

Electrochemical characterization of the bacterial cell surface

Foto omslag gemaakt door
Francis H. M. Cottaar.

619749



Promotoren: Dr. J. Lyklema, hoogleraar in de fysische chemie, met
bijzondere aandacht voor de grensvlak en kolloïdchemie
Dr. A. J. B. Zehnder, hoogleraar in de microbiologie

Co-promotor: Dr. W. Norde, universitair hoofddocent bij de vakgroep
Fysische en Kolloïdchemie

Electrochemical characterization of the bacterial cell surface

Albert van der Wal

Proefschrift

ter verkrijging van de graad van
doctor in de landbouw- en milieuwetenschappen
op gezag van de rector magnificus,
Dr. C. M. Karssen,
in het openbaar te verdedigen op
woensdag 31 januari 1996
des namiddags te vier uur in de Aula
van de Landbouwuniversiteit te Wageningen

This research was funded by grant C6-1/ 8973 from The Netherlands Integrated Soil Research Programme. It was carried out at the Department of Physical and Colloid Chemistry and at the Department of Microbiology of the Wageningen Agricultural University, Wageningen, The Netherlands.

THESIS
LANDBOUWUNIVERSITEIT
WAGENINGEN

CIP-DATA KONINKLIJKE BIBLIOTHEEK, DEN HAAG

Wal, Albert van der

Electrochemical characterization of the bacterial cell
surface / Albert van der Wal. - [S.l. : s.n.]

Thesis Landbouwniversiteit Wageningen. With ref. - With
summary in Dutch.

ISBN 90-5485-492-8

Subject headings: surface charge / colloid stability /
electrokinetic potential.

Stellingen

I

Stellingen bij een proefschrift behoren aan dezelfde eisen te voldoen als die welke gelden voor een wetenschappelijke theorie. Dat betekent o.a. dat ze bediscussieerbaar, bekritiseerbaar en tenslotte ook weerlegbaar moeten zijn.

II

De interpretatie van bacteriehechting volgens Van Loosdrecht *et al.* is gebaseerd op een verwarrende synthese van de oppervlakte-vrije energie benadering en de DLVO theorie.

Van Loosdrecht, M. C. M., W. Norde, J. Lyklema and A. J. B. Zehnder. 1990. Hydrophobic and electrostatic parameters in bacterial adhesion. Aquatic Sciences, 52/1. 103-114.

III

Bij de verklaring van de correlatie tussen hechtingsgedrag van bacteriecellen en de positie van het iso-elektrisch punt, wordt door Rijnaarts *et al.* ten onrechte geen rekening gehouden met electrostatistische effecten.

Rijnaarts, H. H. M., W. Norde, J. Lyklema and A. J. B. Zehnder. 1995. The isoelectric point of bacteria as an indicator for the presence of cell surface polymers that inhibit adhesion. Colloids and Surfaces B: Biointerfaces. 4. 191-197.

IV

De door Einolf en Carstensen voorgestelde procedure voor de berekening van de elektrokinetische potentiaal leidt tot absurd hoge waarden bij lage zoutconcentraties. Dat komt omdat ze de celwandgeleiding uitsmeren over de hele cel en bovendien geen rekening houden met concentratiepolarisatie.

Einolf, C. W., Carstensen, E. L. 1967. Bacterial conductivity in the determination of surface charge by microelectrophoresis. Biochim. Biophys. Acta, 148. 506-516.

V

Dat de elektroforetische beweeglijkheid van kolloïdale deeltjes in het lage concentratiegebied toeneemt bij verhoging van de zoutsterkte is reeds lange tijd bekend. Dit verschijnsel moet echter niet toegeschreven worden aan een 'opladende werking van het co-ion', maar lijkt te worden veroorzaakt door de geleiding van tegenionen langs het deeltjesoppervlak.

Kruyt, H. R. 1924. Inleiding tot de fysische chemie, de kolloïdchemie in het bijzonder, voor biologen en medici, Amsterdam, pag. 111.

VI

Het biologische gegeven dat een vrouw slechts een beperkt aantal jaren vruchtbaar is voorkomt dat de volwassenheid eindelijk lang wordt uitgesteld.

VII

Als de volgelingen van Charles Darwin (1809-1882) het werk van diens tijdgenoot Louis Pasteur (1822-1895) zorgvuldig zouden bestuderen, dan zullen ze ontdekken dat de evolutieleer feitelijk gebaseerd is op de morsdode theorie van de Spontane Generatie.

VIII

Met hun besef dat de werkelijkheid wezenlijk geordend is staan het christendom en de natuurwetenschappen broederlijk tezamen tegenover de levensovertuiging van hedendaagse filosofen.

IX

De spectaculaire vooruitgang van de natuurwetenschappen heeft niet alleen geleid tot een primitieve, mechanistische visie op de werkelijkheid, maar ook tot een overschatting van het menselijk kenvermogen.

X

Door de vervanging van het scheppingsverhaal door een moderne wetenschappelijke kosmogonie zijn ook de christelijke morele beginselen op losse schroeven komen te staan.

XI

Wie in de politiek raak wil schieten moet net boven zijn doel mikken. Dat is de wet van de zwaartekracht.

XII

Door de salarisopbouw parabolisch te laten verlopen met het maximum zo rond het veertigste levensjaar, worden de bestedingsmogelijkheden beter in overeenstemming gebracht met zowel prestatie als behoeftepatroon.

XIII

Men kan Gods nabijheid slechts ervaren in het besef dat Hij oneindig ver van de mens is verwijderd.

XIV

De altijd aanwezige tegenwind op het Groningse platteland vermindert weliswaar het fietsplezier, maar maakt dat de Groningers wel tegen een stootje kunnen.

Stellingen behorend bij het proefschrift "Electrochemical characterization of the bacterial cell surface" van Albert van der Wal, Landbouwwuniversiteit Wageningen, 31 januari 1996.

**Aan mijn vader en grootvader
uit hoogachting en dankbaarheid**

Voorwoord

Met het proefschrift dat nu voor U ligt is een belangrijk deel van het werk dat ik de afgelopen vier jaar heb gedaan op schrift gesteld. Het onderzoek is uitgevoerd op het grensvlak van de fysische en kolloïdchemie en de microbiologie. Al tijdens mijn studie heeft Marc van Loosdrecht mij ingeleid in de wereld van de gehechte micro-organismen en mij destijds reeds gewezen op het belang van een kwantitatieve beschrijving van de elektrische eigenschappen van bacteriecellen. Gedurende mijn gehele aanstelling heb ik van de expertise van beide vakgebieden gebruik mogen maken. Huub Rijnaarts was altijd bereidt om naar mijn gedachtenspinsels te luisteren en heeft mij vele malen van goede adviezen voorzien. Bovendien bleef het laboratorium onder zijn toezicht ordelijk en goed geoutilleerd. Ik had mij geen betere collega kunnen wensen. Ook Fonds en Gosse stonden altijd klaar om mijn vragen te beantwoorden. En natuurlijk niet te vergeten Wim, Carolien en Francis die mij hebben geholpen met diverse analyses.

Het niveau van een proefschrift hangt niet alleen af van de inzet van de promovendus, maar wordt minstens evenveel bepaald door de kwaliteit van de begeleiding. Wat dat laatste betreft, daaraan heeft het niet ontbroken. Zo kon ik tijdens het onderzoek voor lastige problemen telkens een beroep doen op de jarenlange ervaringen van maar liefst drie begeleiders, die tesamen het gehele vakgebied van de fysische en kolloïdchemie tot en met de microbiologie bestrijken. Zo'n luxe valt een jonge beoefenaar van de wetenschap maar zelden ten deel. Een woord van dank is daarom dan ook op zijn plaats.

Beste Willem, zeer geleerde co-promotor. Jouw kamerdeur stond altijd open. Het verschijnen van mijn silhouet op de deurempel was reeds voldoende om mij een plaats aan te bieden en om de zaak eens rustig te bekijken. Was ik te enthousiast dan schroomde je niet enkele vragen te stellen, waaruit bleek dat het allemaal niet zo eenvoudig ligt. Daarentegen was je altijd bereid om een helpende hand te bieden wanneer het onderzoek minder succesvol verliep.

Beste Hans, hooggeleerde promotor. Telkens wanneer ik met jou praat dan moet ik een natuurlijke neiging om U te zeggen onderdrukken. De meeste hoogleraren bekleden hun ambt vanaf een zeker moment in hun leven. Bij jou denk ik echter altijd dat je als professor bent geboren. Je hebt belangrijk bijgedragen aan de inhoud van dit proefschrift en mij er bovendien telkens op gewezen dat de onderzoeksresultaten helder en duidelijk gepresenteerd dienen te worden.

Beste Alex, hooggeleerde promotor. Als animator van het bacteriehechtings-project heb je altijd veel belangstelling getoond in de voortgang van het werk. Door jouw gedegen microbiologische kennis is het onderzoek al vanaf de beginfase voorspoedig verlopen. Bovendien weet ik nu dat je met een microscoop meer kunt zien dan je op het eerste gezicht denkt.

Johan Kijlstra heeft mij nog net voor zijn vertrek naar Bayern de eerste beginselen van de elektrokinetiek bijgebracht. Het vullen van de diëlectrische cel met bacteriën lag in het begin wel wat gevoelig. Zoiets doe je niet zomaar. Toen echter alle metingen met silica en hematiet waren afgerond en de meetcel al helemaal rood was gekleurd, mochten die beestjes er wel in. Bij de interpretatie van de elektrokinetische metingen heb ik veel hulp gehad van Marcel Minor. Zonder zijn enthousiasme en gedegen kennis van zaken hadden de hoofdstukken drie en vier nooit in de huidige vorm opgeschreven kunnen worden.

Een prettig voordeel van natuurwetenschappelijk onderzoek is dat gebruik kan worden gemaakt van ontdekkingen en inzichten van vroeger tijden. Naast het doen van onderzoek heb ik daarom het bestuderen van oude en nieuwe geschriften erg belangrijk gevonden. Met name de zogenaamde AIO discussie groepjes, waarin diverse hoofdstukken van FICS werden behandeld, waren voor mij erg leerzaam. Het is nu eenmaal gemakkelijker om in een groep en onder deskundige begeleiding het wiel opnieuw uit te vinden.

Sinds Herman naast mijn kamer zijn intrek nam heb ik geleerd dat het aloude gezegde "een goede buur is beter dan een verre vriend" in brede zin moet worden opgevat. Zonder zijn gedegen kennis van de electrochemie zou mijn leven waarschijnlijk een ander verloop hebben gekend. Arie is eigenlijk steeds een beetje mijn begeleider gebleven en met Luuk ben ik nog steeds niet uitgepraat.

Ik heb in de afgelopen jaren veel geleerd van Arjan, Gerton, Maarten en Inge, die in het kader van een afstudeervak mij hebben geholpen bij de totstandkoming van het onderzoek. Een wel heel bijzondere ervaring was de samenwerking met Masashi Sakai. De communicatie in een voor ons beiden vreemde taal, bleek geen enkele belemmering te zijn voor urenlange conversaties. Een woord van dank ook voor José Manuel, die mij geduldig de ingewikkelde regels van de spaanse grammatica heeft bijgebracht. Als AIO verkeer je in de gelukkige omstandigheid dat je je kamer mag delen met anderen. Jacomien, Gea en Janet, hartelijk dank voor de geboden gezelligheid en afleiding. Dat laatste geldt ook voor Raquel, die mij niet alleen voortdurend heeft aangemoedigd om het boekje af te maken, maar vooral ook om dat een beetje snel te doen.

Tenslotte, voor degene die geïnteresseerd is in dit onderzoek, maar helaas onvoldoende tijd heeft om zich in alle details ervan te verdiepen, is er een engelse samenvatting met daarin de belangrijkste resultaten en conclusies. Voor de welwillende doch niet begripende lezer is er een vereenvoudigde samenvatting in gewoon nederlands. In de hoop daarmee recht te doen aan de gevarieerdheid van het lezerspubliek, wens ik U veel leesplezier toe.

Bert

Contents

1. Introduction

General background	1
The bacterial cell as a charged colloidal particle	1
Characterization techniques of the electrical double layer	2
Relevance of double layer characterization in bacterial adhesion studies	2
Choice of the bacterial strains	4
Aim and outline of this thesis	5
References	6

2. Chemical analysis of isolated cell walls of Gram-positive bacteria and the determination of the cell wall to cell mass ratio

Introduction	9
Materials and methods	
Bacterial cultivation and preparation	11
Strain identification	11
Cell wall isolation	11
Phospholipid analysis	12
Elimination and determination of D-lactate	12
Amino acid analysis of the isolated walls	13
Electron microscopy	13
Results	
Removal of membrane fragments from the cell wall sample	13
D-lactate elimination	15
Peptidoglycan levels in the wall	15
Amino acid analysis	18
Cell wall mass	18
Discussion	20
Conclusions	22
Acknowledgement	23
References	23

3. Determination of the total charge in the cell walls of Gram-positive bacteria

Introduction	27
Materials and methods	
Bacterial cultivation and preparation	30
Cell wall isolation	30
Cell wall proteins	30
Contact angle measurements	30
Surface/cell wall mass ratio	31
Cell wall volume	31
Potentiometric proton titration	31
Results and discussion	
Chemical composition of the cell walls	32
Purity of the cell wall samples	33
Proton titration of isolated walls	36
Proton titration of whole bacterial cells	36
Cell wall surface charge	37
Esin-Markov analysis	38
Titratable cell wall groups	41
Titration of carboxyl-, amino- and phosphate groups	44
Estimates of the amounts of carboxyl-, amino- and phosphate groups	47
Donnan potential	50
Henderson-Hasselbalch analysis	52
Conclusions	54
References	56

4. Conductivity and dielectric dispersion of Gram-positive bacterial cells

Introduction	59
Theory	61
Experimental	
Bacterial cultivation and preparation	65
Volume fraction	65
D.c. conductivity	66
Dielectric spectroscopy	66
Results	
D.c. conductivity	66

Dielectric dispersion	70
Discussion	71
Conclusions	73
References	74
 5. The electrokinetic potential of bacterial cells	
Introduction	77
Theory	79
Materials and methods	
Bacterial cultivation and preparation	82
Electrophoresis	82
Potential profile across the bacterial wall	82
Results	83
Discussion	89
Conclusions	91
References	91
 Summary and concluding remarks	97
Samenvatting	98
Curriculum Vitae	102

Chapter 1

Introduction

General background

Microorganisms are present in a diverse variety of natural environments, including fresh water lakes, corral reefs, hot springs, desert soils, the oral cavity and intestines. These organisms are the main participants in the mineralisation processes of organic matter and in this respect play an important role in the maintenance of life on earth ¹⁴. From the early beginning of human existence they have been used for biotechnological purposes, especially fermentation processes and are therefore among the oldest domestic organisms ⁴. Microorganisms are generally much smaller than 0.1 mm and can therefore not be seen with the naked eye. Hence, the microbial world remained undiscovered until the invention of microscopes. A scientist endowed with great skills in both constructing microscopes and observing the microbial world was Antonie van Leeuwenhoek (1632-1723). He saw many of the unicellular microorganisms for the first time and often described them with great accuracy ¹⁶. In the centuries thereafter many individual microbial species have been isolated from their natural environments, after which they were characterized with biochemical, physico-chemical and genetic methods. Such characterization studies, in turn, contribute to gain better insight in the behaviour of microorganisms in their original ecological habitats and may reveal their potential abilities for biotechnological applications, as well.

Most microorganisms belong either to the group of the procaryotes, which comprises the bacteria, or to that of the eucaryotes, which includes algae, fungi, yeast and protozoa. The cells of the procaryotes are generally excellent candidates for colloid chemical studies, because they have relatively simple structures and are usually of colloidal size, in the order of 1 micrometer. Moreover, they are able to reproduce themselves in such a way that populations with billions of identical cells can be obtained. The cell dimensions of most eucaryotic cells are in the range of 10 to 100 micrometer, which is generally too large to allow colloid-chemical characterization techniques ^{14, 16}.

The bacterial cell as a charged colloid particle

The inner core of the bacterial cell consists of cytoplasm and is surrounded by the cytoplasmic membrane. The outermost structure of the bacterial cell is its wall,

which is in direct contact with the external environment. The bacterial wall is generally charged due to the presence of carboxyl, phosphate and amino groups. The degree of dissociation of these ionizing groups is determined by the pH and the concentration of the surrounding electrolyte solution. The presence of the charged cell wall groups gives rise to the formation of an electrical double layer. The compensating charge mainly consists of counterions that can penetrate into the porous cell wall and to a minor extent of co-ions that are expelled from it. The extension of the double layer into the surrounding solution depends on the salt concentration. In low salt aqueous systems, such as streams and fresh water lakes, the diffuse countercharge may be smeared out over distances of the order of ten nanometer, whereas in more saline systems, like estuary, sea water and most bodyfluids, the compensating charge will be at close distance from the bacterial wall.

Characterization techniques of the electrical double layer

There are, in principle, several techniques to obtain information on the composition of the electrical double layer⁹. Potentiometric and to a lesser extent conductometric titrations are widely used to assess the surface charge density.

The response of colloidal particles to an external field may contribute to a further characterization of the electrical double layer. A very well-known example of such a dynamic study is microelectrophoresis, in which the velocity of a colloidal particle is measured in an electric field. More direct information about the ionic atmosphere of the double layer can be obtained from static conductivity and from dielectric dispersion studies. However, the interpretation of electrokinetic measurements is not trivial and is very much dependent on the model used for the electrical double layer.

Relevance of double layer characterization in bacterial adhesion studies

Bacterial cells in natural environments tend to accumulate at the solid-liquid interface. There is substantial experimental evidence that the degree of attachment is influenced by such cell surface characteristics as hydrophobicity and cell wall charge^{13, 15, 18}. This suggests that the adhesion behaviour of bacterial cells may be described by classical physico-chemical theories. In the widely used "surface free energy approach" bacterial cell adhesion is interpreted in terms of the cell surface hydrophobicity, measured as the contact angle of a water droplet on a lawn of bacterial cells. However, in this concept it is not trivial to account for the effect of the cell wall charge on the adhesion process.

One of the oldest theories for particle deposition is the classical DLVO theory, developed by Deryaguin and Landau³ and Verwey and Overbeek¹⁹. According to this theory the interaction Gibbs energy between the particle and the macroscopic surface is considered to be determined by the sum of Van der Waals attraction forces and electrostatic forces due to overlap of the electrical double layers. Previous studies indicate that the DLVO theory can be of help to describe the initial processes of bacterial cell adhesion¹⁸. More recent work has shown that, besides the DLVO type interactions, cell wall polymers protruding in the surrounding solution can also have great impact on the adhesion process, especially at higher salt concentrations¹³. So far, these studies were at best semi-quantitative.

For the application of the DLVO theory to bacterial cell adhesion in a more quantitative way, a number of complications arise¹⁷. Firstly, in order to quantify the electrostatic interactions, one needs to know the value of the electrical potential at the bacterial cell surface. Unfortunately, this potential is unmeasurable and therefore electrokinetic techniques, such as electrophoresis, are generally used to obtain information about the potential at the plane of shear, the so-called ζ -potential. However, the value obtained for the ζ -potential depends on the model used for the interpretation of the electrophoretic mobility. Bacterial cells are generally large colloidal particles, which implies that, for not too low electrolyte concentrations, the electrical double layer is thin relative to the particle radius. At first sight one might therefore consider to use the classical Helmholtz-Smoluchowski equation¹⁰ for the conversion of the electrophoretic mobility into the ζ -potential. However, in this theory it is assumed that the ionic atmosphere of the electrical double layer is not deformed by the external electric field. This assumption holds as long as the conduction of ions along or in the particle surface is negligibly small. For bacterial cells surface conduction effects may be considerable, even at low ζ -potentials, depending on the amount of mobile ions in the bacterial wall. This implies that the ζ -potential cannot unambiguously be calculated from electrophoretic mobility measurements, unless quantitative information on the cell wall conductivity is available⁶. Except from the pioneering work of Carstensen et al.^{1, 2} and more lately of Kijlstra et al.⁷ such measurements have not been performed.

Because of the difficulties in the calculation of the ζ -potential the electrostatic state of bacterial cell surfaces is often poorly characterized only in terms of the measured electrophoretic mobility. Although this is the most common approach, it also implies that any theory for particle deposition, including the DLVO theory, can

at best serve as a qualitative guide to describe the (initial) processes of bacterial cell adhesion.

Another major problem in the application of the DLVO theory stems from the uncertainty in the value that has to be assigned to the Hamaker constant, which is needed to assess the Van der Waals attraction forces. It requires quantitative knowledge of the chemical composition of the bacterial wall. For most bacterial cells this information is not available and so far estimations of the values of the Hamaker constants are very much limited¹².

From the above considerations we reach the conclusion that detailed information of both the chemical cell wall structure and the composition of the electrical double layer are prerequisites to gain further insight into the mechanism of bacterial cell adhesion. This issue essentially formulates the theme of this thesis.

Choice of the bacterial strains

The main division between bacterial cells is based on their reaction to Gram staining, developed by Hans Christian Joachim Gram (1853-1938)^{5, 8, 11}. The distinction between Gram-positive and Gram-negative bacterial cells is related to differences in the cell wall structure. The walls of Gram-positive cells consist of a thick network of peptidoglycan strings and associated biopolymers such as teichoic acid, teichuronic acid and proteins. The walls of the Gram-negative bacterial cells are complex multilayered structures. They contain a thin peptidoglycan layer and are surrounded by an asymmetric outer membrane, which consists of a phospholipid and a lipopolysaccharide layer.

For the time being, Gram-positive strains are more suitable for colloid-chemical characterization studies, because of their less complex cell wall structures. A relevant criterium in selecting the bacterial strain is the position of the point of zero charge (p.z.c.), because it is the reference point for the charge formation. Charge reversal of the bacterial wall should preferably occur in the pH range accessible by proton titration, which allows determination of the absolute charge density. In practice this means that the p.z.c. should be at pH values higher than 3. Five Gram-positive bacterial strains, including four coryneforms and a *Bacillus brevis*, have been selected for physico-chemical characterization studies of their cell surfaces.

The growth curve of all these bacterial strains clearly showed distinguishable lag, exponential and stationary phase. The change in the cell surface characteristics during growth was followed by measuring the water contact angle, the electrophoretic mobility at pH 7 and the position of the isoelectric point in a monovalent electrolyte solution. These measurements indicated that after the

exponential growth phase no significant surface changes occurred. The bacterial cells were therefore harvested when growth was completed and before cell lysis occurred, i.e. in the (early) stationary state.

Aim and outline of this thesis

The aim of this thesis is to systematically investigate the properties of the electrical double layer of bacterial cell surfaces. Such a study can only become successful if different experimental techniques are applied. The approach in the present study is such that the characteristics of the electrical double layer at rest can be compared with its dynamic properties. In order to assess the total surface charge density, cell walls have been isolated and subsequently titrated with acid and base. Investigations of the electrokinetic properties of bacterial cell suspensions include static conductivity, dielectric dispersion and electrophoresis studies. Comparison between the different techniques not only reveals detailed double layer characteristics, but also provides good tests to check the consistency of the experimental results.

The relation between the cell surface charge and the chemical composition of the wall is studied in chapters 2 and 3. The chemical analysis of the bacterial wall, given in chapter 2, includes quantitative determination of the peptidoglycan and protein content. In the same chapter a new method is presented to determine the dry weight wall fraction in the bacterial cell. The results of the potentiometric proton titrations with isolated walls and whole cells are presented in chapter 3. Analysis of these titration curves provides information on the number of carboxyl, phosphate and amino groups in the bacterial wall. It is shown that these numbers are in excellent agreement with those estimated from the chemical composition. Moreover, the titration results are converted into absolute cell wall charge densities.

Information on the occurrence of surface conductance in the cell wall and the diffuse part of the double layer is extracted from static conductivity and dielectric dispersion studies. The results are presented in chapter 4 and show that the counterions in the bacterial wall are rather mobile. Chapter 5 deals with the interpretation of the electrophoretic mobility of bacterial cells, taking into account possible surface conductance effects. It is demonstrated that the classical Helmholtz-Smoluchowski equation for the conversion of the electrophoretic mobility into the ζ -potential is only valid for not too low electrolyte concentrations.

References

1. **Carstensen, E. L., H. A. Cox, W. B. Mercer, L. A. Natale** 1965. Passive electrical properties of microorganisms. I. Conductivity of *Escherichia coli* and *Micrococcus lysodeikticus*, *Biophys. J.* **5**, 289-299.
2. **Carstensen, E. L., R. E. Marquis** 1968. Passive electrical properties of microorganisms. III. Conductivity of isolated bacterial cell walls., *Biophys. J.* **8**, 536-548.
3. **Deryaguin, B. V., L. D. Landau** 1941. *Acta Physico Chim.* **14**, 633.
4. Genesis 9:21.
5. **Hancock, R. E. W.** 1991. Bacterial outer membranes: evolving concepts. Specific structures provide Gram-negative bacteria with several unique advantages, *ASM news* **57**, 175-182.
6. **Kijlstra, J.** 1992. Double layer relaxation in colloids. Thesis, Wageningen Agricultural University.
7. **Kijlstra, J., A. Van der Wal** 1995. Electrokinetic behaviour of bacterial suspensions, *Bioelectrochem and Bioenergetics* **37**, 149-151.
8. **Koch, A. L.** 1990. Growth and form of the bacterial cell wall, *American Scientist* 327-341.
9. **Lyklema, J.** 1995. Fundamentals of interface and colloid science, Academic press limited, London etc., vol. II, chapter 3.
10. **Lyklema, J.** in press. Fundamentals of interface and colloid science, Academic press limited, London, vol. II, chapter 4.
11. **Neifhardt, F. C., J. L. Ingraham, M. Schaechter** 1990. Physiology of the bacterial cell. A molecular approach, Sinauer associates, inc., Sunderland, Massachusetts.
12. **Nir, S.** 1976. Van der Waals interactions between surfaces of biological interest, *Progr. Surf. Sci.* **8**, 1-58.
13. **Rijnaarts, H. H. M.** 1994. Interactions between bacteria and solid surfaces. In relation to bacterial transport in porous media. Thesis, Wageningen Agricultural university, The Netherlands.
14. **Schlegel, H. G.** 1993. General microbiology seventh edition, University press, Cambridge.
15. **Sjollem, J.** 1990. Direct observation of particle deposition in a parallel plate flow cell. Application to oral streptococci and polystyrene particles. Thesis, University of Groningen, The Netherlands.
16. **Stanier, R. Y., J. L. Ingraham, M. L. Wheelis, P. R. Painter** 1986. The microbial world fifth edition, Prentice-Hall, New Jersey.
17. **Tadros, T. F.** 1980. Particle surface adhesion, In *Microbial adhesion to surfaces*, R. C. W. Berkeley, J. M. Lynch, J. Melling, P. R. Rutter, B. Vincent, Eds. Ellis Horwood Limited, London, 93-116.

18. **Van Loosdrecht, M. C. M.** 1988. Bacterial adhesion. Thesis, Wageningen Agricultural University, The Netherlands.
19. **Verwey, E. J. W., J. T. G. Overbeek** 1948. Theory of the Stability of Lyophobic Colloids, Elsevier, Amsterdam.

Chapter 2

Chemical analysis of isolated cell walls of Gram-positive bacteria and the determination of the cell wall to cell mass ratio

Abstract

Cell walls of five Gram-positive bacterial strains, including four coryneforms and a *Bacillus brevis* strain have been isolated and subsequently chemically analysed. The peptidoglycan fraction in the walls of the coryneform bacteria is rather high and constitutes about 23 to 31 % of the cell wall dry weight. The protein content is somewhat lower and in the range of 7 to 14 %. The peptidoglycan in the wall of the *B. brevis* strain forms a thin layer and contributes only about 5 % to the cell wall dry weight. The high amount of proteins in the *B. brevis* cell wall (>56 %) can be attributed to a so called S(urface)-layer.

The wall contribution to the total cell mass is calculated from a comparison of D-lactate concentrations in hydrolysates of whole cells and isolated walls. D-lactate concentrations are measured enzymatically after purification of the samples with active carbon. The optimum condition for the quantitative elimination of D-lactate from the peptidoglycan appears to be at 120 °C and 4 N HCl. The wall fraction for the cells of the coryneform bacteria are in the range of 26-32% and is about 75% for the *B. brevis* cells.

Introduction

All bacterial cells are surrounded by rigid walls, which protect the cytoplasm and the fragile plasma membrane from influences of the outer environment. These walls also maintain the shape of the cells and give protection against osmotic lysis¹⁵. Thanks to extensive studies between 1950 and 1980, detailed knowledge is now available about function and chemical composition of the walls^{21, 22}. Following the pioneering work of Cummins and Harris, cell wall analysis is nowadays a valuable technique for the classification of Gram-positive bacteria^{8, 27}.

Classical studies of the cell wall composition require disruption of the cells by mechanical forces and the subsequent isolation and purification of the wall fragments¹³. Although the isolation procedure may lead to undesired losses of

cell wall constituents, these studies generally give precise information on the wall composition. More rapid and also less risky methods involve the analysis of whole cells¹². However the information obtained in this way has generally a more qualitative character.

In Gram-positive bacteria the wall accounts for a considerable proportion of the cell dry weight. Early estimates of the wall contribution to the total cell mass were based on quantitative recoveries of cell wall material²⁵. A more sophisticated method for the determination of the fraction of cell weight represented by wall material has been given by Marquis¹⁶. According to his method whole cells, suspended in protoplast-stabilising-media, are treated with lysozyme, which dissolves the cell envelope. The wall weight can then be determined after centrifugation and drying of the supernatant solution. Although this method can give reliable results, the applicability is limited, because not all bacterial strains have cell envelopes which can be completely hydrolysed by lysozyme.

In 1968 Tipper^{19, 28} proposed an analytical method for the quantitative determination of muramic acid in isolated cell walls. In his procedure, D-lactate is eliminated from muramic acid by alkaline hydrolysis of cell wall material followed by an enzymatic determination of the D-lactate concentration. Few years later Hadzija^{11, 19} also presented a simple colorimetric method for the quantitative determination of D-lactate in cell wall hydrolysates.

In the present paper the chemical structure of isolated cell walls of five Gram-positive bacteria, including four coryneforms and a *Bacillus brevis* strain, has been analysed. The peptidoglycan content in the bacterial wall is determined according to a procedure, which is based on Tipper's enzymatic method. The fraction and composition of the cell wall proteins is assessed from an amino acid analysis of isolated cell walls.

The wall fraction of the bacterial cell is calculated from a comparison between the content of D-lactate in isolated walls with that in whole cells. For that purpose Tipper's enzymatic method for hydrolysed cell wall material has been extended to allow the determination of D-lactate concentrations in hydrolysates of whole cells, as well.

Materials and Methods

Bacterial cultivation and preparation

The *Rhodococcus erythropolis* A177 and the *Rhodococcus opacus* C125 were cultivated in mineral medium described by Schraa et al.²⁴ without adding yeast extract. Ethanol (50 mM) was used as the sole carbon and energy source. *Corynebacterium* sp. strain DSM 6688² and *Corynebacterium* sp. strain DSM 44016² were cultivated in brain heart infusion broth (Merck, 40 g/l deionized water). Growth of *Bacillus brevis* ATCC 9999 in culture media as described by Mateo et al.¹⁷ did not result in full separation of the individual cells in the stationary growth phase. Therefore, the following medium was used (in g/l): 2.2 NH₄Cl, 0.27 KH₂PO₄, 0.05 KNO₃, 0.2 MgCl₂·6H₂O, 0.06 CaCl₂·2H₂O, 0.01 FeCl₃·6H₂O, 0.35 MgSO₄·7H₂O, 7.5 casamino acids and 2.5 glycerol. Trace elements (1 ml/l) and vitamins solution (1 ml/l) were added²⁴.

Bacteria were grown at 30 °C on a rotary shaker and harvested in the early stationary growth phase by centrifugation for 10 min at 20,000 g and 4 °C. The cells were washed three times in deionized water.

Strain identification

Rhodococcus erythropolis A177 and *Rhodococcus opacus* C125¹⁴ were identified by Dr. B. Bendinger (pers. communication) as members of the genus *Rhodococcus* upon the combination of their diagnostic cell wall components¹⁰ (see also appendix A). Species attribution was done by Dr. S. Klatte (pers. communication) based upon the quantitative composition of fatty acid methyl esters, mycolic acid methyl esters and physiological reaction profiles.

Cell wall isolation

Cells in a 4 M guanidinium HCl solution were disrupted by exposing them five times to French press, the coryneforms at 20,000 psi and *B. brevis* at 15,000 psi. The degree of disruption was monitored by phase microscopy. The disrupted cells were centrifuged at 30,000 g and the pellet resuspended in 4 M guanidinium HCl. If necessary the French press procedure was repeated once more. The broken cells were washed several times in 1 M KNO₃, centrifuged at 1,500 g to remove intact cells and coarse debris. The cell walls were collected at 20,000 g. The pellet was washed with milliQ water and aliquotes were freeze-dried for phospholipid, D-lactate and amino acid analysis. Electron micrographs showed cell wall samples to be free of whole cells.

Phospholipid analysis

Phospholipid concentrations were determined according to a modified method of Bartlett and Bligh ^{1, 7}. Freeze-dried cells (10-60 mgr d.w.) or cell walls (20 and 30 mg) were rehydrated for 10 hours in 2.4 ml milliQ water, extracted for at least 10 hours with 3 ml chloroform and 6 ml methanol and another 10 hours after addition of 3 ml chloroform and 3 ml water. Separation into a chloroform and a water/methanol phase was usually complete within 24 hours. In case emulsification occurred in the chloroform phase these emulsions were broken either by gently shaking or by centrifugation. An aliquot of the chloroform phase was dried at 100 °C for about 30 min in the oven and the residue was destructed in 0.4 ml 30% perchloric acid in sealed tubes to 180 °C for 30 min. If the sample was not colourless, 50 µl 30% hydrogen peroxide was added after which the sample was again heated at 180 °C for 20 min. The amount of phosphate was determined by adding 1.8 ml milliQ, 0.1 ml molybdate-reagent (50 g/l (NH₄)₆Mo₇O₂₄·4H₂O) and 0.1 ml ANSA-reagent (410 g/l Na₂S₂O₅, 21 g/l Na₂SO₃, 5 g/l 1-amino-2-hydroxy-4-naphtalenesulfonic acid). After 15 min in a boiling bath the extinction was measured with a spectrophotometer at a wavelength of 820 nm. The destruction of β-glycerophosphate was used as a standard.

For total phosphate determination in the isolated walls 1 mg sample was hydrolysed in 0.4 ml 30% perchloric acid. The amount of total phosphate was measured according to the colorimetric method described above.

Reagents were stored at 4 °C in dark coloured bottles. All glassware was cleaned carefully in nitric acid and all chemicals used were free of phosphate.

Elimination and determination of D-lactate

D-lactate was eliminated from the peptidoglycan of whole bacterial cells by hydrolysis of 50 mg freeze-dried cells in sealed tubes at 110 °C and 120 °C in hydrochloride concentrations between 1 and 6 M for 24 hours. The hydrolysed cells were neutralised with potassium hydroxide. An aliquot, which contained 8 mg hydrolysed cell wall material, was purified by adding 1 ml active carbon (W100, 150 g/l, pH 10) and H₂O up to a final volume of 2 ml. After 1 hour equilibration the active carbon was removed by a syringe filter (0.2 µm). D- and L-lactate concentrations in the filtrate were measured enzymatically (enzymes were purchased from Boehringer Mannheim). A cuvette was filled with 1 ml filtrate, 1 ml glycylglycine buffer (79.2 g/l glycylglycine, 14.7 g/l L-glutamate and sodium hydroxide to a final pH value of 10), 0.2 ml NAD⁺ (35 mg/ml) and 20 µl glutamate-pyruvate transaminase (approx. 1500 U/ml). After 5 min. the absorption was

measured with a spectrophotometer at a wavelength of 340 nm. Either 20 μ l L- or D- lactate dehydrogenase (approx. 5000 U/ml) was added and after 40 min the increase in absorption was measured. Absorption is linear with D- and L-lactate concentration for the range from 2 to 25 μ g per cuvette.

The hydrolysis of freeze-dried cell walls was performed with 20 mg of material, at temperatures and hydrochloric acid concentrations where D-lactate is optimally liberated from the peptidoglycan, which was at 4 M hydrochloric acid and 120 °C. The concentrations of D- and L-lactate were determined according to the same procedure as that for the whole cells.

Amino acid analysis of the isolated walls

For the amino acid analysis isolated cell walls were hydrolysed according to the same procedure as for the D/L-lactate elimination. The amino acid composition was determined with a biotronic LC 6000E amino acid analyser (column: Durrum DC6A Resin), according to the procedure given by Spackman and Benson^{4, 26}.

Electron microscopy

For the preparation of cross-sections, cells were fixed in 3% (v/v) glutaraldehyde. After centrifugation the cells were treated with 1% OsO₄ and subsequently dehydrated in graded ethanol and impregnated with epoxypropane. The cells were embedded in Epon 812. Ultra-thin sections of 50-70 nm were cut on a Reichert Ultracut Emicrotome. After staining with uranyl acetate, sections were examined with a Jeol EM 1200 ex II transmission electron microscope.

For shadow-casting with palladium a formvar-coated copper grid (150 mesh, Ø 3 mm) was laid on a drop of an unfixed cell suspension for 15 min. The grid was washed three times on a drop of deionized water. The air-dried grid was coated with a 1-2 nm thick layer of palladium in a Balzers coater BAE 80T at 5.10⁻⁵ mbar with a fixed angle of 30° from a distance of 15 cm. The samples were examined with a Jeol EM 1200 ex II transmission electron microscope.

Results

Removal of membrane fragments from the cell wall sample

The ratio of phospholipids in the isolated cell walls and in whole cells is used as an indicator for the removal of membrane fragments.

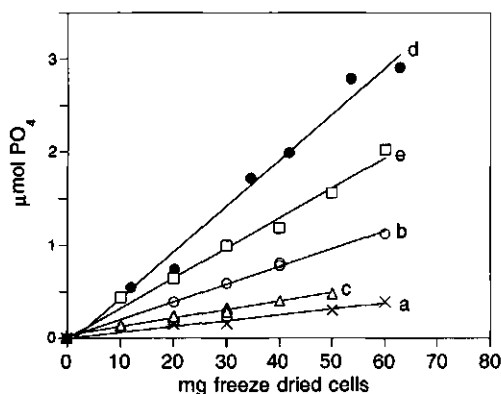


Figure 1: Phospholipids extracted from whole cells of *Corynebacterium* sp. strain DSM 44016 (x) (a), *Corynebacterium* sp. strain DSM 6688 (o) (b), *Rhodococcus erythropolis* A177 (Δ) (c), *Rhodococcus opacus* C125 (\bullet) (d) and *Bacillus brevis* ATCC 9999 (\square) (e).

The results of the phospholipid extractions from whole cells are given in figure 1 for all five bacterial strains. The number of phospholipid molecules extracted strongly depends on the nature of the bacterial strain used and is the highest for *Rhodococcus opacus* C125. Assuming the cross-sectional area of a phospholipid molecule to be about 0.30 nm^2 and a cell wall surface area of $100 \text{ m}^2/\text{g}$ wall (chapter 3) it follows that approximately 16% of the total phospholipids in the cell membrane is extracted. For all other bacterial strains the extraction procedure is less complete. Phospholipids are surface-active molecules and are therefore expected to accumulate in the water-chloroform interface. Hence, the above procedure for the phospholipid determination does not yield the total amount of phospholipids.

In table 1 the fraction of phospholipids removed from the cell walls has been calculated from a comparison between the phospholipids extracted from the isolated walls and whole cells.

At least 70-80% of the cytoplasmic membrane has been removed from the isolated cell walls of the coryneforms and approximately 34% from *B. brevis* cell walls. However, these values may be underestimated, because in case of extraction of whole cells phospholipids have to diffuse through the cell wall. Especially for *B. brevis*, which has a dense protein rich S-layer, phospholipid extraction from whole cells may be incomplete. The removal of phospholipids from the isolated walls is therefore most likely somewhat higher than those values given in tabel 1.

strain	phospholipids extracted $\mu\text{mol P/g}$ cell wall		phospholipid removed from walls during isolation	total phosphate in the isolated walls $\mu\text{mol P/g}$ cell wall
	whole cells	isolated walls		
<i>Corynebacterium</i> sp. strain DSM 44016	19.7	3.3	83%	150
<i>Corynebacterium</i> sp. strain DSM 6688	70.4	20	71%	240
<i>Rhodococcus</i> <i>erythropolis</i> A177	35.4	8.1	77%	260
<i>Rhodococcus opacus</i> C125	172.4	29	83%	290
<i>Bacillus brevis</i>	42.7	27	34%	110

Table 1: Removal of phospholipids from isolated cell walls based on a comparison between the extracted phospholipids in isolated walls and in whole cells. The extracted phospholipids are expressed in $\mu\text{mol P}$ per g cell wall material.

The amount of total phosphate in the isolated cell walls is higher than that of the extracted phospholipids, (table 1), indicating a likely occurrence of phosphate in the walls of the coryneform bacteria and the *B. brevis* strain.

D-lactate elimination

The elimination of D-lactate from the walls of whole cells is given in fig. 2^{a-e} for different bacteria at two temperatures and various acidities. As expected, D-lactate elimination is facilitated by increasing the hydrochloric acid concentration. However, the influence of the temperature is less systematic. *Rhodococcus erythropolis* A177, *Corynebacterium* sp. strain DSM 6688 and *B. brevis* ATCC 9999 show less complete hydrolysis at 110 °C than at 120 °C, whereas in the case of *Rhodococcus opacus* C125 and *Corynebacterium* sp. strain DSM 44016 the temperature hardly affects the elimination of D-lactate. The amount of L-lactate is essentially constant for hydrochloric acid concentrations between 0 and 4 M. At 5 and 6 M HCl a slight increase of L-lactate is observed, which may reflect the breakdown of unstable molecules to give lactate.

For any strain, the liberation of D-lactate is incomplete at HCl concentrations lower than 4 M, regardless of temperature.

4 M HCl at a temperature of 120 °C seems to be optimal for complete elimination of D-lactate from the peptidoglycan structure in the bacterial wall.

Peptidoglycan levels in the wall

The amount of D-lactate released from the peptidoglycan by acid hydrolysis of isolated cell walls is given in table 2. In the same table the peptidoglycan fraction

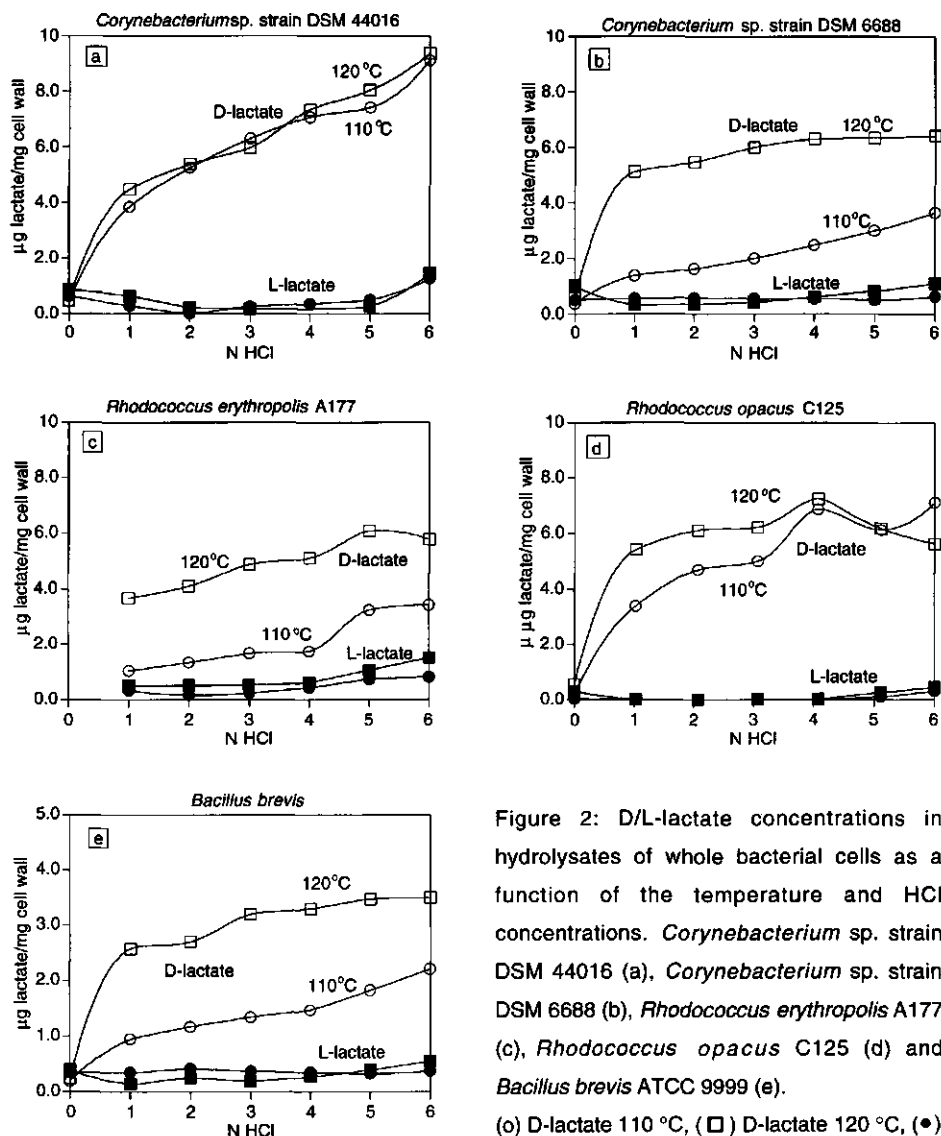


Figure 2: D/L-lactate concentrations in hydrolysates of whole bacterial cells as a function of the temperature and HCl concentrations. *Corynebacterium* sp. strain DSM 44016 (a), *Corynebacterium* sp. strain DSM 6688 (b), *Rhodococcus erythropolis* A177 (c), *Rhodococcus opacus* C125 (d) and *Bacillus brevis* ATCC 9999 (e). (○) D-lactate 110 °C, (□) D-lactate 120 °C, (●) L-lactate 110 °C, (■) L-lactate 120 °C.

in the bacterial wall is estimated from the D-lactate content under the assumption that the peptidoglycan of the coryneforms and the *B. brevis* belongs to the A1γ type, according to the classification scheme of Schleifer and Kandler²³.

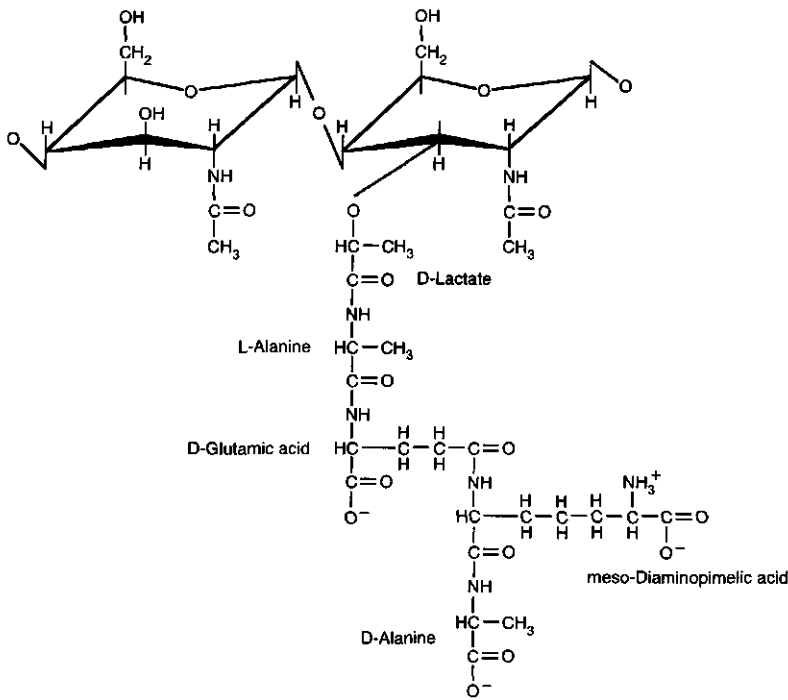


Figure 3: Most likely peptidoglycan structure present in the walls of the coryneforms and *Bacillus brevis*. *Rhodococcus erythropolis* A177 and *Rhodococcus opacus* C125 contain N-glycolylmuramic acid instead of N-acetylmuramic acid.

strain	D-lactate μmol/g cell wall	peptidoglycan	proteins	cell wall fraction	d _{cw} (nm)
<i>Corynebacterium</i> sp. strain DSM 44016	220	23 %	14 %	32 %	60 ±10
<i>Corynebacterium</i> sp. strain DSM 6688	260	27 %	14 %	27 %	35 ±5
<i>Rhodococcus</i> <i>erythropolis</i> A177	222	24 %	10 %	26 %	35 ±5
<i>Rhodococcus opacus</i> C125	302	31 %	7 %	29 %	35 ±5
<i>Bacillus brevis</i>	44	5 %	56 %	75 %	75 ±25

Table 2: Cell wall contribution to the total cell mass and the relative fractions of the peptidoglycan and proteins in the isolated walls. d_{cw}: cell wall thickness as determined from electron micrographs. M_w (primary peptidoglycan) is 1003 for N-acetyl residues and 1035 for the N-glycolyl residues in the glycan moiety.

Peptidoglycan is an important cell wall constituent of the coryneform bacteria and determines about 23 to 31 % of the cell wall dry weight.

The peptidoglycan in the cell walls of the *B. brevis* strain accounts for about 5 % of the cell wall dry weight. This suggests that there are other more dominant compounds present in the *B. brevis* cell wall.

Amino acid analysis

The results of the amino acid analysis of the isolated cell walls of the five bacterial strains are given in table 3. Glutamic acid, alanine and m-diaminopimelic acid are present in high amounts in the walls of the coryneforms. They most likely originate from the peptidoglycan. Several other amino acids are also found, but at lower levels, indicating the presence of low amounts of proteins in the isolated cell wall sample. The contribution of the proteins to the cell wall dry weight of the coryneform bacteria ranges from 7 to 15 %.

For the coryneform bacteria the ratios between alanine, glutamic acid and m-diaminopimelic acid are given in table 4. As expected from the peptidoglycan structure, the amount of alanine is about 2 to 3 times higher than that of m-diaminopimelic acid. The somewhat higher amount of glutamic acid compared to that of m-diaminopimelic acid is probably caused by the presence of cell wall proteins.

The relatively low amount of m-diaminopimelic acid in the walls of *B. brevis* indicates that, in line with the D-lactate analysis, peptidoglycan is a minor cell wall constituent. Most of the glutamate and alanine must originate from cell wall proteins, because their levels are much higher than that of the m-diaminopimelic acid. Moreover, the presence of high amounts of a number of other amino acids also suggests that an important part of the cell wall consists of proteins. Taking into account that other amino acids may be present besides the ones examined, the protein fraction in the cell wall should be at least 56%, see table 2.

Cell wall mass

The cell wall contribution to the total cell mass is calculated from a comparison between the D-lactate concentration measured in hydrolysates of whole cells and that of the isolated walls. The results are included in table 2. For the coryneform bacteria the wall contributes by about 26-32 % to the cell dry weight, while in the case of *B. brevis* 75 % of the cell mass consists of cell wall. This is consistent with estimates of the wall thickness based on electron micrographs. The cell walls of the *B. brevis* strain have a thickness ranging from 50 to 100 nm, whereas those of the coryneforms are about 30 to 70 nm (table 2).

Amino acid	<i>Corynebacterium</i> sp. strain		<i>Rhodococcus</i>		<i>Bacillus brevis</i>
	DSM 44016	DSM 6688	<i>erythropolis</i>	<i>opacus</i> C125	
Aspartate	132	162	66	36	402
Asparagine					
Threonine	96	108	162	36	264
Serine	102	66	96	36	168
Glutamate	527	485	474	420	612
Glutamine					
Glycine	216	216	222	42	348
Alanine	749	611	947	660	468
Valine	102	132	72	84	336
Cysteine	0	0	0	0	0
Methionine	6-12	0	30	30	72
Isoleucine	84	108	36	42	264
Leucine	138	162	120	108	360
m-Diamino-pimelic acid	377	-	306	270	48
Tyrosine	24	12	0	0	96
Phenylalanine	57	48	30	72	168
Lysine	36	108	24	12	282
Histidine	24	24	6	6	84
Arginine	54	60	18	6	198

Table 3: The amino acid composition in the walls of the five bacterial strains (in $\mu\text{mol/g}$ freeze dried cell wall). The diamino acid m-diaminopimelic has previously been detected in the walls of *Corynebacterium* sp. strain DSM 6688². Its amount could not be determined in this study due to the presence of a perturbing peak in the chromatogram. For the same reason the amount of m-diaminopimelic acid in the walls of *Corynebacterium* sp. strain DSM 44016 may be somewhat overestimated. The D and L configurations of the amino acids have the same retention times. Asparagine is converted into aspartate during acid hydrolysis and glutamine into glutamate.

strain	molar ratios for the peptidoglycan peptides		
	Alanine	Glutamic acid	m-Diamino-pimelic acid
<i>Corynebacterium</i> sp. strain DSM 44016	2	1.4	1
<i>Corynebacterium</i> sp. strain DSM 6688	2	1.6	-
<i>Rhodococcus erythropolis</i> A177	3.1	1.5	1
<i>Rhodococcus opacus</i> C125	2.4	1.6	1

Table 4: Molar ratios between the peptidoglycan amino acids for the four coryneform bacteria.

Discussion

Elimination of D-lactate from the peptidoglycan is facilitated by both increasing HCl concentrations and increasing temperature. However, at the same time these extreme conditions may favour the production of lactate from other molecules, for instance alanine. This type of reactions may produce racemic mixtures, in which half of the produced lactate will be in the D and the other half in the L configuration. The increase in the concentration of L-lactate during hydrolysis under extreme conditions can thus be used as an indicator of the D-lactate production.

Direct measurement of D-lactate in hydrolysates of whole cells is impossible due to the high background absorption at 340 nm. Active carbon (W100) almost entirely removed the strongly absorbing molecular structures, probably emanating from carbohydrates. According to BET-analysis, this active carbon has a total surface area of 522 m²/g. Porosity analysis indicates that most of the surface area is determined by micropores rather than by mesopores. The removal by adsorption was performed in an alkali environment in order to increase the electrostatic repulsion between the lactate and the active carbon. The measured adsorption of lactate to the active carbon was less than 1 nmol/m², which in our systems can be considered as negligible. Hence the purification of the sample was effective without affecting the lactate.

The colorimetric method of Hadzija ^{11, 19} has also been used to measure D-lactate in isolated walls and in whole cells. The reproducibility appeared to be rather poor for isolated cell walls and was absent in the case of whole cells. Moreover, the colorimetric method was not specific for lactate. Ethanal, propanal and ethanol, for example, also gave positive reactions. Therefore the applicability of Hadzija's method is limited and the quantitative determination of muramic acid in bacterial cell walls with this method is prone to erroneous results.

Information about the sequence of the amino acids in the peptide moiety of the peptidoglycan can be obtained from partial acid hydrolysis of the cell walls and the subsequent identification of the oligopeptides ²³. Such experiments have not been performed in the present study. However, the A1 γ peptidoglycan type is considered to be a characteristic of the genera *Corynebacterium* and *Rhodococcus* ^{10, 23}. This implies that the peptide moiety of the peptidoglycan is a composition of L-alanine, D-glutamic acid, m-diaminopimelic acid and D-alanine and that the cross-linking between the peptidoglycan units is direct, that is without any interpeptide bridge. Indeed, the results of the amino acid analysis support the proposed structure of the peptide string. This peptide string is attached to N-

acetylmuramic acid, in case of the two *Corynebacteria*, and to N-glycolylmuramic acid for the two *Rhodococcus* species.

The vast majority of the strains of the genus *Bacillus* belong to the directly cross-linked m-diaminopimelic acid A1 γ peptidoglycan type ²³. This structure was for example found in the cell walls of another *B. brevis* strain (ATCC 8246) ²³. Amino acid analysis of the isolated walls of *B. brevis* has revealed the presence of m-diaminopimelic acid, which can only originate from the peptidoglycan. It can therefore be concluded that the peptidoglycan of *B. brevis* ATCC 9999 most likely belongs to the A1 γ type.

The ratios of the amino acids: alanine, glutamic acid and m-diaminopimelic acid in the peptidoglycan matrix should be between 3:1:1 and 2:1:1, depending on the degree of cross-linking. For an A1 γ peptidoglycan type, cross-linking occurs between the amino group of the m-diaminopimelic acid on position 3 and the carboxyl group of the D-alanine on position 4 of another primary peptidoglycan unit, coupled by the simultaneous elimination of the end D-alanine. In principle, the degree of cross-linking can be determined from the ratio between the peptidoglycan amino acids. However, during hydrolysis of the isolated cell walls, amino acids are released from both peptidoglycan and cell wall proteins. Hence, without further information about the composition of these proteins, no accurate estimation of the degree of cross-linking between the peptidoglycan units can be obtained.

From the amino acid analysis of the *B. brevis* cell walls it is concluded that proteins give a substantial contribution to the cell wall dry weight. Beveridge ⁵ has revealed the presence of a S-layer on the surface of *B. brevis* ATCC 8246 cells by electron microscopy. An S-layer is a planar array of (glyco)proteinaceous subunits, which are situated on top of the peptidoglycan containing matrix ⁶. Our electron micrographs also showed an electron-dense layer in the outermost cell wall. The proteins in the cell wall are therefore most likely situated in the protein-rich S-layer. The strains of the genera *Corynebacterium* and *Rhodococcus* also contain cell wall polysaccharides, such as arabinose and galactose ^{2,3} (see also appendix A). Phosphate groups may be involved in the binding of the polysaccharides to the peptidoglycan matrix ¹⁸. The relatively low amounts of total phosphate in the isolated cell walls indicate that teichoic acid is not an important cell wall component. Cell walls, which lack teichoic acid often contain high concentrations of neutral polysaccharides ²⁷. X-ray photoelectron spectroscopy studies of isolated walls and whole cells of the coryneform bacteria show that the polysaccharides may determine 30 to 40 % of the cell wall dry weight ⁹.

The coryneform bacteria all contain mycolic acid (long-chain 2-alkyl-3-hydroxy-acid²⁰) in their cell walls. Estimates of the number of carbon atoms in the mycolic acids of the four coryneforms have been given by Bendinger et al.^{2, 3}. So far, the mycolic acid fraction in the cell walls has not been quantified. However, the strong hydrophobic characteristics^{3, 29} and the high C-H content of the cell surfaces of all four coryneforms⁹ indicate that the mycolic acids may give an important contribution to the cell wall dry weight.

Conclusions

The D configuration of the lactic acid is a unique cell wall constituent and therefore a good probe for the quantitative determination of muramic acid in whole cells and isolated walls. The proposed method for determining the wall content in bacterial cells is not restricted to Gram-positive strains, but is generally applicable, as peptidoglycan is a cell wall component of all procaryotic organisms²³. Accurate information about the cell wall composition and the wall fraction in bacterial cells is of relevance for physico-chemical studies, including determination of the cell wall charge and heavy metal uptake by bacterial cells.

In principle, the proposed method allows determination of D-lactate concentrations in systems such as the soil, lake water or biofilters, which can be used as an indicator for the growth of bacterial cells.

Appendix A

strain	glycolyl type of peptidoglycan	arabino-galactan	fatty acids	mena-quinones	main polar lipids
<i>Rhodococcus erythropolis</i> A177	+	+	S, U, T	MK-8(H ₂)	DPG, PE, PI, PIM
<i>Rhodococcus opacus</i> C125	+	+	S, U, T	MK-8(H ₂)	DPG, PE, PI, PIM

Results of the chemotaxonomical analysis of the strains *Rhodococcus erythropolis* A177 and *Rhodococcus opacus* C125. **fatty acids**: S, straight chain, saturated; U, straight chain, mono-unsaturated; T, tuberculostearic acid; **mena-quinones**: The number of isoprenyl groups in the side chain and the number of hydrogenated double bonds are indicated. **polar lipids**: DPG, diphosphatidylglycerol; PI, phosphatidylinositol; PIM, phosphatidylinositolmannoside; PE, phosphatidylethanolamine. For further information see 2, 14.

Acknowledgement

The authors thank Dr. S. Klatte for the identification of the strains *Rhodococcus erythropolis* A177 and *Rhodococcus opacus* C125, Wim Roelofsen for the amino acid analysis, Francis H. M. Cottaar for preparing the electron micrographs and Dr. P. G. Rouxhet for delivering the *B. brevis* strain. The helpful discussions with Dr. Æ. de Groot, Dr. L. K. Koopal and Dr. J. P. Roozen are recognized. This research was funded by grant C6/8973 from The Netherlands Integrated Soil Research Program.

References

1. **Bartlett, G. L.** 1959. Phosphorus assay in column chromatography, *J. Biol. Chem.* **234**, 466-468.
2. **Bendinger, B., R. M. Kroppenstedt, S. Klatte, K. Altendorf** 1992. Chemotaxonomic differentiation of Coryneform bacteria, *Int. J. Syst. Bacteriol.* **42**, 474-486.
3. **Bendinger, B., H. H. M. Rijnaarts, K. Altendorf, A. J. B. Zehnder** 1993. Physicochemical cell surface and adhesive properties of coryneform bacteria related to the presence and chain length of mycolic acids., *Appl. Environ. Microbiol.* **59**, 3973-3977.
4. **Benson, J. R.** 1973. Applications of the newer techniques of analysis, In *Applications of the newer techniques of analysis*, I. L. Simmons, G. W. Ewing, Eds. Plenum Publishing Corp., New York, 223.
5. **Beveridge, T. J.** 1990. Mechanism of gram variability in select bacteria, *J. Bacteriol.* **172**, 1609-1620.
6. **Beveridge, T. J., L. L. Graham** 1991. Surface layers of bacteria, *Microbiol. Rev.* **55**, 684-705.
7. **Bligh, E. G., W. J. Dyer** 1959. A rapid method of total lipid extraction and purification., *Can. J. Biochem. Physiol.* **37**, 911-917.
8. **Cummins, C. S., H. Harris** 1956. The chemical composition of the cell-wall in some Gram-positive bacteria and its possible value as a taxonomic character, *J. Gen. Microbiol.* **14**, 583-600.
9. **Dufrene, Y., A. Van der Wal, P. G. Rouxhet** To be published. XPS analysis of isolated walls and whole cells of five Gram-positive strains.
10. **Goodfellow, M.** 1992. The family Nocardiaceae, In *The prokaryotes, 2nd ed.*, A. Balows, H. G. Trüper, M. Dworkin, W. Harder, K. H. Schleifer, Eds. Springer-Verlag, New, York, 1188-1213.
11. **Hadzija, O.** 1974. A simple method for the quantitative determination of muramic acid, *Anal. Biochem.* **60**, 512-517.

12. **Keddie, R. M., G. L. Cure** 1977. The cell wall composition and distribution of free mycolic acids in named strains of coryneform bacteria and in isolates from various natural sources., *J. Appl. Bacteriol.* **42**, 229-252.
13. **Keddie, R. M., G. L. Cure** 1978. Cell wall composition of coryneform bacteria, In *Coryneform bacteria*, I. J. Bousfield, A. G. Calley, Eds. Academic press, London, 47-83.
14. **Klatte, S., R. M. Kroppenstedt, F. A. Rainey** 1994. *Rhodococcus opacus* sp. nov., an unusual nutritionally versatile *Rhodococcus* species., *System. Appl. Microbiol.* **17**, 355-360.
15. **Koch, A. L.** 1990. Growth and form of the bacterial cell wall, **78**, 327-341.
16. **Marquis, R. E.** 1968. Salt-induced contraction of bacterial cell walls, *J. Bacteriol.* **95**, 775-781.
17. **Matteo, C. C., M. Glade, A. Tanaka, J. Piret, A. L. Demain** 1975. Microbiological studies on the formation of gramicidin S synthetases, *Biotechn. Bioeng.* **17**, 129-142.
18. **Mc Neil, M., M. Daffe, P. J. Brennan** 1990. Evidence for the nature of the link between the arabinogalactan and peptidoglycan of mycobacterial cell walls., *J. Biol. Chem.* **265**, 18200-18206.
19. **Gerhardt, P, Murray, R. G. E., Costilow, R. N., Nester, E. W., Wood, W. A., Krieg, N. R., G. Briggs Phillips** 1981. Manual of Methods for General Bacteriology. American society for microbiology, Washington, DC.
20. **Minnikin, D. E., M. Goodfellow, M. D. Collins** 1978. Lipid composition in the classification and identification of coryneform and related taxa, In *Coryneform bacteria*, I. J. Bousfield, A. G. Calley, Eds. Academic Press, London, 85-160.
21. **Rogers, H. J., H. R. Perkins, J. B. Ward** 1980. Microbial cell walls and membranes, Chapman and Hall, London, New York.
22. **Salton, M. R. J.** 1964. The bacterial cell wall, Elsevier publishing company, Amsterdam, London, New York.
23. **Schleifer, K. H., O. Kandler** 1972. Peptidoglycan types of bacterial cell walls and their taxonomic implications, *Bacteriol. Rev.* **36**, 407-477.
24. **Schraa, G., M. L. Boone, M. S. Jetten, A. R. W. Van Neerven, P. J. Colberg, A. J. B. Zehnder** 1986. Degradation of 1,4-dichlorobenzene by *Alcaligenes* sp. strain A175., *Appl. Environ. Microbiol.* **52**, 1374-1381.
25. **Shockman, G. D., J. J. Kolb, G. Toennies** 1957. Relation between bacterial cell wall synthesis growth phase, and autolysis, *J. Biol. Chem.* **230**, 961-977.
26. **Spackman, D. H., W. H. Stein, S. Moore** 1958. Automatic reducing apparatus for use in the chromatography of amino acids, *Anal. Chem.* **30**, 1190.
27. **Takeuchi, M., A. Yokota** 1989. Cell-wall polysaccharides in Coryneform bacteria, *J. Gen. Appl. Microbiol.* **35**, 233-252.
28. **Tipper, D. J.** 1968. Alkali-catalyzed elimination of D-lactic acid from muramic acid and its derivatives and the determination of muramic acid., *Biochem.* **7**, 1441-1449.

29. **Van der Wal, A., W. Norde, J. Lyklema, A. J. B. Zehnder** 1996. Determination of the total charge in the cell walls of Gram-positive bacteria, chapter 3, this thesis.

Chapter 3

Determination of the total charge in the cell walls of Gram-positive bacteria.

Abstract

The charge in the bacterial wall originates from the dissociation of acidic groups such as carboxyl, phosphate and amino groups. The degree of dissociation of these chargeable groups is a function of the pH and the activity of the surrounding electrolyte solution. In this study the cell wall charge density of Gram positive bacterial strains, including four coryneforms and a *Bacillus brevis* is assessed by proton titrations of whole bacterial cells and isolated cell walls at different electrolyte concentrations. At neutral pH rather high values between 0.5 and 1.0 C/m² for the cell wall charge density are found. The titration curves for the isolated cell walls are free of hysteresis allowing a rigorous (thermodynamic) analysis. For the coryneform bacteria these curves have a common intersection point between pH 3-4, which is identified as the point of zero charge. The carboxyl and phosphate groups are titrated in distinct pH regions, allowing accurate estimation of their numbers. These numbers compare very well with those based on a chemical analysis of the isolated cell walls. The uncertainty in the estimated number of amino groups is somewhat higher, because these groups are only partly titrated within the pH range accessible by proton titrations.

At electrolyte concentrations below 0.01 M maximum expulsion of co-ions from the cell walls already occurs at relatively low charge densities. At these low electrolyte concentrations the compensating countercharge predominantly consists of counterions that penetrate into the porous cell wall matrix and to a much lower and constant extent by the exclusion of co-ions.

This latter observation considerably facilitates the interpretation of electrokinetic properties of bacterial suspensions such as measured in conductivity and micro-electrophoresis studies.

Introduction

All bacterial cells are surrounded by a porous three-dimensional macromolecular network, which is generally known as the bacterial cell wall or cell envelope. The chemical composition of bacterial walls has been well studied^{17-19, 27}. An important cell wall polymer is peptidoglycan, which is commonly present in the walls of both Gram-positive and Gram-negative bacteria. Gram-positive cell walls

generally contain high peptidoglycan concentrations, whereas in the case of the more complex envelopes of Gram-negative cells this peptidoglycan is restricted to a thin layer between the cytoplasmic and the outer membrane.

Besides peptidoglycan many other macromolecules may be present in the cell wall, including teichuronic acid, (lipo-) teichoic acid, (lipo-) polysaccharides, (lipo-) proteins, enzymes, and mycolic acids. Most of these macromolecules are polyelectrolytes, because they carry charged groups such as carboxyl-, phosphate- or amino groups. The presence of anionic and cationic groups gives the bacterial wall amphoteric properties, which implies that, depending on the pH, the net charge in the wall can be either positive, negative or zero.

Several methods have been proposed to determine the concentrations of the positive and negative groups in the bacterial wall. Among these are: titration of preheated cells with polyelectrolytes ²³, chemical modification of free carboxyl and amino groups in the wall with reactive agents like hydrazine, carbodiimide, diazomethane and fluorodinitrobenzene ^{13, 20}, binding of dyes such as safranin and orange G that are specific for carboxyl and amino groups, respectively ⁴ or potentiometric proton titrations of isolated cell walls ^{3, 4, 13}. All these studies show that in the bacterial cell wall the anionic groups dominate over the cationic groups. This seems to be a general phenomenon and it is in agreement with the observation that most bacterial cells have isoelectric points below pH 4 ⁷.

The rigidity of the cell wall is related to the thickness of the peptidoglycan layer, which has to resist the osmotic pressure. This rigidity is the reason why isolated walls retain their original shapes ¹⁹. More recently, it has been observed that cell walls are elastic, flexible, gel-like structures, that can swell or shrink in radial but not in tangential direction ⁵. It has been shown that the net charge density in the bacterial wall strongly affects its thickness ^{11, 15}.

The chemical affinity of both protons and hydroxide ions for the weak acid and base groups in the bacterial wall is the driving force for the formation of the cell wall charge. These ions are therefore called charge-determining ions. The chemical affinity can be quantified in terms of the intrinsic dissociation constants (pK_a 's) of the weak acid and base groups.

The dissociation and protonation of the acid and base groups in the bacterial wall by the charge-determining ions leads to the spontaneous formation of an electrical double layer. The compensating charge consists of counterions that may penetrate into the porous cell wall matrix, and of co-ions that are expelled from it. This latter phenomenon leads to an increase of the neutral electrolyte

concentration in the solution surrounding the bacterial wall. This is a manifestation of the Donnan effect.

Among the various techniques that can be applied to obtain information on the electrical properties of bacterial cell walls, micro-electrophoresis is most widely used. This electrokinetic technique certainly gives valuable information on the electrokinetic behaviour of bacterial cells. However, in addition to the ζ -potential information about other properties such as the total cell wall charge is needed for a more complete characterization of the electrical double layer of bacterial cell surfaces.

Moreover, interpretation of the electrophoretic mobility in terms of ζ -potential and electrokinetic charge is a complicated task due to the unknown position of the plane of shear and the influence of the mobile countercharge on the effective mobility of the cells. In this respect, static conductivity and dielectric dispersion measurements give additional information about the composition of and ion mobilities in the electrical double layer. We will discuss these subjects in chapter 4 and 5.

For colloidal particles potentiometric and conductometric proton titrations are commonly used to assess the surface charge density. These techniques can also be applied directly to whole bacterial cells, provided leakage of protons through the cytoplasmic membrane is prevented.

In this paper we show that the surface charge density of bacterial cells can be successfully estimated by potentiometric proton titrations of isolated cell wall fragments. We applied this method to Gram-positive bacterial cells including four coryneform bacteria and a *Bacillus brevis* strain. Analysis of the titration curves provides information about the number of carboxyl, phosphate and amino groups in the bacterial wall. These numbers are compared with those estimated by chemical analysis of the isolated cell walls.

The position of the point of zero charge (p.z.c.) appears to be within the pH-range accessible by proton titrations; this allows the determination of the absolute charge density in the bacterial wall. From Esin-Markov and Henderson-Hasselbalch analyses additional information is obtained on the composition of the electrical double layer of bacterial cell surfaces.

Materials and Methods

Bacterial cultivation and preparation

Rhodococcus erythropolis A177 and *Rhodococcus opacus* C125 were cultivated in a mineral medium described by Schraa et al.²² however without adding yeast extract. Ethanol (50 mM) was used as the sole carbon and energy source. *Corynebacterium* sp. strain DSM 6688 and *Corynebacterium* sp. strain DSM 44016 were cultivated in brain heart infusion broth (Merck, 40 g/l deionized water). *Bacillus brevis* ATCC 9999 was cultivated in (g/l): 2.2 NH₄Cl, 0.27 KH₂PO₄, 0.05 KNO₃, 0.2 MgCl₂·6H₂O, 0.06 CaCl₂·2H₂O, 0.01 FeCl₃·6H₂O, 0.35 MgSO₄·7H₂O, 7.5 casamino acids and 2.5 glycerol. Trace elements (1ml/l) and vitamins solution (1 ml/l) were added.²²

The bacterial cells were grown at 30 °C on a rotary shaker and harvested in the early stationary phase by centrifugation for 10 min at 20,000 x g at 4 °C. The cells were washed three times in deionized water.

Cell wall isolation

A French pressure cell was used to disrupt the cells of the coryneforms at a pressure of 20,000 psi and those of *B. brevis* at 15,000 psi. Guanidinium hydrochloride (4 M) was added in order to inactivate autolytic enzymes and to remove the cytoplasmic membrane. The cell wall fraction was obtained by centrifugation, whereafter it was washed several times in 1 M KNO₃ and in demineralised water.

Electron micrographs showed the cell wall preparation to be free of whole cells. During the isolation procedure most of the membrane fragments were removed, which could be deduced from the very low phospholipid concentration in the isolated cell wall samples. Further details of the isolation procedure are described by²⁷.

Cell wall proteins. The presence of removable cell wall proteins was checked by incubating whole cells for 20 minutes at room temperature in 0.2 g/l Tween 20. After centrifugation, the protein concentration in the supernatant was determined with Coomassie brilliant blue G250 as described by Bradford².

Contact angle measurements. The contact angles of water droplets on air-dried bacterial lawns were measured according to the method of Van Loosdrecht et al.²⁸.

Surface/cell wall mass ratio. The cell surface area was determined by two methods: (a) light microscopy and (b) dynamic light scattering. The cell mass was determined by weighing a freeze-dried cell suspension of which the concentration of the cells was determined by counting the cells in a count chamber. The contribution of the wall mass to the total dry weight of a bacterial cell is determined by a method discussed elsewhere.²⁷

Cell wall volume. The cell wall volume was determined by measuring the sedimentation volume after five days in 0.1 M to 1.0 M KNO₃ solutions.

Potentiometric proton titration

All titrations were performed in KNO₃ solutions at 25 °C under flushing with nitrogen using a fully automatic TPC 2000 system (Schott-Nederland) and a pH-glass electrode (Metrohm). The electrode was calibrated over the entire pH-range 2-11.

All cell wall titrations were accompanied by blanc titrations under the same conditions. The ratio between the total volume of titrant needed for the cell walls and the blanc titrations was at least 2:1. The binding of protons and hydroxide ions to the cell walls at a given pH was determined by subtracting the amount of titrant needed for the blanc titrations from those of the cell wall titrations, after correction for volume changes. The amount of titrated material was determined afterwards by weighing the freeze-dried material. The wet cell walls were titrated immediately after isolation, although in some cases they were first stored at -20 °C. Such storage did not lead to noticeable different results. When dispersed in media of high electrolyte concentrations (0.1 M, 1.0 M), 0.6 - 0.8 g dry weight walls of the coryneform bacteria and 2 g dry weight walls of the *B. brevis* were titrated with 1.000 N HNO₃ and 1.000 N KOH.

At lower electrolyte concentrations (0.001M, 0.01M), about 0.2 g dry weight walls of the coryneform bacteria and 0.7 g dry weight walls of the *B. brevis* were titrated with 0.1000 N HNO₃ and 0.1000 N KOH in a pH-range from about 3 to about 10. In all cases the ionic strength was approximately constant during the acid and base titrations. Titrant was added when dpH/dt was less than 0.002 pH units per min. The change in pH was about 1 unit in 30 minutes. The total volume of titrant added during one titration was always less than 10% of the total volume in the cell. For the establishment of the relative positions of the titration curves at different salt concentrations, cell walls were suspended in 0.001 M electrolyte solution and stepwise titrated with KNO₃ up to 1 M electrolyte solution. Increase of the concentration of indifferent electrolyte leads to an concomitant increase of the total

cell wall charge due to improvement of the screening. For those pH-values where the net cell wall charge is negative, protons are released from the wall if the electrolyte concentration is increased, which is measured as a downward pH shift. Similarly, if the net cell wall charge is positive then the pH shifts to higher values. For all five strains salt titrations were performed at pH 3, 4, 5, 6 and 7.

Titration of whole cells of *Rhodococcus erythropolis* were carried out between pH 4 and 10 at 0.1 M KNO₃ under flushing with nitrogen. The cells were titrated at different rates ranging from about one pH unit per 1.5 min to about one pH unit per 100 min. Cells were titrated immediately after harvesting in order to retain some physiological activity. The amount of cells used corresponded to about 0.662 g dry weight.

Results and Discussion

Chemical composition of the cell walls

A detailed description of the chemical composition of the walls of the bacterial cells used in this study is given elsewhere²⁷. The results of that study are briefly summarized. Peptidoglycan is an important constituent of the walls of the coryneforms. It accounts for about 23-31 % of the total dry weight. The peptidoglycan structure of *Corynebacterium* sp. strain DSM 44016, *Corynebacterium* sp. strain DSM 6688 and *B. brevis* is most likely a composition of N-glycolyl-glucosamine, N-acetyl-muramic acid, D-lactate, D- and L-alanine, D-glutamic acid and meso-diaminopimelic acid. The peptidoglycan composition of *Rhodococcus erythropolis* A177 and *Rhodococcus opacus* C125 is almost identical to that of the corynebacteria and *B. brevis*, except that the peptide string is attached to N-glycolyl-muramic acid instead of N-acetyl-muramic acid. The ratio

strain	cell wall to cell mass ratio	peptidoglycan fraction in isolated cell walls	protein fraction in isolated cell walls	No. of carbon atoms in mycolic acid ¹
<i>Corynebacterium</i> sp. strain DSM 44016	32%	23%	14%	34-40
<i>Corynebacterium</i> sp. strain DSM 6688	27%	27%	14%	32-36
<i>Rhodococcus erythropolis</i> A177	26%	24%	10%	34-48
<i>Rhodococcus opacus</i> C125	29%	31%	7%	44-56
<i>Bacillus brevis</i>	75%	5%	56%	—

Table 1: Cell wall composition. ¹ Results taken from Bendinger et al. ¹ (with permission).

of the carboxyl and amino groups in the primary peptidoglycan structure is 3 to 1. The amount of protein in the cell walls of the coryneforms ranges between 7-14% of the total dry weight. The mycolic acids present in the walls of all four coryneforms do not contribute to the cell wall charge.

The peptidoglycan layer of *B. brevis* is relatively thin and amounts to only about 5% of the cell wall dry weight. On top of the peptidoglycan layer there is a thick protein-rich surface layer, the so called S-layer. The contribution of proteins to the cell wall weight is approximately 56%.

The cell wall composition and the cell wall to cell mass ratio of the bacteria used in this study are summarized in table 1.

Purity of the cell wall samples

There are several proofs that the isolated walls resemble those of the whole cells. As can be seen in table 2, the isoelectric points (i.e.p.) of the cell walls are very close to those for the corresponding whole cells, except in the case of

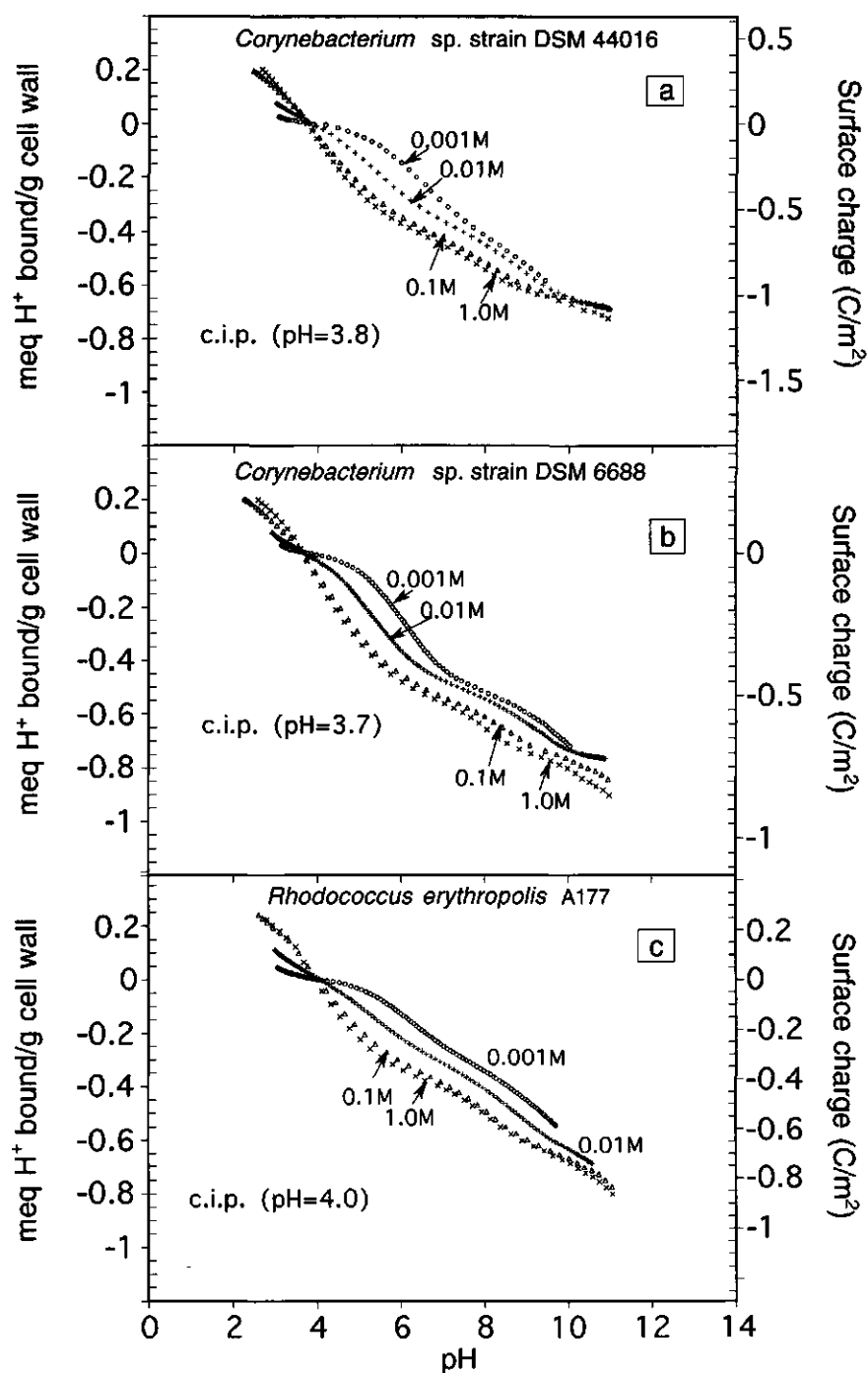
strain	isolated walls			whole cells	
	pH-i.e.p.	pH-c.i.p.	C.A.	pH-i.e.p.	C.A.
<i>Corynebacterium</i> sp. strain DSM 44016	3.3	3.8	95	3.6	103
<i>Corynebacterium</i> sp. strain DSM 6688	3.4	3.7	100	3.2	89
<i>Rhodococcus</i> <i>erythropolis</i> A177	4.1	4.0	70	<2.0	87
<i>Rhodococcus opacus</i> C125	3.6	4.1	68	3.4	70
<i>Bacillus brevis</i>	4.7	5.1	43	4.6	50

Table 2: Comparison between some properties of the isolated walls with those of whole cells. i.e.p.: isoelectric point, c.i.p.: common intersection point and C.A.: (water) contact angle.

Rhodococcus erythropolis A177. Rijnaarts et al. ¹⁶ deduced from adhesion experiments that a thin polysaccharide layer may be present on the cell wall surface of *Rhodococcus erythropolis* A177. It could well be that this layer is removed from the cell wall during the isolation procedure. In this respect it is striking that the i.e.p. of mutated cells of *Rhodococcus erythropolis*, is at pH 3.5, which is close to that for the isolated walls. This observation suggests that these mutants have lost their polysaccharide layer.

The water contact angles measured for whole cells and isolated walls are rather close (table 2), which is another indication that the chemical compositions of isolated walls are similar to those of the whole cells.

There are no indications of removable cell wall proteins.



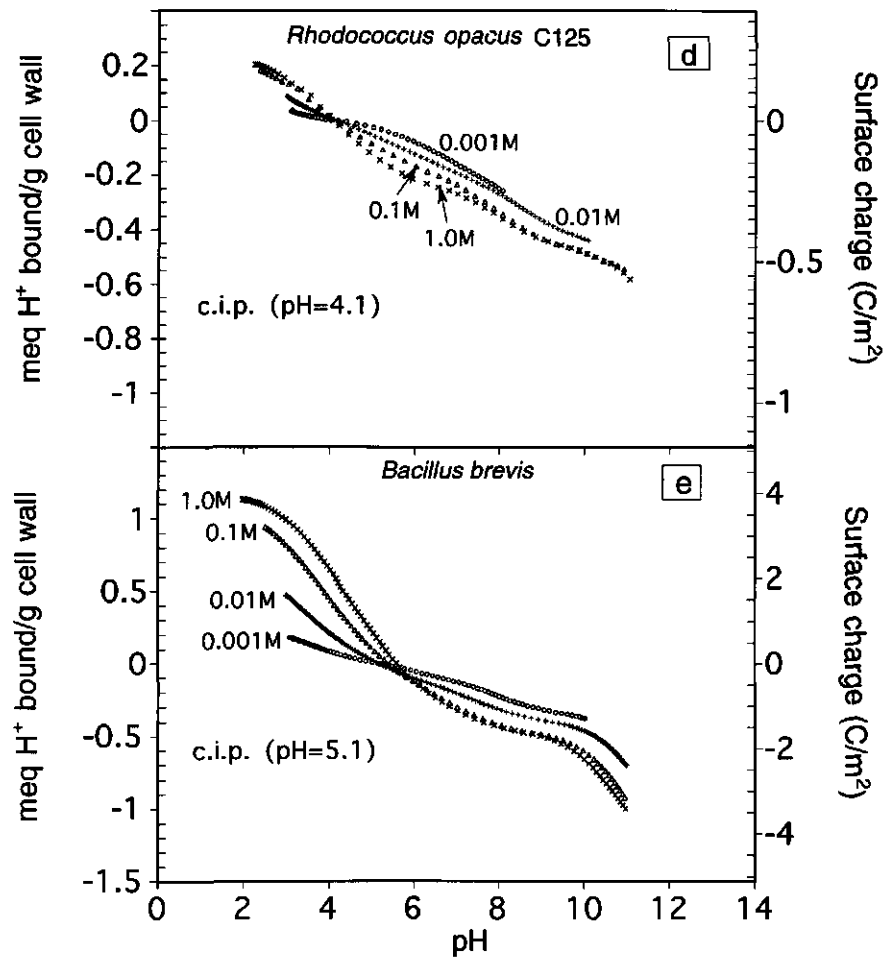


Figure 1: Proton titration curves for isolated walls of *Corynebacterium* sp. strain DSM 44016 (a), *Corynebacterium* sp. strain DSM 6688 (b), *Rhodococcus erythropolis* A177 (c), *Rhodococcus opacus* C125 (d) and *Bacillus brevis* ATCC 9999 (e). (○) 0.001M, (+) 0.01M, (Δ) 0.1M, (x) 1.0M. Proton binding to the cell walls is expressed in meq/ g dry weight.

Proton titration of isolated walls

The results of the potentiometric proton titrations of isolated walls of the five Gram-positive strains are given in figs 1a-e. The acid and base titration curves appear to be free of hysteresis even when the walls are titrated rapidly, with less than 15 minutes between pH 2 and 11. This implies that the titration of the cell walls is not likely to induce irreversible structural changes. Apparently, the weak acid and base groups in the bacterial wall are readily accessible by the protons and hydroxide ions. In fact, this result is not surprising considering that the cell wall has a porous gel-like structure with a relatively high water content. The absence of hysteresis leads to the conclusion that the charging process can be considered as reversible, which implies that the cell wall charge is continually in equilibrium with the surrounding electrolyte solution at any pH and salt concentration. This observation facilitates the interpretation of the titration data, because it allows an analysis using thermodynamics for reversible processes.

Proton titration of whole bacterial cells

The results of the proton titrations of whole cells of *Rhodococcus erythropolis* A177 are given in fig. 2, where pH=4, which is the p.z.c. for the isolated walls, has been chosen as the reference point for the binding of protons to the cells. If the

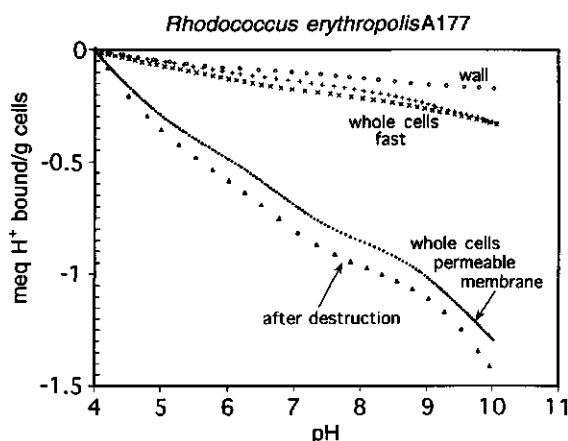


Figure 2: Proton titrations of whole bacterial cells from strain *Rhodococcus erythropolis* A177.

(o) isolated cell walls, (+) and (x) fast base and acid titrations, resp., (●) acid/base titrations after maintaining the cells for 30 h at pH 4. (Δ) acid/base titrations after disruption of the cells by French press. Proton binding in meq/g dry weight cells.

rate of titration is sufficiently high (> 1 pH unit per 1.5 min), only the outermost parts of the cells are titrated. Unlike with isolated cell walls, some hysteresis between the acid and base titrations now does occur. It is probably caused by the diffusion of protons into the cytoplasmic membrane at low pH-values and excretion

of these protons at high pH-values. However, hysteresis is neither found between the acid titrations nor between the base titrations upon repeating titration cycles, which means that the same number of anionic and cationic groups are protonated or dissociated at any titration cycle. The flux of protons into the cell interior is rather small and appears to be about $2 \mu\text{eq H}^+/\text{min g d.w. cells}$ at pH 4, which is negligible on the time scale of the fast proton titrations. Decreasing the rate of titration to one pH unit per 20 min leads to an increase of the hysteresis between the acid and base titration curves and also to an increased number of dissociable groups observed. Titration curves that have been obtained after keeping the cells for several hours (>30 h) at pH 4 show a further increase of the number of chargeable groups, but neither is hysteresis found between acid and base titrations nor between fast (1 pH unit per 1.5 min) and slow (1 pH unit per 100 min) titrations. Moreover, these curves almost coincide with those obtained after destruction of the cells by French press. These results suggest that the cytoplasmic membrane becomes permeable to protons upon exposing the cells to extreme pH values.

Comparison between the fast titration curves with those for the isolated walls, included in fig. 2, shows that in the first case more groups are titrated than those situated in the cell wall only. This difference is probably due to the dissociation and protonation of acid and base groups in the cytoplasmic membrane, which mainly originate from membrane proteins and/or some phospholipids. Especially those groups that are situated in the exterior of the membrane are readily accessible to protons and hydroxide ions. Therefore, estimates of the cell surface charge based on fast proton titrations of whole bacterial cells are expected to be higher than those based on titrations of isolated walls. These complications limit the analysis of the titration curves of whole cells. Nevertheless, fast proton titrations with whole cells may be used as a relatively easy and fast method to obtain semiquantitative information on the cell surface charge density.

Cell wall surface charge

The degrees of dissociation of the carboxyl, amino and phosphate groups in the bacterial wall depend on the pH of the electrolyte solution. The cell wall surface charge density, σ_o , can be directly determined from the difference of the absorbed amounts of protons and hydroxide ions. It is operationally given by:

$$\sigma_o \equiv F (\Gamma_{\text{HNO}_3} - \Gamma_{\text{KOH}}) \quad (1)$$

in which F is Faraday's constant. Γ_{HNO_3} and Γ_{KOH} are the amounts of HNO_3 and KOH absorbed per unit area, respectively.

The absorption of a hydroxide ion in the bacterial wall is effectively the same as the removal of a proton from one of the acidic groups. Therefore, the degree of dissociation is decreased by the absorption of protons and increased by the absorption of hydroxide ions. For colloidal particles the surface charge is usually expressed per unit area. We follow this custom, although it is realized that the surface charge is not restricted to the surface proper, but to a layer which has some depth. The specific surface area is obtained from the cell dimensions and the wall/ cell mass ratio (tables 1 and 3).

strain	Length μm	width μm	d_{cw} nm	S.A. $\text{m}^2/\text{g d.w. wall}$	wall volume ml/g d.w. wall
<i>Corynebacterium</i> sp. strain DSM 44016	1.1	0.8	60 ± 10	61.5	3.7
<i>Corynebacterium</i> sp. strain DSM 6688	2.0	0.7	35 ± 5	102.5	3.6
<i>Rhodococcus</i> <i>erythropolis</i> A177	3.2	1.2	35 ± 5	89.8	3.1
<i>Rhodococcus opacus</i> C125	2.9	1.3	35 ± 5	100.0	3.5
<i>Bacillus brevis</i>	6.0	1.0	75 ± 25	28.3	2.1

Table 3: Estimations of the surface area of the bacterial cells and the cell wall volume. d_{cw} = cell wall thickness, estimated from electron micrographs, S.A. = surface area.

As swelling and shrinking occurs essentially only in radial direction, it may therefore be assumed that the cell wall surface area is approximately constant over the entire titration curves.

The space charge density can be calculated from the surface charge density provided the cell wall thickness and the charge distribution are known.

Esin-Markov analysis

The cell wall charge, σ_o , is not only determined by the pH, but also by the activity of the carrier electrolyte, because its ions screen the lateral interactions between neighbouring charged groups. Therefore, at a given pH, the net cell wall charge increases with increasing electrolyte concentration.

To characterize this influence of electrolyte concentrations on the composition of the electrical double layer the Esin-Markov coefficient (β) has been introduced. For the present system it is defined as ⁹:

$$\beta \equiv \left(\frac{\partial \text{pH}}{\partial \log a_{\pm}} \right)_{\sigma_0} \quad (2)$$

where a_{\pm} is the mean activity of the electrolyte. The Esin-Markov coefficient is an experimentally accessible parameter and equal to the horizontal (i.e. at constant charge) distance between the titration curves at different salt concentrations. Based on thermodynamic arguments it can be shown⁹ that for a 1-1 electrolyte

$$\beta = -1 - 2 \left(\frac{\partial \sigma_-}{\partial \sigma_0} \right)_{a_{\pm}} = 1 + 2 \left(\frac{\partial \sigma_+}{\partial \sigma_0} \right)_{a_{\pm}} \quad (3)$$

where $-\partial \sigma_- / \partial \sigma_0$ and $-\partial \sigma_+ / \partial \sigma_0$ are the differential fractions of the surface charge that is compensated by anions and cations, respectively.

The ionic components of charge, σ_- and σ_+ can be determined by integrating equation (3). Assuming that in the p.z.c. $\sigma_- = \sigma_+ = 0$, we obtain:

$$\sigma_{\pm} = -\frac{1}{2} \sigma_0 \pm \frac{1}{2} \int_0^{\sigma_0} \beta \, d\sigma_0 \quad (4)$$

It appears that for the cell walls of the coryneform bacteria the titration curves at the four electrolyte concentrations have a common intersection point (c.i.p.), which is located between pH 3.7 and 4.1 (see table 2). In the c.i.p. the Esin-Markov coefficient is zero, so that $(\partial \sigma_- / \partial \sigma_0)_{a_{\pm}} = (\partial \sigma_+ / \partial \sigma_0)_{a_{\pm}} = -1/2$, which means that close to the c.i.p. the excess of counterions and the deficit of co-ions equally contribute to the countercharge. Coincidence of the c.i.p. with the i.e.p. indicates that the c.i.p. occurs at the point of zero charge (p.z.c.)¹⁰. In those cases no specific adsorption of ions takes place so that the distribution of the countercharge is solely determined by electrostatics. For the coryneforms, except for *Rhodococcus erythropolis*, the i.e.p.'s seem to be at slightly lower pH values than the c.i.p.'s, which indicates the occurrence of some specific adsorption of nitrate ions to the hydrophobic cell wall material. Unfortunately, the exact positions of the i.e.p.'s are somewhat uncertain due to the formation of aggregates at pH-values close to those of the i.e.p.'s. Despite the remaining uncertainty in locating the exact position of the p.z.c., we have chosen the c.i.p. as the reference point for the charge formation, when representing the titration curves for the coryneforms in figs 1a-e.

The titration curves of the cell walls of *B. brevis* do not show a well defined c.i.p. In this case we have chosen the intersection point of the titration curves at 0.001M and 0.01M as the reference point, because at low salt concentrations the shift of the p.z.c. due to specific adsorption of anions is relatively small. As can be seen in table 2 this intersection point is indeed close to the i.e.p.

According to equation 3 the Esin-Markov coefficient equals -1 in those cases where the countercharge is totally determined by cations and $+1$ if only anions compensate the cell wall charge. However, these extreme values are only attained if the cell wall charge is sufficiently high and if strong specific interactions of NO_3^- and K^+ ions, respectively are absent. We determined the Esin-Markov coefficient for that part of the titration curves where the shift in the pH due to increasing salt concentrations has been directly measured (pH 3-7). The Esin-Markov coefficient is graphically displayed in fig. 3 for *Corynebacterium* sp. strain DSM 44016. For

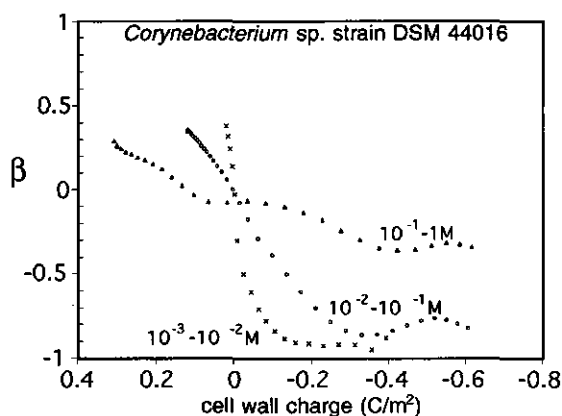


Figure 3: The Esin-Markov coefficient (β) as a function of the pH for the cell walls of *Corynebacterium* sp. strain DSM 44016.

the coryneforms and the *B. brevis* the Esin-Markov coefficients reach a plateau value for negatively charged surfaces, which is almost equal to -1 , for electrolyte concentrations lower than 0.1 M. Physically this means that then most of the negative cell wall charge is compensated by potassium ions and that the negative adsorption of anions only slightly contributes to the countercharge (see figs 4a-e). At higher salt concentrations the Esin-Markov coefficient is less negative, implying that the contribution of excluded nitrate ions to the compensating cell wall charge is higher; more nitrate ions can be expelled from the porous cell wall structure if

the nitrate concentration in solution increases. At high salt concentrations both co- and counterions may therefore equally contribute to the countercharge.

For positively charged cell walls the plateau value of +1 is only obtained for *B. brevis*. For the coryneforms the pH range below the p.z.c., that can be studied is rather small and as a consequence no plateau value could be reached for the Esin-Markov coefficients.

The absolute values of the Esin-Markov coefficients for *B. brevis* at pH-values below the p.z.c. are comparable with those for negatively charged walls and the explanation, given above, also applies, *mutatis mutandis*, for the positively charged wall. At high salt concentrations the Esin-Markov coefficient has a rather high value, which indicates that even in excess electrolyte solution the positive cell wall charge is still predominantly compensated by nitrate ions and to a lesser extent by the negative adsorption of potassium. Apparently at pH-values below the p.z.c. lateral interactions between neighbouring groups still occur, even at high salt concentrations.

The compositions of the countercharge, according to the Esin-Markov analysis, are graphically displayed in figs 4^{a-e}. These graphs show that for salt concentrations up to 0.1 M already at relatively low cell wall charge densities maximum expulsion of co-ions from the cell wall matrix occurs. At salt concentrations lower than 0.01 M the countercharge mainly consists of counterions, whereas the co-ions hardly contribute.

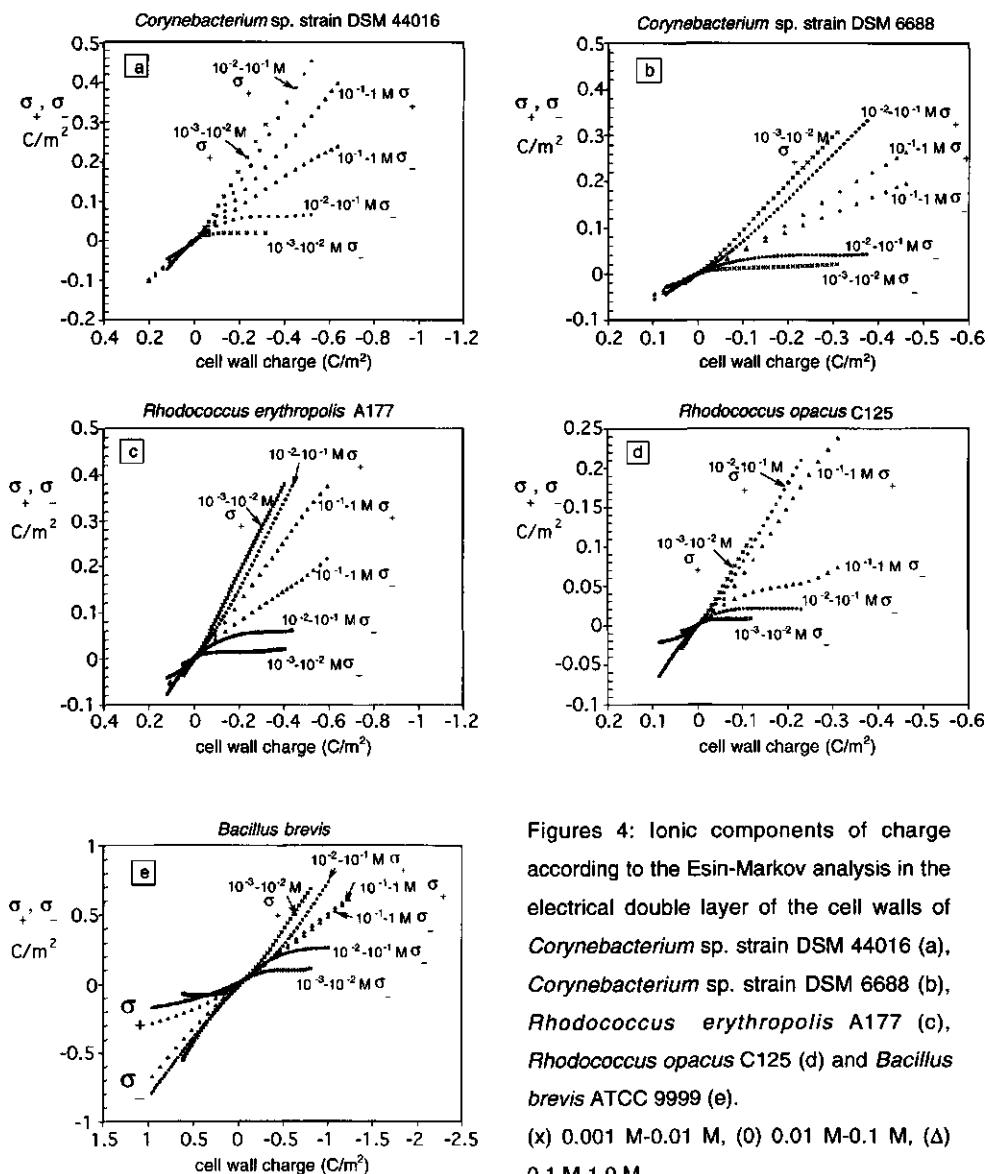
Titratable cell wall groups

The charge in the bacterial wall is determined by the dissociation or protonation of the acid and base groups. The following reactions are likely to occur:



in which L generally represents that part of the cell wall structure to which the titratable group is chemically bound.

Based on reversible titration behaviour we can write the corresponding equilibrium equations:



$$K_{L-\text{COOH}}^{\text{eff}} = \frac{[L-\text{COO}^-] a_{\text{H}^+}}{[L-\text{COOH}]} \quad (9)$$

$$K_{L-\text{NH}_3^+}^{\text{eff}} = \frac{[L-\text{NH}_2] a_{\text{H}^+}}{[L-\text{NH}_3^+]} \quad (10)$$

$$K_{L_2-\text{HPO}_4}^{\text{eff}} = \frac{[L_2-\text{PO}_4^-] a_{\text{H}^+}}{[L_2-\text{HPO}_4]} \quad (11)$$

$$K_{L-\text{H}_2\text{PO}_4}^{\text{eff}} = \frac{[L-\text{HPO}_4^-] a_{\text{H}^+}}{[L-\text{H}_2\text{PO}_4]} \quad \text{and} \quad K_{L-\text{HPO}_4}^{\text{eff}} = \frac{[L-\text{PO}_4^{2-}] a_{\text{H}^+}}{[L-\text{HPO}_4^-]} \quad (12a,b)$$

in which the proton activity in the surrounding electrolyte solution, a_{H^+} , and the effective dissociation constants ($K_{L-\text{COOH}}^{\text{eff}}$, $K_{L-\text{NH}_3^+}^{\text{eff}}$, $K_{L_2-\text{HPO}_4}^{\text{eff}}$, $K_{L-\text{H}_2\text{PO}_4}^{\text{eff}}$ and $K_{L-\text{HPO}_4}^{\text{eff}}$) have the same dimensions: mol/l. The titratable cell wall groups appear in equations 9-12 as cell wall concentrations. However, these groups may also be expressed in terms of activities or mole fractions.

The titration curves can be described with the above given equations 9-12, provided the effective dissociation constants and the concentrations of the different groups are known.

Generally, the effective dissociation constants of the titratable groups in the bacterial wall deviate from those in the isolated state, called K_{chem} , because of electrostatic interactions with neighbouring groups. The nature of L to which the titratable groups are chemically bound and the surrounding medium in which they are located may also contribute to the value of K_{chem} .

The Gibbs energy ($\Delta_{\text{diss}}G$) for the dissociation of a proton from a cell wall group can be divided into a chemical term (ΔG_{chem}), which contains the intrinsic contribution and all other non-electrostatic effects and an electrical term (ΔG_{el}), which originates from electrostatic interactions with surrounding charged groups.

$$\Delta_{\text{diss}}G = \Delta G_{\text{chem}} + \Delta G_{\text{el}} \quad (13)$$

The electrostatic interaction between the proton and the dissociating group is included in ΔG_{chem} . ΔG_{el} therefore represents the additional amount of reversible isothermal work required to transfer a hydrogen ion from the dissociating group in the cell wall to infinity. This electrostatic contribution is:

$$\Delta G_{\text{el}} = -F\psi \quad (14)$$

where ψ is the electrostatic potential in the cell wall at the place of the dissociating group caused by the presence of neighbouring charged groups.

The relation between the standard Gibbs energy of dissociation and the effective dissociation constant is given by:

$$\Delta_{\text{diss}} G^{\circ} = 2.303 RT \text{pK}^{\text{eff}} \quad (15)$$

where R is the gas constant. Combining equations 13, 14 and 15 and introducing:

$$\text{pK}_{\text{chem}} = \Delta G_{\text{chem}}^{\circ} / 2.303 RT \text{ results in:}$$

$$\text{pK}^{\text{eff}} = \text{pK}_{\text{chem}} - 0.434 F\psi/RT \quad (16)$$

Equation 16 formulates how the dissociation of a given cell wall group (K^{eff}) is influenced by the electrostatic potential which originates from the charged groups nearby. This electrostatic effect, which is sometimes called the polyelectrolyte effect, is measured as a shift in the effective dissociation constant to lower or higher values, depending on the sign of ψ .

Indifferent ions screen the lateral interactions between the charged cell wall groups and therefore suppress the polyelectrolyte effect. The electrical contribution to the effective dissociation constant therefore vanishes at high salt concentrations.

Titration of carboxyl-, amino- and phosphate groups

The occurrence of inflection points in the titration curves (figs 1^{a-e}) indicates distinct pH regions, where one (or more) class(es) of groups are consecutively titrated. The pH-values at which these inflection points occur can be judged more accurately from the reciprocal differential titration curves, where $\delta \text{pH} / \delta \text{meq H}^{+}$ bound is plotted vs. pH. Such curves are given in figs 5^{a-e} for the four coryneforms and the *B. brevis*. The maxima in these curves are identified as equivalence points of the titrations of certain types of cell wall groups. The minima provide information about the dissociation constants of the chargeable groups. The pH-range where a certain group is titrated depends on the concentration of indifferent electrolyte in solution. For all five bacterial strains we see that the various titration regions shift to lower pH-values at increasing salt concentrations. This shift is due to the screening of electric repulsion between the negatively charged groups in the bacterial wall. At very high salt concentrations the range of the double layer overlap is so small that the cell wall charges may be considered as individual units.

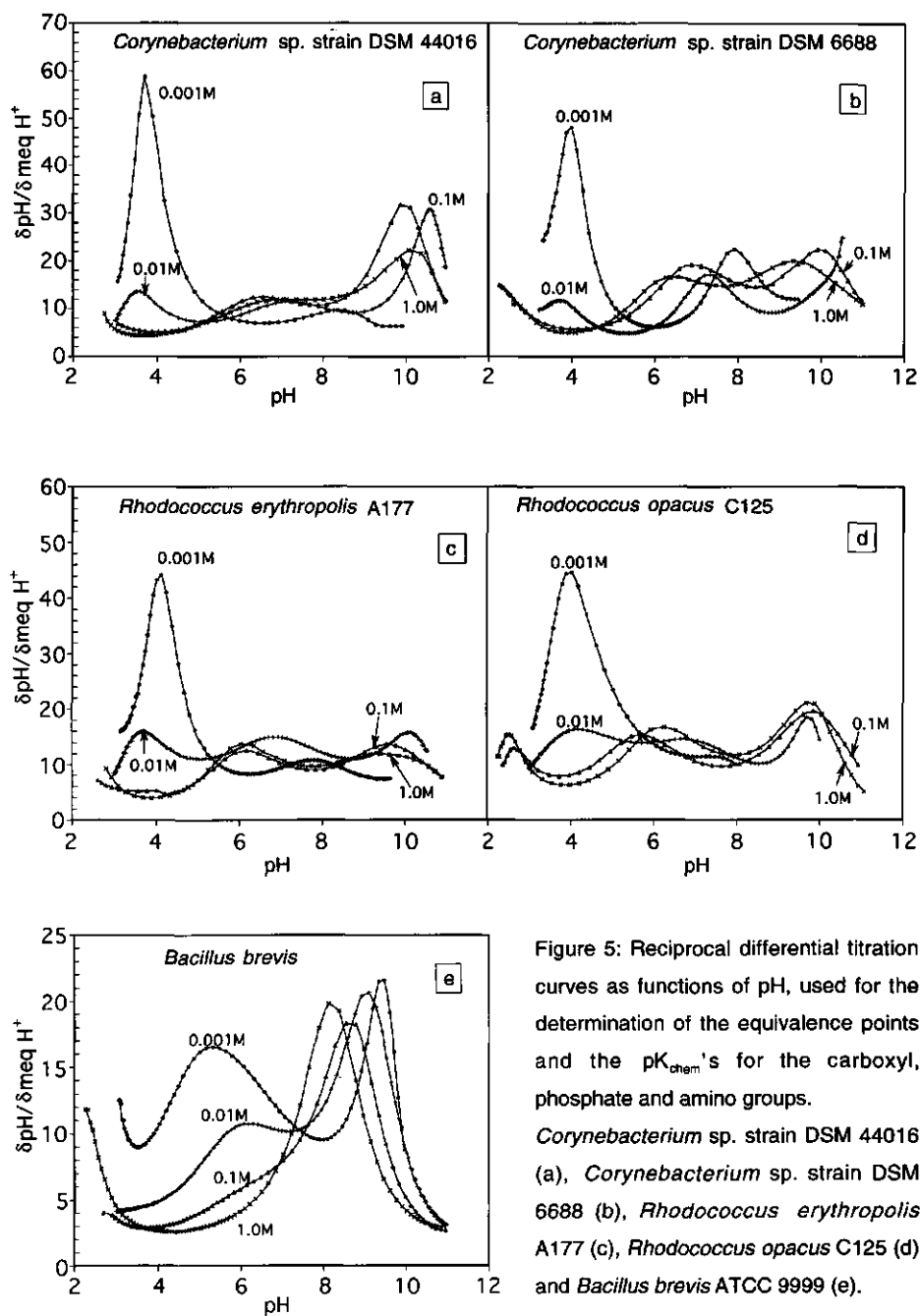


Figure 5: Reciprocal differential titration curves as functions of pH, used for the determination of the equivalence points and the pK_{chem} 's for the carboxyl, phosphate and amino groups.

Corynebacterium sp. strain DSM 44016 (a), *Corynebacterium* sp. strain DSM 6688 (b), *Rhodococcus erythropolis* A177 (c), *Rhodococcus opacus* C125 (d) and *Bacillus brevis* ATCC 9999 (e).

(○) 0.001 M, (+) 0.01 M, (Δ) 0.1 M, (×) 1.0 M.

If we assume that the polyelectrolyte effect is absent in 1 M electrolyte solution it follows from equation 16 that then $pK^{\text{off}} \approx pK_{\text{chem}}$. From figs 5^{a-e} the values of pK_{chem} for the carboxyl, phosphate and amino groups can then be identified as the pH-values at which the differential titration curves at 1 M electrolyte have their minimum values. The most left-hand minimum, which appears at pH=4.1 for the coryneform bacteria and at pH=4.7 for the *B. brevis* is identified as the pK_{chem} of the carboxyl group. For the coryneform bacteria at a pH-value of about 8 a second minimum appears, which is most likely the pK_{chem} of the dissociation of the second hydrogen ion from the phosphate group (see equation 8^b). The amino groups of the cell walls of the coryneform bacteria are titrated at pH-values higher than 10 and the value of pK_{chem} is expected to be between 11 and 12. The amino groups of the *B. brevis* wall are titrated at pH-values > 8 and the pK_{chem} is about 11. In fact, the pK_{chem} 's determined for the carboxyl, phosphate and amino groups are average values. Some groups may have slightly higher or lower values due to effects such as the hydrophobicity of the surrounding medium or the composition of the cell wall structure to which these groups are bound.

The minima in the differential titration curves should correspond with the titration of half of the cell wall groups that are titrated within that particular pH-region. For the carboxyl and phosphate groups, this appears to be the case, as can be seen from the differential titration curves as functions of the amount of protons bound to the wall (see figs 6^{a-e}), where the minima appear to be situated half-way between the bordering maxima. For the amino groups reliable information is difficult to obtain due to the uncertainty in the value of pK_{chem} .

It should be noted that for the coryneform bacteria the estimated value of the pK_{chem} for the carboxyl group is very close to the intrinsic dissociation constant for the carboxyl of the side-chain of, for instance, glutamic acid, i.e., $pK_{\text{intr}} = 4.25$. Apparently, medium effects in the wall are very similar to those in solution, which suggests that the water content in the walls of the coryneforms is rather high. The intrinsic dissociation constant of the side chain amino group of, for instance, lysine is 10.53, which is also within the range of the pK_{chem} estimated from the titration curves.

The value of pK_{chem} for the dissociation of the first hydrogen ion of the phosphate group is expected to be low. Compare for instance the intrinsic pK_a of the phospholipid phosphatidylcholine which is below 2.25⁶. So, it is likely that dissociation of this group occurs beyond the titration region investigated in this study.

The differential titration curves (fig.'s 6^{a-e}) of the coryneform bacteria and the *B. brevis* show a maximum at low salt concentration in the p.z.c. This maximum becomes less pronounced if the salt concentration increases and is completely suppressed in 0.1 M and 1.0 M electrolyte solution. This observation, which is a manifestation of the polyelectrolyte effect, can be explained as follows. Below the p.z.c. the overall potential in the bacterial wall is positive and consequently, according to equation 16, the effective dissociation constant of the carboxyl group shifts to lower values. On the other hand, above the p.z.c., the dissociation of the carboxyl groups is unfavourable. Titration therefore occurs at higher pH-values. At low salt concentration this effect is more pronounced, because the absolute value of the cell wall potential is higher. At higher salt concentrations the electrostatic interactions between the charged groups diminish and the carboxyl groups are therefore titrated in a smaller pH range.

Estimates of the amounts of carboxyl-, amino- and phosphate- groups

Comparison of the number of cell wall groups that are titrated in the different pH-regions as estimated from the differential titration curves (figs 6^{a-e}) with those obtained from the chemical analysis leads to a more complete understanding of the composition of the bacterial wall. The numbers of carboxyl and phosphate groups, which could be determined accurately, are given in table 4. Unfortunately, no precise estimations for the amino groups could be obtained, because these strongly basic groups are titrated at relatively high pH-values. It is not unlikely that at pH=11, more than 50% of the amino groups are still protonated. Therefore, the total number of amino groups in the bacterial wall are expected to exceed those given in table 4.

The numbers of carboxyl and amino groups can be independently calculated from the primary peptidoglycan structure and the amino acid analysis of the cell wall proteins. These results are included in table 4. For the coryneform bacteria most of the carboxyl and amino groups originate from the peptidoglycan, whereas the contributions of the proteins are rather small. On the other hand, with *B. brevis* the carboxyl and amino groups are mainly situated in the protein-rich S-layer and only a minor fraction is in the thin peptidoglycan layer.

For the coryneforms it appears that the number of carboxyl groups estimated from titration analysis are very similar to, although systematically slightly lower than those obtained from the chemical composition of the walls. This difference is not surprising; for two reasons the chemically established number of carboxyl groups in the peptidoglycan structure may be overestimated. First, these estimations are based on the primary peptidoglycan structure. However, some of the carboxyl and

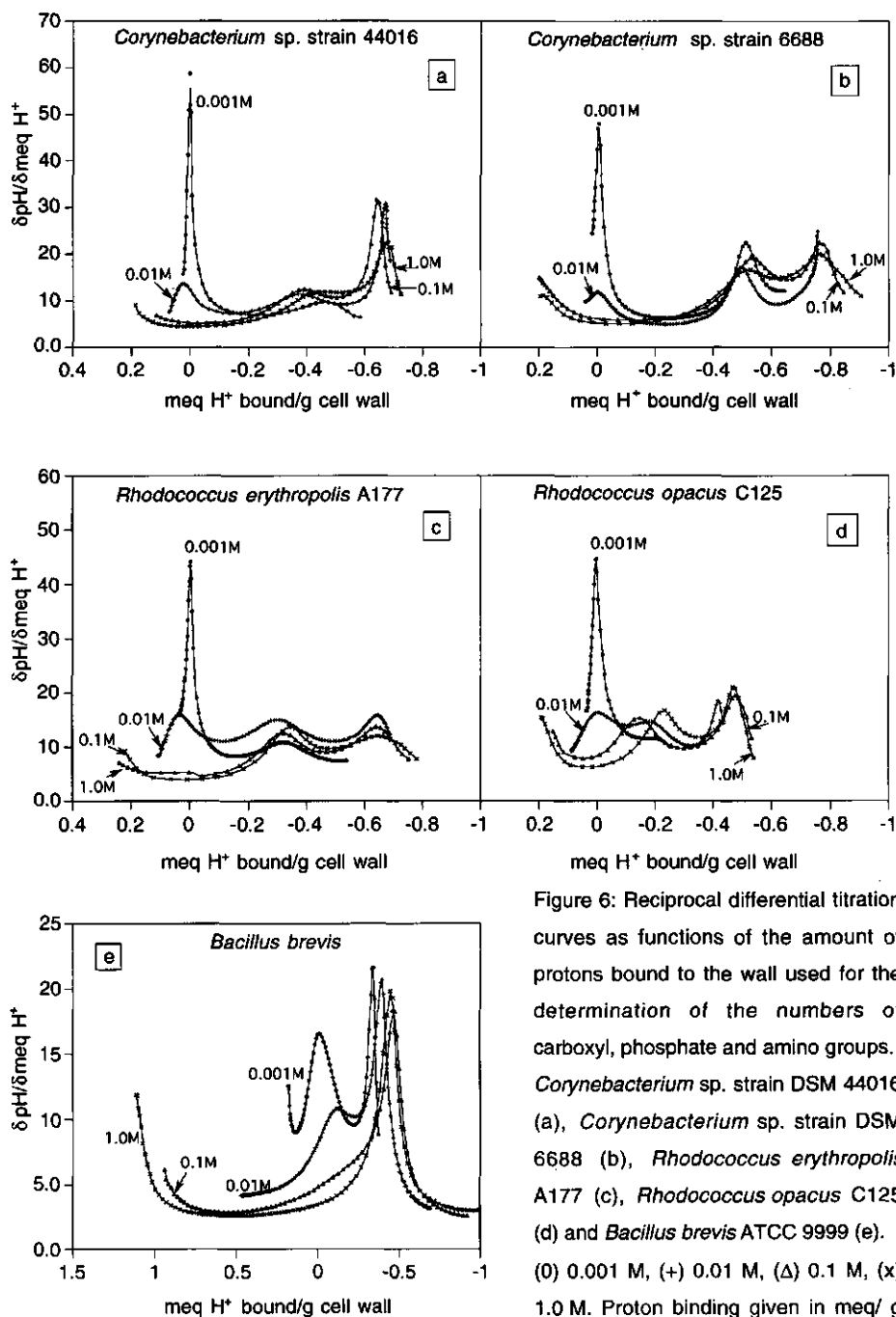


Figure 6: Reciprocal differential titration curves as functions of the amount of protons bound to the wall used for the determination of the numbers of carboxyl, phosphate and amino groups. *Corynebacterium* sp. strain DSM 44016 (a), *Corynebacterium* sp. strain DSM 6688 (b), *Rhodococcus erythropolis* A177 (c), *Rhodococcus opacus* C125 (d) and *Bacillus brevis* ATCC 9999 (e). (0) 0.001 M, (+) 0.01 M, (Δ) 0.1 M, (x) 1.0 M. Proton binding given in meq/g dry weight cell wall.

strain	Titration analysis			Chemical analysis				
	carboxyl	amino	phosphate	carboxyl P.G	proteins	carboxyl P.G	amino proteins	phosphate
<i>Corynebacterium</i> sp. strain DSM 44016	0.66	>0.063	0.22	0.69	0.13	0.23	0.09	0.15
<i>Corynebacterium</i> sp. strain DSM 6688	0.78	>0.11	0.21	0.69	0.16	0.23	0.17	0.24
<i>Rhodococcus</i> <i>erythropolis</i> A177	0.66	>0.10	0.24	0.63	0.07	0.21	0.05	0.26
<i>Rhodococcus</i> <i>opacus</i> C125	0.49	>0.075	0.21	0.72	0.04	0.24	0.02	0.29
<i>Bacillus brevis</i>	1.24	>0.50	0	0.12	>0.89	0.04	>0.44	0.11

Table 4: Comparison between the number of carboxyl-, phosphate and amino groups obtained from titration- and chemical analysis. The titration curves at 0.1 M and 1.0 M are used for the determination of the number of carboxyl and amino groups. The number of phosphate groups is the average of the estimated values at the four electrolyte concentrations. The carboxyl and amino groups estimated from chemical analysis are subdivided into those originating from the peptidoglycan (P.G.) and those from the cell wall proteins. All units are given in mmol/g dry weight cell wall.

amino groups are involved in peptide bonds, which occur between the carboxyl group of the m-diaminopimelic acid of one peptidoglycan unit and the amino group of a m-diaminopimelic acid of another unit. Usually, only a fraction of the m-diaminopimelic acids are used for such cross-linkages between the peptide strings. The number of carboxyl and amino groups involved in cross-linking therefore ranges between 0 and 0.2 mmol/g for the coryneform bacteria and between 0 and 0.04 mmol/g for the *B. brevis*. In the latter case, the loss of titratable groups due to cross-linking is negligible. Second, some carboxyl groups of the peptidoglycan matrix may be amidated, which would result in an additional reduction of the number of titratable carboxyl groups. Amidation of carboxyl groups is a rather common process and has been found to occur in the walls of mycolic acid-containing bacteria^{8, 21, 24}. Amide groups are protonated at pH-values < 1 and are therefore uncharged over the entire pH-range of the titrations. Amidation therefore leads to a reduction of the total number of negative cell wall charges.

As indicated above, the total number of amino groups in the walls of the coryneform bacteria are underestimated by titration analysis. Unfortunately, neither can more accurate estimations be obtained from chemical analysis because the degree of cross-linking between the peptidoglycan units is unknown.

The number of amino groups is therefore expected to be somewhere between 0.1-0.4 mmol/g, which is anyhow much lower than the number of carboxyl groups.

The number of carboxyl and amino groups in the *B. brevis* cell walls estimated from titration analysis are somewhat higher than those estimated from the chemical composition. However, only about 75% of the cell wall composition has been elucidated, so that the total numbers of the carboxyl and amino groups are most likely somewhat higher than the estimates given in table 4. Carboxyl and amino groups are both present in much higher numbers in the *B. brevis* walls than in the walls of the coryneform bacteria.

Only in the walls of the coryneform bacteria are phosphate groups titrated. The estimated number of phosphate groups compare reasonably well with the total amount of phosphate as determined with the colorimetric method. Apparently, all the phosphate groups are terminal groups, which means that per group two hydrogen ions can be bound. However, complete protonation only occurs at very low pH-values, beyond the pH-region accessible to titration. Phosphate groups have also been detected in other mycolic acid-possessing bacteria ¹².

The cell walls of *B. brevis* contain rather low amounts of phosphate groups, which are not titratable in the pH-region 2-11. Apparently, these phosphate groups can only dissociate one proton according to reaction (7), which occurs at pH < 2.

Donnan potential

The electrical potential in the bacterial wall, that causes the polyelectrolyte effect, can be obtained by solving the Poisson equation, taking into account that the space charge density is the sum of the contributions from the fixed cell wall charge together with the (diffuse) countercharge. In order to determine the potential profile across the bacterial wall, the Poisson equation has been solved numerically ²⁵.

A good approximation of the cell wall potential is obtained under the assumption that the fixed cell wall charge is homogeneously distributed and, as the cell wall thickness \gg Debye screening length, fully compensated inside the cell wall. This means that inside the wall the space charge density is zero and that the cell wall potential is approximately constant and equal to the Donnan potential (ψ_{Don}). Assuming that the ion concentration inside the wall is related to the bulk concentration by the Boltzmann factor, the Donnan potential for a 1-1 electrolyte is given by ¹⁴:

$$\psi_{\text{Don}} = \frac{RT}{zF} \operatorname{arcsinh} \frac{z \sigma_0}{2c_b F d_{\text{cw}}} = \frac{RT}{zF} \ln \left[\frac{z \sigma_0}{2c_b F d_{\text{cw}}} + \sqrt{\frac{\sigma_0^2}{4c_b^2 F^2 d_{\text{cw}}^2} + 1} \right] \quad (17)$$

in which z is the valency of the co-ion, T the absolute temperature, c_b the bulk electrolyte concentration (mol/m^3) and d_{cw} the cell wall thickness. Information about the cell wall thickness in aqueous solutions is not available. As a first approximation, d_{cw} is therefore taken equal to the thickness as determined by electron microscopy (table 3). However, especially at low electrolyte concentrations the cell walls may be somewhat swollen, because of repulsion between the charged cell wall groups. Analysis of the titration curves according to the Henderson-Hasselbalch approach suggests that the cell walls of the coryneforms in 0.001 M solution are at least twice as thick as determined with electron microscopy. Measurements of the sedimentation volume of isolated walls also indicate that the cell wall thickness is influenced by the concentration of the electrolyte ions in solution. For instance, the ratio of the sedimentation volume of the cell walls of *Corynebacterium* sp. strain DSM 44016 appears to be 1.8, 1.3, 1.1 and 1 in 0.001 M, 0.01 M and 0.1 M and 1 M electrolyte solution, respectively.

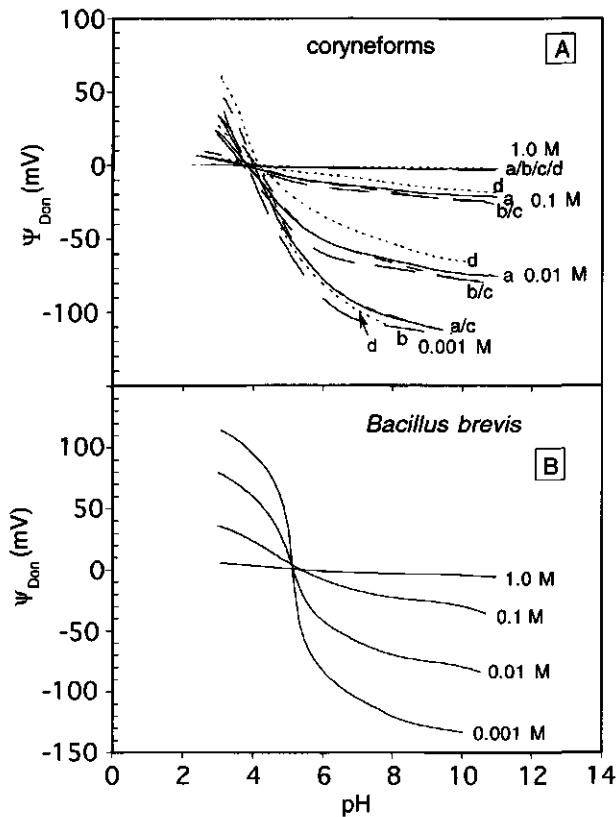


Figure 7: Estimated Donnan potentials at different electrolyte concentrations in the cell walls of the coryneforms (A) and *Bacillus brevis* (B). For the coryneforms d_{cw} in 0.001 M solution is taken twice the thickness as determined from electron micrographs.

Corynebacterium sp. strain DSM 44016 (—) (a), *Corynebacterium* sp. strain DSM 6688 (— —) (b), *Rhodococcus erythropolis* A177 (— — —) (c), *Rhodococcus opacus* C125 (.....) (d) and *Bacillus brevis* ATCC 9999 (— · —) (e).

Figs 7 A and B give the Donnan potentials, calculated from the titration curves (figs 1a-e). These graphs demonstrate that the cell wall charge is very effectively screened by the electrolyte ions. For example, at pH 7 the Donnan potential decreases from values higher than 100 mV to approximately 0 mV upon increasing the electrolyte concentration from 1 mM to 1 M. Swelling or shrinking of the bacterial wall upon changing the electrolyte concentration only slightly influences the Donnan potential. This allows rather accurate estimation of ψ_{Don} , despite remaining uncertainties in the exact value of d_{cw} .

Donnan potentials level off with increasing pH, especially at low electrolyte concentrations, notwithstanding the increase in the cell wall charge. Donnan potentials are therefore much less sensitive to changes in the pH of the electrolyte solution than the cell wall charge density (figs 1a-e).

Information about the composition of the countercharge can also be obtained from the Donnan model. In this model the relation between the ionic components of charge, σ_+ and σ_- , and the Donnan potential is given by:

$$\sigma_+ = F d_{\text{cw}} c_b [\exp(-F\psi_{\text{Don}}/RT) - 1] \text{ and } \sigma_- = - F d_{\text{cw}} c_b [\exp(F\psi_{\text{Don}}/RT) - 1] \quad (18a,b)$$

The results, given in figs 8a-e, show the same trends as those deduced from the Esin-Markov analysis (figs 4a-e). At 0.001 M and 0.01 M the co-ions hardly contribute to the countercharge. Moreover, the expulsion of co-ions reaches its maximum value at relatively low charge densities. In 0.1 M electrolyte solution a considerable fraction of the countercharge is determined by the deficit of co-ions. At this electrolyte concentration a plateau value is only obtained for the *B. brevis* cell walls due to its very high surface charge. The charge density in the walls of the coryneforms is too low to expel all co-ions into the surrounding electrolyte solution. At 1 M salt concentration, co- and counterions approximately equally contribute to the countercharge.

According to the Donnan-model, the maximum expulsion of co-ions from the walls of the coryneforms and *B. brevis* in 0.001 M and 0.01 M solution is 0.005 à 0.01 C/m² and 0.03 à 0.07 C/m², respectively. For *B. brevis* at 0.1 M salt concentration the plateau value corresponds with 0.6 C/m². These values are in agreement with those estimated from the Esin-Markov analysis.

Henderson-Hasselbalch analysis

Further information about the cell wall composition is obtained by analysing the titration curves using the Henderson-Hasselbalch equation, which is given by:

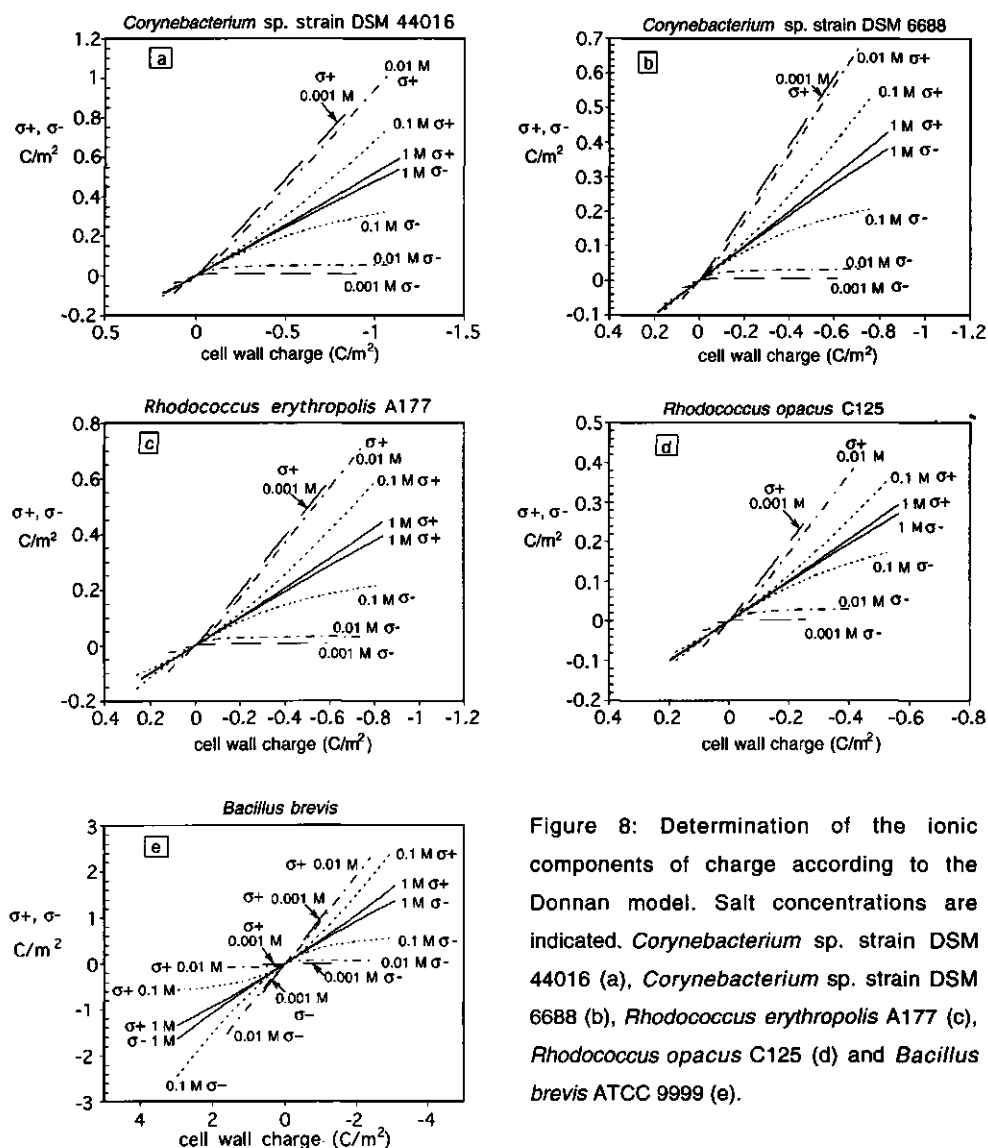


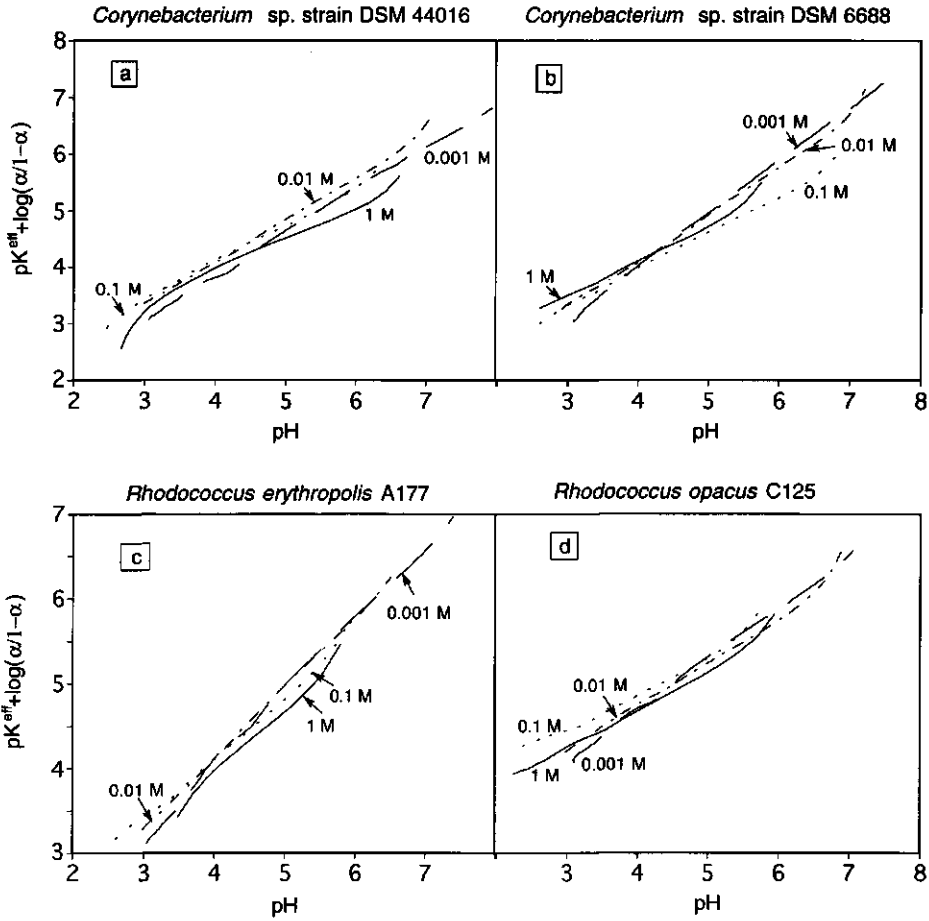
Figure 8: Determination of the ionic components of charge according to the Donnan model. Salt concentrations are indicated. *Corynebacterium* sp. strain DSM 44016 (a), *Corynebacterium* sp. strain DSM 6688 (b), *Rhodococcus erythropolis* A177 (c), *Rhodococcus opacus* C125 (d) and *Bacillus brevis* ATCC 9999 (e).

$$\text{pH} = \text{pK}_{\text{a}_i}^{\text{eff}} + \log \frac{\alpha_i}{1 - \alpha_i} \quad (19)$$

This equation can be obtained from any of the equations 9-12, by introducing the degree of dissociation, α_i , which is the fraction of a class of groups i that is dissociated. The Henderson-Hasselbalch equation can, in principle, be applied to all the titratable cell wall groups, provided that the number of groups within each titratable class are known and the dissociation constants of the different classes are at least several pH-units apart. Moreover, the variation of pK_{chem} within a certain titratable class should be small. These conditions are satisfied in the case of the carboxyl groups in the walls of the coryneform bacteria, because most of these groups originate from three amino acids of the peptidoglycan, whose intrinsic dissociation constants are very similar. The Henderson-Hasselbalch approach cannot be applied to the carboxyl groups in the walls of *B. brevis*, because these groups originate from many different amino acids whose intrinsic dissociation constants are fairly different. Moreover, medium effects may play an important role, as many amino acids are situated in the protein-rich S-layer.

For the calculation of pK^{eff} for the titration of the carboxyl groups in the walls of the coryneforms we have used equation 16, assuming that $\text{pK}_{\text{chem}} = 4.1$ equating the electrostatic potential in the wall to the Donnan potential. The results of the Henderson-Hasselbalch analysis at different electrolyte concentrations are given in the figs 9a-d. These figs show that the plots of $\text{pK}^{\text{eff}} + \log(\alpha/1 - \alpha)$ as functions of the pH, lead to approximately straight lines with slopes equal to one. Deviations from that line may be caused by inaccuracies in the estimation of the cell wall thickness and the determination of the degree of dissociation, due to overlap in the titration regions of the different cell wall groups, specially at high salt concentrations. At 0.001 M a straight line is only obtained if the cell wall is taken twice the thickness as determined by electron microscopy. This suggests that the cell walls may swell considerably upon decreasing the electrolyte concentration from 0.01 M to 0.001 M.

The Henderson-Hasselbalch plots for the various coryneform bacteria are almost identical, implying that, at least as far as the dissociable groups is concerned, the compositions of the cell walls are very similar for these strains.



Figures 9: Henderson-Hasselbalch plots for the carboxyl groups corrected for the polyelectrolyte effect in isolated walls of *Corynebacterium* sp. strain DSM 44016 (a), *Corynebacterium* sp. strain DSM 6688 (b), *Rhodococcus erythropolis* A177 (c) and *Rhodococcus opacus* C125 (d). (— — —) 0.001 M, (— — —) 0.01 M, (- · - ·) 0.1 M, (——) 1.0 M.

Conclusions

It can be concluded that detailed information about the characteristics of the electrical double layer of bacterial cell surfaces can be extracted from proton titration studies with bacterial cells and isolated cell walls. A rigorous

(thermodynamic) analysis of the titration curves for isolated cell walls was possible due to the absence of hysteresis between the acid and base titrations. This indicates that the chargeable cell wall groups are readily accessible to the protons and hydroxide ions.

Information about the ionic composition of the countercharge has been obtained from Esin-Markov analysis of the titration curves. This approach also is purely thermodynamic and based on first principles. It does not require a model for the electrical double layer and is therefore generally applicable, including to porous surfaces such as those of bacterial cells.

Determination of the ionic components of charge according to the Donnan model is based on several assumptions and requires detailed information about the structure of the bacterial wall. Exact solutions of the Poisson equation show that only in the outermost cell wall layers the cell wall potential deviates substantially from the Donnan potential²⁵. Both Esin-Markov analysis and the Donnan model approach lead to the same conclusion that at salt concentrations lower than 0.01 M the cell wall charge is predominantly compensated by counterions, with the excluded co-ions hardly contributing to the countercharge. Because of this fact the influence of the co-ions on the electrokinetic properties of bacterial suspension may be neglected, which considerably facilitates the interpretation of conductivity and micro-electrophoresis studies^{25, 26}.

The composition of the ionic components of charge only depends on the surface charge density and is insensitive to the nature of the chargeable cell wall groups. At given σ_0 the relative contribution of the co- and counterions to the countercharge for the coryneform bacteria and the *B. brevis* strain are therefore very similar, despite differences in the chemical structure of their cell walls.

The anionic and cationic groups in the bacterial wall could be identified and their numbers determined by representing the differential titration curves as functions of pH and cell wall charge. The carboxyl and phosphate groups in the bacterial wall were almost entirely titrated in the pH range accessible by proton titration, allowing precise estimation of their numbers. On the other hand, estimates for the number of amino groups in the bacterial wall were less accurate, because these groups are partly titrated beyond the pH range where precise titration measurements are feasible.

In order to calculate the space charge density in the bacterial wall, the cell wall thickness is an important parameter. Exact measurements of the cell wall thickness in aqueous solutions have not been performed. However, Henderson-Hasselbalch analyses for the titration of the carboxyl groups of the coryneforms

bacteria and sedimentation measurements indicate that the bacterial cell wall expands and shrinks upon changes in the bulk electrolyte concentration. Obviously, additional experimental work, especially with Gram-negative bacterial strains is required before more general conclusions about the charge formation in bacterial cell surfaces can be drawn.

References

1. **Bendinger, B., H. H. M. Rijnaarts, K. Altendorf, A. J. B. Zehnder** 1993. Physicochemical cell surface and adhesive properties of coryneform bacteria related to the presence and chain length of mycolic acids., *Appl. Environ. Microbiol.* **59**, 3973-3977.
2. **Bradford, M. M.** 1976. A rapid and sensitive method for the quantification of microgram quantities of protein utilizing protein-dye binding., *Anal. Biochem.* **72**, 248-254.
3. **Carstensen, E. L., R. E. Marquis** 1968. Passive electrical properties of microorganisms. III. Conductivity of isolated bacterial cell walls., *Biophys. J.* **8**, 536-548.
4. **Czerkawski, J. W., H. R. Perkins, H. J. Rogers** 1963. A study of the composition and structure of the cell wall mucopeptide of *Micrococcus lysodeikticus*., *Biochem. J.* **86**, 468-474.
5. **Doyle, R. J., R. E. Marquis** 1994. Elastic, flexible peptidoglycan and bacterial cell wall properties., *Trends in Microbiol.* **2**, 57-60.
6. **Gutman, M., E. Nachliel** 1990. The dynamic aspects of proton transfer processes, *Biochim. Biophys. Acta.* **1015**, 391-414.
7. **Harden, V. P., J. O. Harris** 1952. The isoelectric point of bacterial cells, *J. Bacteriol.* **65**, 198-202.
8. **Kato, K., J. L. Strominger, S. Kotani** 1968. Structure of the cell wall of *Corynebacterium diphtheriae*. I. Mechanism of hydrolysis by the L-3 enzyme and the structure of the peptide., *J.* **7**, 2762-2773.
9. **Lyklema, J.** 1972. The Esin and Markov coefficient for double layers with colloid chemical importance, *J. Electroanal. Chem.* **37**, 53-60.
10. **Lyklema, J.** 1984. Points of zero charge in the presence of specific adsorption., *J. Colloid Interface Sc.* **99**, 109-117.
11. **Marquis, R. E.** 1968. Salt-induced contraction of bacterial cell walls, *J. Bacteriol.* **775**-781.
12. **Mc Neil, M., M. Daffe, P. J. Brennan** 1990. Evidence for the nature of the link between the arabinogalactan and peptidoglycan of mycobacterial cell walls., *J. Biol. Chem.* **265**, 18200-18206.
13. **Neihof, R. A., W. H. Echols** 1978. Chemical modification of the surfaces of bacterial cell walls., *Physiol. Chem. & Physics* **10**, 329-343.

14. **Ohshima, H., T. Kondo** 1991. On the electrophoretic mobility of biological cells., *Biophys. Chem.* **39**, 191-198.
15. **Ou, L. T., R. E. Marquis** 1970. Electromechanical interactions in cell walls of Gram-positive cocci., *J. Bacteriol.* **101**, 92-101.
16. **Rijnaarts, H. H. M., W. Norde, E. J. Bouwer, J. Lyklema, A. J. B. Zehnder** 1993. Bacterial adhesion under static and dynamic conditions., *Appl. Environ. Microbiol.* **59**, 3255-3265.
17. **Rogers, H. J., H. R. Perkins, J. B. Ward** 1980. Microbial cell walls and membranes, Chapman and Hall, London, New York.
18. **Rouxhet, P. G., N. Mozes, P. B. Dengis, Y. F. Dufrêne, P. A. Gerin, M. J. Genet** 1994. Application of X-ray photoelectron spectroscopy to microorganisms, *Colloids Surf. B: Biointerfaces* **2**, 347-369.
19. **Salton, M. R. J.** 1964. The bacterial cell wall, Elsevier publishing company, Amsterdam, London, New York.
20. **Salton, M. R. J.** 1961. Studies of the bacterial cell wall. VIII. Reaction of walls with hydrazine and with fluorodinitrobenzene, *Biochim. Biophys. Acta* **52**, 329-342.
21. **Schleifer, K. H., O. Kandler** 1972. Peptidoglycan types of bacterial cell walls and their taxonomic implications, *Bacteriol. Rev.* **36**, 407-477.
22. **Schraa, G., M. L. Boone, M. S. Jetten, A. R. W. Van Neerven, P. J. Goldberg, A. J. B. Zehnder** 1986. Degradation of 1,4-dichlorobenzene by *Alcaligenes* sp. strain A175., *Appl. Environ. Microbiol.* **52**, 1374-1381.
23. **Terayama, H.** 1954. Application of the method of colloid titration to the study of bacteria, *Arch. Biochem. Biophys.* **50**, 55.
24. **Vacheron, M. J., M. Guinand, G. Michel, J. M. Ghuysen** 1972. Structural investigations on cell walls of *Nocardia* sp., *Eur. J. Biochem.* **29**, 156-166.
25. **Van der Wal, A., M. Minor, W. Norde, J. Lyklema, A. J. B. Zehnder** 1996. The electrokinetic potential of bacterial cells, chapter 5, this thesis.
26. **Van der Wal, A., M. Minor, W. Norde, A. J. B. Zehnder, J. Lyklema** 1996. Conductivity and dielectric dispersion of Gram-positive bacterial cells, chapter 4, this thesis.
27. **Van der Wal, A., W. Norde, B. Bendinger, A. J. B. Zehnder, J. Lyklema** 1996. The chemical composition of Gram-positive bacterial cell walls and the determination of the cell wall to cell mass ratio, chapter 2, this thesis.
28. **Van Loosdrecht, M. C. M., J. Lyklema, W. Norde, G. Schraa, A. J. B. Zehnder** 1987. The role of bacterial cell wall hydrophobicity in adhesion., *Appl. Environ. Microbiol.* **53**, 1893-1897.

Chapter 4

Conductivity and dielectric dispersion of Gram-positive bacterial cells.

Abstract

The conductivity of bacterial cell suspensions has been studied over a wide range of ionic strengths and is interpreted in terms of their cell-wall properties. The experimental data have been analysed after improving the high κa double layer theory of Fixman, by accounting for ionic mobility in the hydrodynamically stagnant layer, i.e. in the bacterial wall.

Static conductivity and dielectric dispersion measurements both show that the counterions in the porous gel-like cell wall give rise to a considerable surface conductance. From a comparison of the mobile charge with the total cell wall charge it is inferred that the mobilities of the ions in the bacterial wall are of the same order but somewhat lower than those in the bulk electrolyte solution. The occurrence of surface conductance reduces the electrophoretic mobility in electrophoresis studies. If this effect is not taken into account, the ζ -potential will be underestimated, especially at low electrolyte concentrations.

Introduction

The electrical properties of bacterial cell surfaces are related to the chemical composition of the bacterial wall. The charge in the cell wall matrix originates from acidic groups such as carboxyl, phosphate and amino groups, which may be present in high concentrations^{3, 25}. Most bacterial walls contain higher concentrations of anionic groups than of cationic groups, which results in a negative cell wall charge at neutral pH. This charge is mainly compensated by counterions that penetrate into the porous cell wall and to a minor extent by co-ions that are expelled from it. Detailed information on the composition of the electrical double layer is of interest for such studies as adhesion of microbial cells and binding of (heavy) metals to microorganisms. For example, in studies concerning bacterial cell adhesion, micro-electrophoresis may be of help in order to quantify the electrostatic interactions between the cell and the solid surface²⁷. However, the interpretation of the electrophoretic mobility in terms of ζ -potential

and electrokinetic charge requires information about the mobile charge inside the bacterial wall. A full characterisation of the electrical double layer of bacterial surfaces can therefore only be obtained from a combination of different experimental techniques.

In a previous study²⁵ we have shown that the total cell wall charge can be determined by potentiometric proton titrations of isolated cell wall fragments. In that study it has been found that the cell wall charge density (σ_o) can be as high as 0.5-1.0 C/m², which may give rise to an appreciable surface conductance within the hydrodynamically stagnant layer. The contribution of the counterions in the bacterial wall to the surface conductance depends on their concentrations, their mobilities and the ease by which they can migrate into the wall at one side of the cell and leave it at the other. In fact, from a comparison between the mobile cell wall charge and the titration charge information can be obtained about the state of ion-binding within the cell wall matrix.

The contribution of the mobile charge in the bacterial wall to the total surface conduction can be inferred from conductivity studies with bacterial suspensions. So far, such studies have hardly been reported in the literature, except for the pioneering work of Carstensen, Einolf and Marquis^{2-4, 10, 16}. Unfortunately, the theories available at that time, to extract the mobile cell wall charge from the measured conductivity of the suspension, were still rather poor. For instance, for the interpretation of their experimental data, Carstensen et al. used Maxwell's equation that has been derived for uncharged, conducting colloidal particles at low volume fractions. This equation leads to wrong estimates of the mobile cell wall charge, especially at low electrolyte concentrations where the electrical double layer may be slightly out of equilibrium due to the occurrence of concentration polarisation. This last effect has been taken into account in more recent theories as derived by Dukhin, O'Brien and Fixman (see for instance^{7, 8, 11, 12, 19}). These approaches are based on the observation that for colloidal particles, for which the electrical double layer is very thin in comparison with the radius of curvature of the particle surface, the ion distribution inside the double layer may be considered to be in local equilibrium with the surrounding electrolyte solution just outside the double layer. These theories account for surface conduction, caused by the diffuse double layer ions, beyond the slip plane, but ignore any conductivity within the hydrodynamically stagnant layer. In this paper possible ion mobility behind the slip plane is incorporated in the high κa double layer theory of Fixman. This extended theory is used for the analysis of the electrokinetic properties of bacterial suspensions such as the conductivity in static electric fields and the dielectric response in low frequency dielectric dispersion studies.

Theory

The conductivity of a dilute suspension of nonconducting charged spherical colloidal particles (\hat{K}_{susp}) is simply related to the volume fraction (ϕ) and the induced dipole strength ($\hat{\mu}$) of the dispersed particles and is given by:^{5, 9}

$$\Delta\hat{K} = \hat{K}_{\text{susp}} - \hat{K}_L = 3\phi \frac{\hat{\mu}}{a^3 E} \hat{K}_L \quad (1)$$

where for any \hat{K} :

$$\hat{K} = K + i\omega\epsilon \quad (2)$$

in which a is the particle radius, E the strength of the externally applied electric field, \hat{K}_L the bulk electrolyte conductivity, K the conductivity, $\epsilon = \epsilon_r \epsilon_0$ the dielectric permittivity, ϵ_r the relative dielectric permittivity, ϵ_0 the dielectric permittivity of vacuum and ω the frequency. $\Delta\hat{K}$, \hat{K}_{susp} , \hat{K}_L and $\hat{\mu}$ are frequency-dependent complex quantities. In static electric fields ($\omega=0$) equation (1) holds if the ions in the electrolyte solution have the same mobilities^{17, 22}, which is the case for the systems under consideration in this study. The induced dipole strength of the charged particle is caused by the polarisation of the double layer and reflects the perturbation in ion densities and the applied electric field.

For colloidal suspensions at least two distinct relaxation frequencies can be distinguished.

In the high frequency regime, i.e. at frequencies in the MHz region, the relaxation mechanism of interest is that of the readjustment of the diffuse layer ions to the applied electric field leading to a stationary electrical current in any section of the double layer. The relaxation time is of order $1/\kappa^2 D$ (where D is the diffusivity of the ions), which is about 10^{-7} s in 1 mM (1-1) electrolyte.

The dispersion in the low frequency regime is related to changes in the ion densities beyond the double layer. The occurrence of these ion perturbations can be visualized by considering the flux balance of the individual ion species in the double layer. Inside the double layer the electric current is mainly carried by counterions and to a much lower extent by co-ions, whereas the current flowing out into the surrounding electrolyte solution is made up by equal contributions of both ion species. The unbalance of charge carriers in- and outside the double layer leads to the formation of excess concentrations of neutral salt at one side of the particle and to a deficit at the other side. The development of these

concentration gradients outside the double layer influence the ion fluxes inside the double layer and consequently the particle dipole strength¹⁸.

The increased salt concentration has to diffuse away into the surrounding electrolyte solution over distances of the order of the particle radius. The dispersion in the low frequency regime for not too small colloidal particles therefore occurs in the kHz region. The corresponding relaxation time is of order a^2/D .

At frequencies below 1 kHz, i.e. at approximately static conditions, the ion gradients can fully develop and therefore $\Delta\hat{K}$ is essentially constant. Consequently, in d.c. conductivity studies only the real parts of \hat{K}_{susp} , \hat{K}_L and $\hat{\mu}$ have to be considered. In static electric fields information about the induced dipole strength is obtained by measuring the conductivity increment as a function of the volume fraction. The static dipole strength can be related to the specific surface conductivity (K^o) by the dimensionless surface conduction parameter (Rel):

$$\text{Rel} = \frac{K^o}{K^L a} \quad (3)$$

The Rel value is a measure of the surface conductivity relative to the bulk conductivity.

At low volume fractions in a solution of a symmetrical electrolyte, in which the ions have the same mobility, assuming that only the counterions contribute to the conduction in the electrical double layer, the static dipole strength is characterised by*

$$\mu = -\frac{a^3}{2} E \left(1 - \frac{3\text{Rel}}{1+2\text{Rel}} \right) \quad (4)$$

At high Rel values (Rel > 1), the tangential flow of ions along the particle surface due to diffusion, conduction and convection leads to a relatively high contribution to the suspension conductivity and to the development of the ion gradients outside the double layer. On the other hand, at low Rel values (Rel < 1) the flux of ions along the surface is small in comparison with those in the bulk electrolyte and consequently concentration polarisation is less important. At very low Rel values

* Equation 4 is equal to Dukhin's equation⁸ (or see for instance²³ eq.12), Hunter and O'Brien's equation (see for example¹² eq. 13.6.18) and can be derived from Fixman's¹¹ eq. 3.6.

($Re \approx 0$) the particles can be considered as uncharged non-conducting spheres. For $Re = 1$ the static dipole strength is 0 and the suspension conductivity is independent of the volume fraction of the particles, i.e. particle and surrounding electrolyte solution are isoconducting. For bacterial suspensions it is worthwhile to determine the exact position of the isoconductance point (i.c.p.) as in this condition the determination of the magnitude of the induced dipole strength is insensitive to errors in the volume fraction.

The surface conduction parameter (Re) is related to the mobile countercharge density in the electrical double layer. Taking Fixman's derivation of the integrated flux balance (eq 3.6¹¹) assuming that the net tangential flux of the co-ions is zero and introducing surface conductance behind the plane of shear, according to the procedure of Kijlstra et al.¹³, it is derived that:

$$Re = \frac{1}{\kappa a} \left[\left(1 + \frac{K^{\sigma,i}}{K^{\sigma,d}} \right) + 3 \frac{m}{z^2} \right] \left[\exp \left(\frac{zF\zeta}{2RT} \right) - 1 \right] = \frac{1}{K^L a} \left[u^i \sigma_c^i + \left(1 + 3 \frac{m}{z^2} \right) u^L \sigma_c^d \right] \quad (5)$$

where z is the valency of the co-ion ($z\zeta > 0$), ζ the ζ -potential, F Faraday's constant, R the gas constant and T the absolute temperature. The reciprocal Debye screening length, κ , is defined by:

$$\kappa^2 = \frac{2cz^2F^2}{\epsilon RT} \quad (6)$$

in which c is the electrolyte concentration (mol.m^{-3}). The non-dimensional ionic drag coefficient, m , is given by:

$$m = \frac{2\epsilon RT|z|}{3\eta F|u^L|} \quad (7)$$

where η is the viscosity of the electrolyte ($m \approx 0.16$ for KNO_3 at 298 K) and $K^{\sigma,i}/K^{\sigma,d}$ the ratio of the conductivities of countercharges behind and beyond the plane of shear

$$\frac{K^{\sigma,i}}{K^{\sigma,d}} = \frac{u^i \sigma_c^i}{u^L \sigma_c^d} \quad (8)$$

u^j and u^l are the mobilities of the counterions inside the plane of shear and in the diffuse part of the double layer, respectively. σ_c^j is the countercharge due to the counterions behind the plane of shear and σ_c^d is the diffuse countercharge due to the excess of counterions outside the slip plane:

$$\sigma_c^d = -\frac{2czF}{\kappa} \left[\exp\left(\frac{zF\zeta}{2RT}\right) - 1 \right] \quad (9)$$

The mobility of the counterions in the diffuse part of the double layer (u^l) is assumed to be equal to that in the bulk solution, while the mobility of the ions inside the plane of shear (u^j) may deviate from the bulk value. In the limiting case that the ions in the stagnant layer are immobile ($K^{\sigma,j} = 0$), the surface conductance is only determined by the diffuse countercharge outside the plane of shear and consequently eq. 5 reduces to Fixman's equation. In the other limit, if surface conductance is almost entirely due to the mobile charge behind the plane of shear ($K^{\sigma,j} \gg K^{\sigma,d}$), eq. 5 reduces to:

$$\text{ReI} \approx \frac{u^j \sigma_c^j}{K^{\sigma,j} a} \quad (10)$$

For the bacterial cells under study it has been shown²⁵ that, at neutral pH and not too high salt concentrations, the compensating cell wall charge almost entirely consists of counterions that are situated in the cell wall, i.e. behind the plane of shear ($|\sigma_o| \approx |\sigma_c^j| \gg |\sigma_c^d|$). Analysis of the d.c. conductivity measurements therefore allows rather accurate estimates of the mobilities of these ions, despite uncertainties in the exact values of the ζ -potential.

Information about the induced dipole strength ($\hat{\mu}$) can also be obtained from dielectric spectroscopy, where the complex conductivity increment ($\Delta\hat{K}$) of a colloidal suspension at a given volume fraction, is studied as a function of the frequency. The response in the low frequency regime can be very high, because of concentration polarization. Above the relaxation frequency, the ion gradients of neutral electrolyte beyond the double layer can no longer fully develop and consequently the dielectric permittivity of the suspension drops down. However, the suspension conductivity increases with increasing frequency, because the absence of concentration polarization leads to a higher contribution of the mobile charge to the suspension conductivity. The frequency dependencies of ϵ and K contain the same information and are related by the Kramers-Kronig relation,

which gives a model-independent check of the consistency of the experimental data ¹³.

The interpretation of dielectric dispersion data requires the time-dependent solution for the induced dipole strength. For this purpose we used the extended Fixman theory according to Kijlstra et al. ¹³, in which surface conductance in the hydrodynamically stagnant layer is accounted for. From this theory the dielectric increment ($\Delta\epsilon_r$) and the conductivity increment (ΔK) are to a good approximation given by ¹⁵:

$$\Delta\epsilon_r = \frac{9}{16} \phi \epsilon_r^{\text{es}} (\kappa a)^2 \left(\frac{2 \text{Re}l}{1 + 2 \text{Re}l} \right)^2 \frac{1}{(1 + \omega\tau)(1 + \sqrt{\omega\tau})} \quad (11)$$

$$\Delta K = \frac{9}{8} \phi K^L \left(\frac{2 \text{Re}l}{1 + 2 \text{Re}l} \right)^2 \frac{\omega\tau\sqrt{\omega\tau}}{(1 + \omega\tau)(1 + \sqrt{\omega\tau}) - \frac{\text{Re}l}{1 + 2 \text{Re}l} \omega\tau\sqrt{\omega\tau}} \quad (12)$$

respectively. Here ϵ_r^{es} is the relative dielectric permittivity of the electrolyte solution and $\tau = a^2/2D$ the relaxation time.

These equations show that the particles radius (a) and the surface conduction parameter ($\text{Re}l$) have a strong influence on $\Delta\epsilon_r$ and ΔK . For very high values for $\text{Re}l$, both $\Delta\epsilon_r$ and ΔK reach limiting values.

Experimental

Bacterial cultivation and preparation

Corynebacterium sp. strain DSM 6688 and *Corynebacterium* sp. strain DSM 44016 were cultivated in brain heart infusion broth (Merck, 40 g/l deionized water). *Rhodococcus erythropolis* A177, *Rhodococcus opacus* C125 and *Bacillus brevis* ATCC 9999 were cultivated in mineral media as described elsewhere ²⁵. All bacterial cells were grown at 30 °C on a rotary shaker and harvested in the early stationary phase by centrifugation for 10 min at 20,000 x g at 20 °C and washed at least four times in KNO_3 solutions, at concentrations according to the experimental needs.

Volume fraction

Volume fractions of the bacterial suspensions were estimated from the cell dimensions and the cell concentrations as determined in a cell counting chamber.

For *Corynebacterium* sp. strain DSM 44016, which forms approximately spherical cells, the volume fraction was estimated viscometrically, using an Ostwald-viscometer.

D.c. conductivity

Conductivities of the cell suspensions were measured at pH 6.5-7.0 and 25 °C with a conductivity cell at a frequency of 3.7 kHz and an effective field strength of 80 V/m. The applied frequency is sufficiently high to prevent electrode polarization but low enough to ensure static conditions ¹³. The electrophoretic contribution of the bacterial cells to the suspension conductivities is less than 1%.

Dielectric spectroscopy

Complex conductivities of the bacterial suspensions were measured at pH 6.5 and 25 °C with a dielectric spectrometer as described by Kijlstra et al. ¹⁴, which contained a four-electrode set-up in order to eliminate effects due to electrode polarization. The equipment was optimized for the frequency range of approximately 500 Hz-500 kHz. Measurements are performed in approximately 1 mM KNO₃ at 25 °C and an effective field strength of approximately 13 V/m using bacterial suspensions of volume fractions between 0.01 and 0.1. A complete frequency scan took about 20 s, which is sufficiently fast to prevent complications due to leakage of ions through the cytoplasmic membrane.

Results

D.c. conductivity

Figures 1a-e show that the measured suspension conductivities of the five bacterial strains at given electrolyte solutions are linear with the volume fractions for ϕ up to 0.3. This implies that particle interaction is essentially absent, allowing analysis of the d.c. conductivity measurements according to the theory for dilute suspensions. The slopes of the curves are negative within the range of electrolyte concentrations studied, implying that the conductivity of the cells is lower than that of the bulk electrolyte. At high electrolyte concentrations, the bacterial cell conductivity becomes negligible in comparison with the bulk electrolyte solution and the slope of the curves approach the limit of $-1.5\phi K^L$, which is Maxwell's result for dilute suspensions of uncharged nonconducting spherical particles. At low electrolyte concentrations the slopes of the curves are

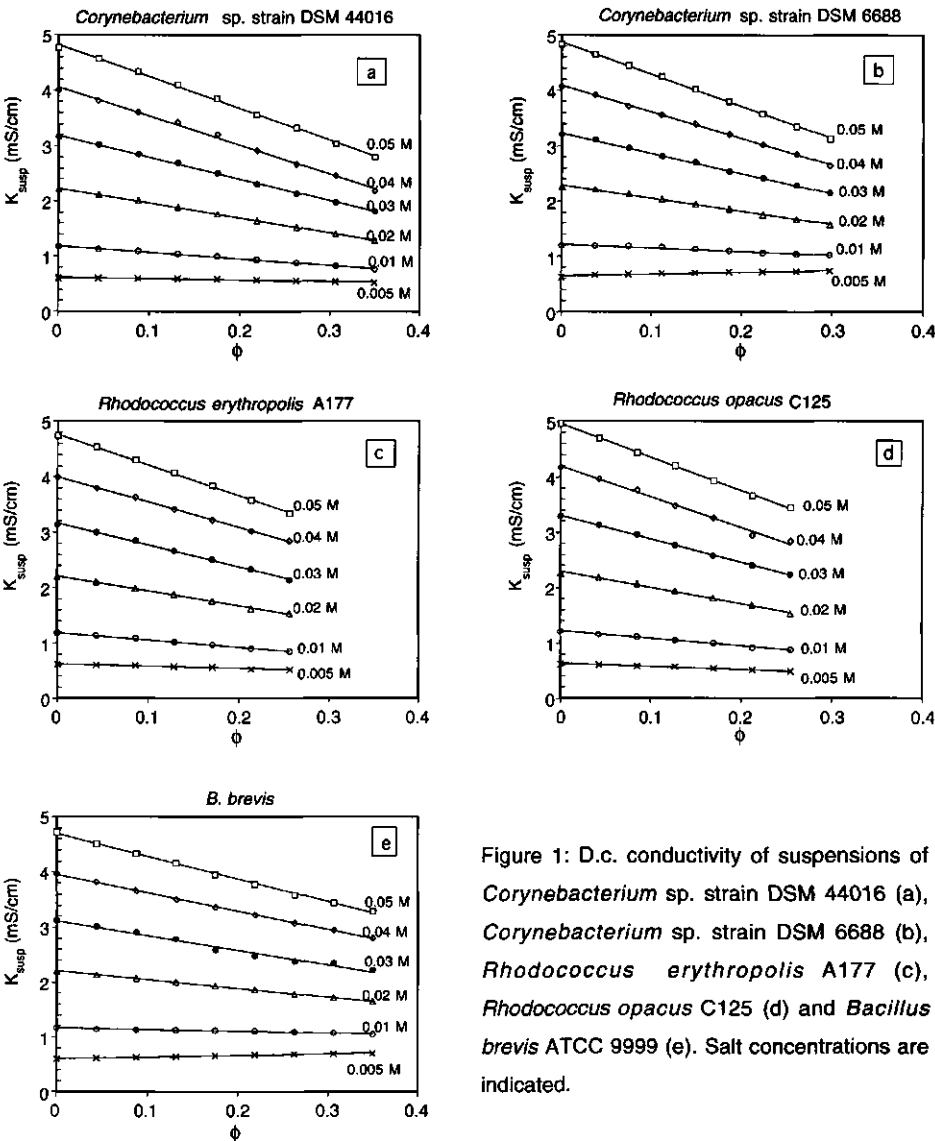


Figure 1: D.c. conductivity of suspensions of *Corynebacterium* sp. strain DSM 44016 (a), *Corynebacterium* sp. strain DSM 6688 (b), *Rhodococcus erythropolis* A177 (c), *Rhodococcus opacus* C125 (d) and *Bacillus brevis* ATCC 9999 (e). Salt concentrations are indicated.

expected to be positive. However, in this region no accurate conductivity measurements could be performed due to leakage of ions through the cytoplasmic membrane, leading to a spurious change of K^L during the course of the experiment. Because of this complication, ReI and K^σ tend to be overestimated at low electrolyte concentrations. Notwithstanding these uncertainties, it may be

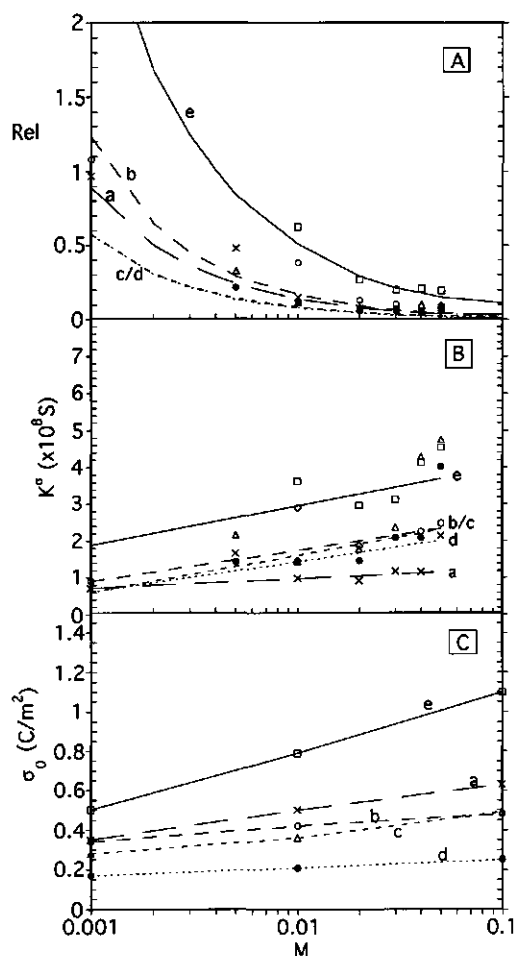


Figure 2: Calculated values for Rel (A) and surface conductivity (K^σ) (B) from d.c. conductivity studies. Rel and K^σ at 0.001 M are calculated from dielectric dispersion studies (see fig. 3). For comparison values for the surface charge density (σ_0)²⁵ at neutral pH are given in (C). *Corynebacterium* sp. strain DSM 44016 (x — —) (a), *Corynebacterium* sp. strain DSM 6688 (o — —) (b), *Rhodococcus erythropolis* A177 (Δ - - -) (c), *Rhodococcus opacus* C125 (\bullet ) (d) and *Bacillus brevis* ATCC 9999 (\square — —) (e). Curves for Rel computed from eq. (10). For discussion see text.

estimated that the conductivities of the cells are equivalent to those of an electrolyte solution of about 1 - 2 mM for the coryneforms and approximately 5 mM for *B. brevis*. At very high electrolyte concentrations the slopes of the curves hardly deviate from those for uncharged particles, leading to relatively large errors in the determination of Rel and K^σ . Moreover, the cell suspensions flocculate and K_{susp} may no longer be linearly dependent on ϕ . The values calculated for Rel and K^σ , as given in the figures 2^A and 2^B, are therefore most reliable in the concentration range 0.01 M-0.04 M.

Figure 2^A shows that for the coryneform bacteria at increasing electrolyte concentrations Rel decreases to values <0.1 , while for *B. brevis* Rel becomes <0.2 . In order to interpret the calculated Rel -values in terms of K^σ , for non-spherical cells one has to assign an effective particle radius. For the coryneforms this effective radius is chosen such that the surface area is equal to that of the non-spherical cells. For the cylindrical cells of *B. brevis*, the effective radius is chosen to be equal to half the width of the cells, which can be considered as the shortest length scale. Consequently, the calculated K^σ -values give the lower limit for the surface conductivity. Cell dimensions and effective radii are given in table 1.

strain	Morphology	Length μm	width μm	a^{eff} nm	$K^{\sigma,i}/K^{\sigma,d}$	ζ (mV) 1mM 10mM		u^i/u^L
<i>Corynebacterium</i> sp. strain DSM 44016	spherical	1.1	0.8	570	15	-70	-46	0.25 ± 0.05
<i>Corynebacterium</i> sp. strain DSM 6688	elliptical	2.0	0.6	640	40	-48	-33	0.40 ± 0.20
<i>Rhodococcus</i> <i>erythropolis</i> A177	cylindrical	2.9	1.9	1067	13	-102	-60	0.38 ± 0.20
<i>Rhodococcus opacus</i> C125	cylindrical	3.2	1.2	1074	16	-75	-54	0.62 ± 0.20
<i>Bacillus brevis</i>	cylindrical	6.0	1.0	>500	>130	-58	-25	>0.50

Table 1: Estimates of the effective cell radius, a^{eff} , and the averaged ion mobilities in the wall, u^i , normalized on $u^L = 7.52 \times 10^{-8} \text{ m}^2/\text{Vs}$ for the strains studied. ζ -potentials are estimated from the measured electrophoretic mobilities according to ²⁴. u^i is calculated from eq. (10). The conductivity ratio $K^{\sigma,i}/K^{\sigma,d}$ at 0.01 M is calculated from eq. 5 and the Rel values given in fig. 2^A. For further explanation see text.

The calculated surface conductivities, K^σ , for all bacterial cells tend to increase slightly with increasing electrolyte concentrations and are found to be higher for *B. brevis* than for the coryneforms. These trends agree with those for the total surface charge density as determined by proton titrations of isolated cell walls ²⁵, fig. 2^C. For all bacterial cells studied the values for $K^{\sigma,i}/K^{\sigma,d}$ are very high, varying from 13 to >100 , as can be seen in table 1. This means that surface conductance is almost entirely due to the counterions in the bacterial wall, i.e. within the hydrodynamically stagnant layer. Information about the mobilities of the ions at the different electrolyte concentrations in the cell wall matrix is obtained from eq.(10) under the approximation that $\sigma_o \approx -(\sigma_c^i + \sigma_c^d)$. These results are included in table 1 and demonstrate that the ion mobilities in the bacterial wall are of the same order, but lower than those in the bulk solution. The spread in the calculated ion

mobilities in the wall at different electrolyte concentrations is due to the combined effect of errors in the estimates of the total cell wall charge (σ_o), the surface conductivity (K^o), the volume fractions of the cell suspensions and deviations from the spherical shape of the cells. The averaged ion mobilities are used in order to extrapolate values of Rel to low electrolyte concentrations, where direct d.c. conductivity measurements cannot be performed. The calculated curves for Rel as a function of the electrolyte concentration are included in fig. 2A. These curves describe the experimental values for Rel at the higher electrolyte concentrations reasonably well. Moreover, the extrapolated values for Rel at 1mM electrolyte solution for *Corynebacterium* sp. strain DSM 44016 and *Corynebacterium* sp. strain DSM 6688 are in very good agreement with Rel -values as determined by dielectric dispersion measurements, so that the extrapolation procedure is satisfactory.

Dielectric dispersion

Experimental results for the dispersion in the low frequency regime, are given in figures 3a,b for *Corynebacterium* sp. strain DSM 44016 and *Corynebacterium* sp. strain DSM 6688, respectively. In the frequency range 800Hz-500kHz the response showed excellent linear dependency on the volume fraction up to 0.15 of the suspended cells. Below 800 Hz the spread in $\Delta\epsilon_r$ was rather high especially at volume fractions below 2%. Hardly any aggregation was observed for the cells of the two coryneforms studied. Suspensions of the approximately spherical cells of *Corynebacterium* sp. strain DSM 44016 appeared to be homodisperse, as evidenced by light-microscopy. Moreover, the relaxation frequencies for both ΔK and $\Delta\epsilon_r$ agree perfectly with the cell radius, as determined with dynamic light scattering. In the case of *Corynebacterium* sp. strain DSM 6688 the relaxation frequencies for both ΔK and $\Delta\epsilon_r$ are at slightly lower frequencies than expected, corresponding with an effective particle radius, which is about 1.4 times higher than that given in table 1. This may be caused by systematic errors in the estimation of the effective particle radius, although the observed heterodispersity in the cell size may also play a role. The drawn curves in figs 3a,b, are theoretical results for three different values for K^o . They show that the experimental results can be reasonably well described by the Fixman theory, after incorporation of surface conductivity behind the slip plane. Moreover, the measured dielectric and conductivity increment approximately lead to the same estimate for K^o . These K^o and the corresponding Rel values, extracted from the dielectric dispersion measurements at 1 mM electrolyte concentration, are included in the figs 2A, B.

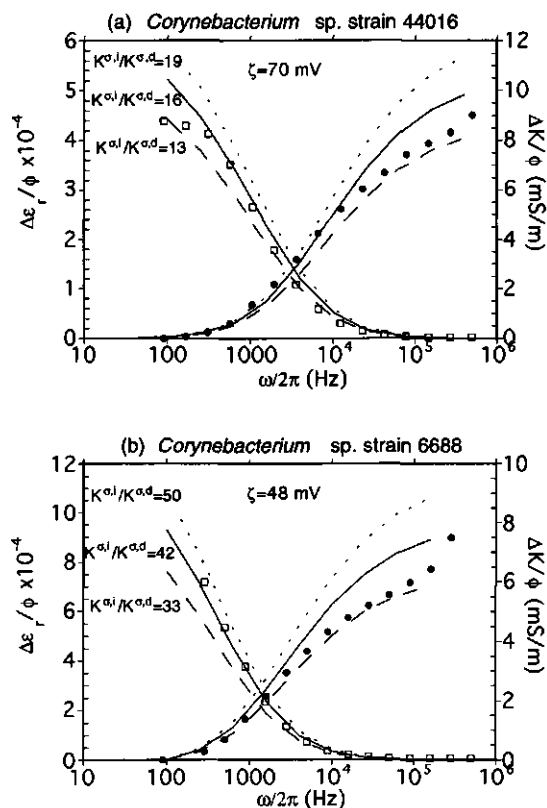


Figure 3: Dielectric dispersion of *Corynebacterium* sp. strain DSM 44016 (a) and *Corynebacterium* sp. strain DSM 6688 (b). (\square) $\Delta\epsilon_r/\phi$ and (\bullet) $\Delta K/\phi$ are measured values. The lines are theoretical curves calculated with the extended Fixman theory according to Kijlstra et al. 13. $a=570$ nm for *Corynebacterium* sp. strain DSM 44016 (a) and $a=890$ nm for *Corynebacterium* sp. strain DSM 6688 (b). (.....), (—), (— — —) are calculated for $K^\sigma = 8.5, 7.2, 5.8$ ($\times 10^{-9}$ S) (a) and $10.6, 9.0, 7.1$ ($\times 10^{-9}$ S) (b) respectively.

Discussion

D.c. conductivity and dielectric dispersion studies provide in principle the same information about electrical double layers. However, the experimental conditions under which these data are obtained are rather different. D.c. conductivity studies require very accurate knowledge of the composition of the background electrolyte, which, especially at low electrolyte concentrations, cannot easily be obtained. The conductivity of the bulk electrolyte may be influenced by phenomena such as leakage of ions through the cytoplasmic membrane and negative adsorption of electrolyte (both leading to an increased bulk conductivity) or by ion uptake in the cytoplasm and specific adsorption of ions (which would decrease the bulk conductivity). These effects, which are expected to vary linearly with the bacterial

cell volume fraction, cannot be easily quantified and the interpretation of the suspension conductivity measurements at low electrolyte concentrations is therefore rather risky. On the other hand, dielectric dispersion measurements of cell suspensions are hardly sensitive to changes in the composition of the background electrolyte. However, the experimental accuracy decreases with increasing electrolyte concentrations, because of the increasingly unfavourable signal to noise ratio. Dielectric measurements are therefore limited to electrolyte concentrations lower than approximately 2 mM¹⁴. In practice, d.c. conductivity and dielectric dispersion studies therefore give complementary information about the occurrence of surface conductance at high and low electrolyte concentrations, respectively.

Correct determination of the volume fractions of the bacterial cell suspensions is another delicate issue, particularly when the cells are non-spherical. An overestimation of the volume fraction would lead to an overestimation of ReI and K^{σ} in d.c. conductivity studies, but to an underestimation of their values in dielectric dispersion studies. Generally, it is believed that the external water fraction in a bacterial cell pellet varies between 30 and 50%¹, which is of the same order as those found for plugs of spherical latex particles²³. According to our estimates, the external water fractions in the bacterial pellets are 30% for *Corynebacterium* sp. strain DSM 44016 and *Bacillus brevis*, 40% for *Corynebacterium* sp. strain DSM 6688 and 50% for *Rhodococcus erythropolis* A177 and *Rhodococcus opacus* C125.

Fixman and O'Brien^{11, 20} have shown, by comparing their analytical equations with exact numerical calculations, that, under the condition of $\kappa a > 50$, the approximation for large κa gives very reliable results for colloidal particles where the diffuse countercharge may be as high as 0.1 C/m². The requirement that surface conductance should be restricted to a sufficiently thin layer holds for the bacterial cells studied, because the cell wall thickness is small (< 10%) in comparison with the particle radius. The fact that the relaxation frequency of the approximately spherical cells of *Corynebacterium* sp. strain DSM 44016 is found to be in excellent agreement with the independently determined cell radius and ion mobilities, is further support for the fact that the high κa double layer theory works reasonably well for spherical bacterial cells.

The error in the estimates for K^{σ} and u^j made by treating non-spherical cells as equivalent spheres, requires some attention. The procedure chosen to assign an effective particle radius is somewhat arbitrary. However, the aspect ratio of the cells of the coryneforms studied is only about 2 or 3, so that alternative averaging procedures also lead to approximately the same estimate for the effective particle

radius. Preliminary analytical equations for the static dipole moment of cylindrical and spheroidal particles show that, treating the non-spherical cells as equivalent spheres, may cause a slight over- or underestimation of ReI and consequently of K'' , depending on the electrolyte concentration^{6, 21}. Previous studies^{25, 26} have shown that the chemical compositions of the cell walls of the various coryneforms are very similar. The surface conductances are therefore also expected to be similar, as appears to be the case.

In the derivation of the analytical equations for the dielectric response, the dielectric permittivity of the particle is assumed to be zero. Nevertheless, the dielectric permittivity of the inner core of the bacterial cells, which is determined by the cytoplasm, will be of the same order as that of the surrounding electrolyte solution. In static electric fields the polarisation of the particle does not change the ion fluxes in the double layer and consequently this dielectric permittivity has no influence on the particle dipole strength. In time-dependent studies, the dielectric constant of the particle only has a minor effect on the dielectric and conductivity increment, as has been shown by comparison with exact numerical results¹¹.

In the high κa approximation it is assumed that the cell surface is impervious for ions, so that the normal component of the ion flux is equal to zero at the surface. For bacterial cells this condition holds, because the ions from the cytoplasm cannot freely pass the cell membrane. These ions are therefore not expected to influence the particle dipole strength.

Analysis of the d.c. conductivity and dielectric measurements based on the high κa approximation leads to consistent estimates of the surface conductance. The values obtained for the ion mobilities in the bacterial wall are physically realistic and support the concept of the bacterial wall as a porous gel-like structure in which the ions are rather mobile due to the relatively high water content.

Conclusions

It can be concluded that the high κa double layer theory as derived by Dukhin, O'Brien and Fixman can be of help in the evaluation of the electrokinetic properties of biological systems such as bacterial cell suspensions. However, these theories should be extended to account for the finite conductivity of ions in the bacterial wall. Development of the theory to include non-spherical particles is necessary. It is remarkable that all Gram-positive bacteria studied, have high surface conductances. Its consequences for the interpretation of the electrophoretic mobility should therefore be considered. It would be of interest to

compare the results obtained with bacterial cells with those of model colloids, of which the hard core is surrounded by a thick polyelectrolyte layer. Unfortunately, these type of experiments have not been performed so far.

The walls of Gram-negative bacteria are less thick than those of the Gram-positive bacteria and also possess a second, outer membrane. For these cells, surface conductance may therefore play a less pronounced, although still considerable, role in electrophoresis studies.

References

1. **Bakker, E. P., H. Rottenberg, S. R. Caplan** 1976. An estimation of the light-induced electrochemical potential difference of protons across the membrane of *Halobacterium Halobium*, *Biochimica Biophysica Acta* **440**, 557-572.
2. **Carstensen, E. L., H. A. Cox, W. B. Mercer, L. A. Natale** 1965. Passive electrical properties of microorganisms. I. Conductivity of *Escherichia coli* and *Micrococcus lysodeikticus*, *Biophys. J.* **5**, 289-299.
3. **Carstensen, E. L., R. E. Marquis** 1968. Passive electrical properties of microorganisms. III. Conductivity of isolated bacterial cell walls., *Biophys. J.* **8**, 536-548.
4. **Carstensen, L. C.** 1967. Passive electrical properties of microorganisms. II. Resistance of the bacterial membrane., *Biophys. J.* **7**, 493-503.
5. **DeLacey, E. H. B., L. R. White** 1981. Dielectric response and conductivity of dilute suspensions of colloidal particles, *J. Chem. Soc. Faraday Trans. 2* **77**, 2007-2039.
6. **Dukhin, S. S.** 1993. Non-equilibrium electric surface phenomena., *Adv Coll Int Sci.* **44**, 1-134.
7. **Dukhin, S. S., B. V. Derjaguin** 1974. Nonequilibrium double layer and electrokinetic phenomena., In *Surface and Colloid Science*, E. Matijevic, Eds. Wiley, New York, 1974, vol. 7.
8. **Dukhin, S. S., N. M. Semenikhin** 1970. *Kolloidn. Zh.* **32**, 360-368.
9. **Dukhin, S. S., V. N. Shilov** 1974. Dielectric phenomena and the double layer in disperse systems and polyelectrolytes, Wiley, New York.
10. **Einolf, W. C., E. L. Carstensen** 1973. Passive electrical properties of microorganisms. V. Low-frequency dielectric dispersion of bacteria., *Biophys. J.* **13**, 8-13.
11. **Fixman, M.** 1983. Thin double layer approximation for electrophoresis and dielectric response, *J. Chem. Phys.* **78**, 1483-1491.
12. **Hunter, R. J.** 1989. Foundations of colloid science, Oxford university press, Oxford, vol. 2, chapter 13, 786-826.

13. **Kijlstra, J., H. P. Van Leeuwen, J. Lyklema** 1992. Effects of surface conductance on the electrokinetic properties of colloids., *J. Chem. Soc. Faraday trans.* **88**, 13441-3449.
14. **Kijlstra, J., R. A. J. Wegh, H. P. Van Leeuwen** 1994. Impedance spectroscopy of colloids, *J. Electroanal. Chem.* **366**, 37-42.
15. **Lyklema, J.** 1995. Fundamentals of interface and colloid science, Academic press, London, vol. II., chapter 4.
16. **Marquis, R. E., E. L. Carstensen** 1973. Electric conductivity and internal osmolality of intact bacterial cells., *J. Bacteriol.* **113**, 1198-1206.
17. **O'Brien, R. W.** 1981. The electrical conductivity of a dilute suspension of charged particles., *J. Colloid Interface Sci.* **81**, 234-248.
18. **O'Brien, R. W.** 1986. The high-frequency dielectric dispersion of a colloid., *J. Colloid Interface Sci.* **113**, 81-93.
19. **O'Brien, R. W.** 1983. The solution of the electrokinetic equations for colloidal particles with thin double layers, *J. Colloid Interface Sci.* **92**, 204-216.
20. **O'Brien, R. W., R. J. Hunter** 1981. The electrophoretic mobility of large colloidal particles., *Can. J. Chem.* **59**, 1878-1887.
21. **O'Brien, R. W., D. N. Ward** 1988. The electrophoresis of a spheroid with a thin double layer, *J. Colloid Interface Sci.* **121**, 402-413.
22. **Teubner, M.** 1983. On the conductivity of a dilute suspension of charged particles., *J. Colloid Interface Sci.* **92**, 284-286.
23. **Van der Put, A. G., B. H. Bijsterbosch** 1980. Electrical conductivity of dilute and concentrated aqueous dispersions of monodisperse polystyrene particles. Influence of surface conductance and double-layer polarization., *J. Colloid Interface Sci.* **75**, 512-524.
24. **Van der Wal, A., Minor, M., W. Norde, J. Lyklema, A. J. B. Zehnder** 1996. The electrokinetic potential of bacterial cells, chapter 5, this thesis.
25. **Van der Wal, A., W. Norde, J. Lyklema, A. J. B. Zehnder** 1996. Determination of the total charge in the cell walls of Gram-positive bacteria, chapter 3, this thesis.
26. **Van der Wal, A., W. Norde, B. Bendinger, A. J. B. Zehnder, J. Lyklema** 1996. The chemical composition of Gram-positive bacterial cell walls and the determination of the cell wall to cell mass ratio, chapter 2, this thesis.
27. **Van Loosdrecht, M. C. M., W. Norde, J. Lyklema, A. J. B. Zehnder** 1990. Hydrophobic and electrostatic parameters in bacterial adhesion., *Aquat. Sci.* **52**, 103-114.

Chapter 5

The electrokinetic potential of bacterial cells

Abstract

Microelectrophoresis studies are of relevance in the characterization of the electrical double layer of bacterial cell surfaces. In order to interpret the electrophoretic mobility in terms of the ζ -potential, the classical Helmholtz-Smoluchowski equation is regularly used. However, this equation has been derived under several more or less restrictive conditions, which are easily violated by complex colloidal systems, such as bacterial cell suspensions.

In recent theories as derived by Dukhin, O'Brien and Fixman, the effect of double layer polarization on the electrophoretic mobility of colloidal particles is accounted for. These theories predict that, at high surface charge densities, the electrophoretic mobility may be strongly retarded compared to the Helmholtz-Smoluchowski equation. In this paper the effect of the mobile charge in the bacterial wall on the electrophoretic mobility is considered. For this purpose a comprehensive equation for the electrophoretic mobility has been derived, which also includes surface conduction within the hydrodynamically stagnant layer. To that end, Fixman's theory, valid for large κa , has been modified.

It is shown that cell wall conduction can have a considerable effect on the electrophoretic mobility of bacterial cells, especially at low salt concentrations. In 1 mM and 10 mM electrolyte solution, the classical Helmholtz-Smoluchowski equation underestimates the ζ -potential by approximately a factor of 2 and 1.3, respectively.

Obviously a full description of the composition of the electrical double layer of bacterial cell surfaces cannot be based on electrophoretic mobility measurements only, but should be obtained from a combination of experimental techniques, including titration and conductivity measurements.

Introduction

Electrophoretic techniques are very powerful tools in the characterization of the electrical double layer of bacterial cell surfaces. In bacterial adhesion studies, for example, electrophoretic mobility measurements are widely performed in order to obtain information about the magnitude of the electrostatic interaction between the bacterial cell and the solid surface. For this purpose the electrokinetic potential (ζ)

is sometimes calculated from the electrophoretic mobility by applying the well known Helmholtz-Smoluchowski equation, which is given by:

$$u = \frac{\epsilon}{\eta} \zeta \quad (1)$$

where u is the electrophoretic mobility, $\epsilon = \epsilon_r^{\text{es}} \epsilon_0$, in which ϵ_r^{es} and ϵ_0 are the relative dielectric constant of the electrolyte solution and the dielectric constant of vacuum, respectively and η the viscosity of the solution ^{2, 20, 39, 45}. The applicability of eq (1) to bacterial cells rests on several assumptions such as: (i) the radius of curvature of the particle surface is large compared to the Debye-screening length (κ^{-1}), (ii) the particle surface is non-conducting, (iii) the applied electric field strength and the field of the double layer are additive, (iv) the charge is homogeneously distributed over the particle surface, (v) the viscosity, dielectric constant and ion conductivities in the double layer, outside the plane of shear, are equal to their bulk values ^{4, 16}. As the validity of all these assumptions for bacterial cells is uncertain, it is nowadays common practice to present experimentally measured electrophoretic mobility values instead of ζ -potentials ^{1, 11, 17, 21, 26, 33, 37}. This approach suffices for many qualitative studies concerning bacterial adhesion, but for a more quantitative analysis, reliable estimates of the electrokinetic potential are required.

For bacterial cells the effect of surface conductance on the electrophoretic mobility has first been considered by Einolf and Carstensen ⁷. In their analysis they apply the Henry and Booth theories for conducting particles ^{3, 12}. However, at low electrolyte concentrations their calculated ζ -potentials are unrealistically high. This is caused by an overestimation of the effect of surface conductance on the electrophoretic mobility, which finds its origin in their ignoring concentration polarization ⁴⁰.

From recent theories as derived by Dukhin et al.⁶, O'Brien et al.²⁷ and Fixman ⁹ for dielectric particles with very thin double layers compared to the particle radius (a), it follows that double layer relaxation can have a considerable effect on the electrokinetic properties of colloidal suspensions. From these theories the large κa approximation of Fixman has been extended in order to account for ion conduction in the hydrodynamically stagnant layer. This extended theory has been used for the analysis of conductivity measurements of bacterial suspensions in order to determine the amount of mobile charge in the bacterial cell wall ⁴¹. This charge determines the particle dipole strength and consequently influences both the static conductivity and the dielectric response of bacterial suspensions. On the other hand, it reduces the electrophoretic mobility at given ζ -potential. In this paper a simplified equation for the electrophoretic mobility is presented from the large κa

theory of Fixman. This equation applies to colloidal particles with high surface conductance and arbitrary ζ -potentials. It is demonstrated that for bacterial cells already for low ζ -potentials deviations from Smoluchowski's equation occur.

In another paper ⁴² it was shown that the charge density of bacterial cell surfaces can be determined from proton titrations with isolated cell walls. In addition, the mobility of the counterions in the cell wall matrix has been established from conductivity measurements ⁴¹. From a combination of these results, surface conductance can be estimated over a wide range of pH-values, which is of relevance in the calculation of the ζ -potential from electrophoretic mobility measurements. Moreover, from a comparison between the ζ -potential and the potential profile, which follows from the solution of the Poisson-Boltzmann equation for the cell wall charge, information about the cell wall flexibility and the position of the plane of shear is obtained.

Theory

The electrokinetic potential of a colloidal particle is not directly measurable, but can be inferred from electrokinetic measurements, such as micro-electrophoresis, provided an appropriate model of the electrical double layer under dynamic conditions is available. The governing equations that have to be considered in order to interpret the electrophoretic velocity are the Poisson and Boltzmann equations for the potential and ion distribution, the ion conservation equations together with the Nernst-Planck equation for the ion fluxes and the Navier-Stokes equation for the fluid flow. These coupled non-linear electrokinetic equations can be linearized provided the applied electric field strength is not too high. Exact numerical solutions for the electrophoretic mobility of spherical particles with arbitrary particle radius have first been given by Wiersema et al.⁴⁴ and have later been improved by O'Brien and White ²⁹. Accurate analytical equations for particles with large ka in a symmetrical electrolyte have been derived by a number of investigators, including Dukhin et al., O'Brien et al. and Fixman ^{6, 9, 27}. These equations may be applied to bacterial cells, provided the mobile charge in the hydrodynamically stagnant layer, i.e. in the bacterial wall, is explicitly taken into account. As shown by Kijlstra et al. ¹⁸ the concept of finite surface conduction behind the plane of shear can easily be incorporated in Fixman's theory, where the co- and counterions are supposed to have the same mobilities. In this theory, the boundary conditions for solving the electrokinetic equations are specified such that the fluid velocity is zero on the plane of shear and equal to minus the electrophoretic velocity far away in the electrolyte solution. The particle surface is assumed to be impenetrable for ions, which means that the ion flux of the

individual species normal to the particle surface should be balanced by their tangential flux. Moreover, far from the particle surface the field strength becomes equal to that of the applied field and the ion concentration to that of the bulk electrolyte solution. In addition to Kijlstra et al.¹⁸, it is assumed that the tangential flux of the co-ions in the double layer is negligibly small. This latter assumption simplifies the analytical equation for the electrophoretic mobility considerably. The following result is obtained²⁴:

$$\frac{\eta F}{\epsilon RT} u = \frac{F\zeta}{RT} + \frac{2\text{Re}l}{1+2\text{Re}l} \left\{ \frac{2}{z} \ln 2 - \frac{2}{z} \ln \left(1 + \exp \left(\frac{zF\zeta}{2RT} \right) \right) \right\} \quad (2)$$

where F is Faraday's constant, R the gas constant, T the absolute temperature, z the valency of the co-ion ($z\zeta > 0$) and $\text{Re}l$ is given by:

$$\text{Re}l = \frac{1}{\kappa a} \left[\left(1 + \frac{K^{\sigma,i}}{K^{\sigma,d}} \right) + 3 \frac{m}{z^2} \right] \left[\exp \left(\frac{zF\zeta}{2RT} \right) - 1 \right] = \frac{1}{K^L a} \left[u^i \sigma_c^i + \left(1 + 3 \frac{m}{z^2} \right) u^L \sigma_c^d \right] \quad (3)$$

in which a is the particle radius, u^L and u^i are the ion mobilities in the bulk and cell wall, respectively and K^L the bulk conductivity. The reciprocal Debye screening length (κ) is given by:

$$\kappa^2 = \frac{2cz^2F^2}{\epsilon RT} \quad (4)$$

in which c is the electrolyte concentration (mol.m^{-3}). The non-dimensional ionic drag coefficient, m , is given by:

$$m = \frac{2\epsilon RT|z|}{3\eta F|u^L|} \quad (5)$$

For the electrolyte solution used in this study, KNO_3 , m is approximately 0.16 at 298 K. The conductivity ratio, $K^{\sigma,i}/K^{\sigma,d}$ is defined by:

$$\frac{K^{\sigma,i}}{K^{\sigma,d}} = \frac{u^i \sigma_c^i}{u^L \sigma_c^d} \quad (6)$$

where σ_c^i the countercharge density due to the counterions in the bacterial wall, $K^{\sigma,i}$ the cell wall conductivity and $K^{\sigma,d}$ the conductivity caused by the diffuse counterions. σ_c^d is the diffuse countercharge due to the excess of counterions:

$$\sigma_c^d = -\frac{2czF}{\kappa} \left[\exp\left(\frac{zF\zeta}{2RT}\right) - 1 \right] \quad (7)$$

The leading term in eq.(2) is the Smoluchowski expression. The effect of surface conduction on the electrophoretic mobility is reflected in the second term, involving Rel. Eq.(2) for the electrophoretic mobility, in the absence of surface conduction behind the plane of shear, ($K^{\sigma,i}/K^{\sigma,d} = 0$), has also been derived by Shubin et al.³⁶ from the large κa theory of Hunter and O'Brien¹⁴.

The effect of surface conduction on the electrophoretic mobility is illustrated in figure 1 for $\kappa a = 56$. If the counterions behind the plane of shear are considered to

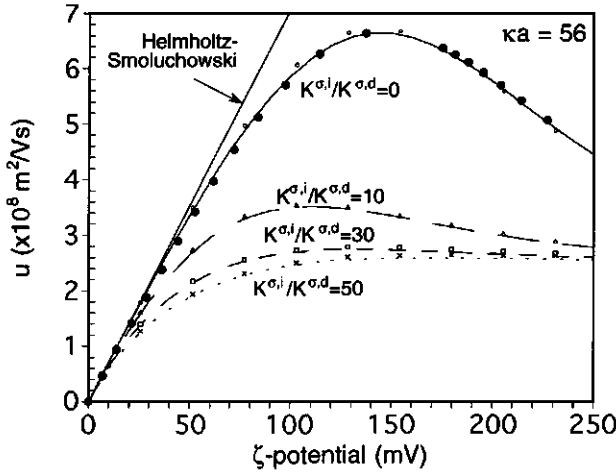


Fig. 1: Electrophoretic mobility versus the ζ -potential for $\kappa a = 56$. The curves are calculated with eq.(2) and the symbols are computed according to the extended Fixman theory of Kijlstra et al.¹⁸. (o —) $K^{\sigma,i}/K^{\sigma,d} = 0$, (Δ —) $K^{\sigma,i}/K^{\sigma,d} = 10$, (\square - -) $K^{\sigma,i}/K^{\sigma,d} = 30$, (x) $K^{\sigma,i}/K^{\sigma,d} = 50$. (●) exact numerical results²⁹ for $K^{\sigma,i}/K^{\sigma,d} = 0$. The Helmholtz-Smoluchowski result is indicated.

be immobile ($K^{\sigma,i}/K^{\sigma,d} = 0$), then the obtained curve approximately coincides with exact numerical solutions of the linearized electrokinetic equations according to O'Brien and White²⁹. The results obtained with eq. (2) show excellent agreement with those calculated with the extended Fixman equation for the mobility according

to Kijlstra et al. ¹⁸. This also justifies the restriction that is made regarding the boundary condition for the co-ion. Fig.1 illustrates that already at relatively low ζ -potentials the electrophoretic mobility is retarded due to surface conduction behind the slip plane and its effect on double layer relaxation. For intermediate to high values of the conductivity ratio ($10 < K^{\sigma,l}/K^{\sigma,d} < 50$) and ζ -potentials higher than 60-70mV, the mobilities become nearly independent of the ζ -potential. Hence, in this region no accurate estimates of the electrokinetic potential can be obtained from electrophoretic mobility measurements.

Materials and methods

Bacterial cultivation and preparation

Corynebacterium sp. strain DSM 6688 and *Corynebacterium* sp. strain DSM 44016 were cultivated in brain heart infusion broth (Merck, 40 g/l deionized water). *Rhodococcus erythropolis* A177, *Rhodococcus opacus* C125 and *Bacillus brevis* ATCC 9999 were cultivated in mineral media as described elsewhere ⁴³. All bacterial cells were grown at 30 °C on a rotary shaker and harvested in the early stationary phase by centrifugation for 10 min at 20,000 x g at 20 °C and washed at least four times in KNO₃ solutions, at concentrations according to the experimental needs.

Electrophoresis

The electrophoretic mobilities of the bacterial cells were measured in KNO₃ solutions at 22 °C with a laser-Doppler velocimetric device (Zetasizer 3; Malvern Instruments, Ltd., Worcestershire, Great Britain). The applied field strength was approximately 2500 V/m. Velocity measurements were performed at least at two positions in the capillary. The pH of the diluted cell suspensions was adjusted by adding HNO₃ or KOH of the same ionic strength and its value was determined before and after the mobility measurements.

Potential profile across the bacterial wall

The electrical potential, $\psi(x)$, in the bacterial wall and in the surrounding electrolyte solution is related to the space charge density, $\rho(x)$, according to the Poisson equation, which for a flat geometry is given by:

$$\frac{d^2\psi}{dx^2} = -\frac{\rho(x)}{\epsilon} \quad (8)$$

in which x is the normal distance from the bacterial surface with its origin at the interface between the wall and the surrounding electrolyte solution. The dielectric constant (ϵ) in the bacterial wall may deviate from that in the electrolyte solution. Outside the bacterial wall, the space charge density is fully determined by the distribution of the electrolyte ions, whereas inside the wall the fixed charges (ρ_{fix}), which are assumed to be homogeneously distributed, also contribute. Equation 8 is solved numerically according to the integration procedure of Runge-Kutta together with the Newton-Raphson iteration method³⁸. In the inner core of the bacterial wall, the potential is approximately constant, because all fixed cell wall charges are fully compensated by electrolyte ions. One boundary condition is therefore given by: $d\psi/dx = 0$ in the inner core. The other boundary condition is obtained from the continuity condition at the interface between the wall and the electrolyte solution: $\epsilon_r^{\text{cw}} (d\psi/dx)_{x \uparrow 0} = \epsilon_r^{\text{es}} (d\psi/dx)_{x \downarrow 0}$, in which $(d\psi/dx)_{x \downarrow 0} = -\sqrt{8cRT/\epsilon} \sinh(F\psi_0/2RT)$. ψ_0 is the potential at $x=0$. The relative dielectric constant of the cell wall material (ϵ_r^{cw}) is chosen equal to 60.

Results

The effect of the cell wall charge density and the extent of screening of this charge by counter- and co-ions were investigated by measuring the electrophoretic mobility as a function of the pH and the concentration of the electrolyte solution. The results, presented in fig.'s 2^{a-e}, demonstrate that the absolute values of the electrophoretic mobility of the different bacterial cells generally increase with the increasing cell wall charge and decrease with increasing electrolyte concentration. For all electrolyte concentrations studied it appears that with increasing pH the electrophoretic mobilities level off or that even their absolute values diminish, for instance as with the coryneform bacteria in 1 mM electrolyte solution. In addition, three of the four coryneforms investigated show that at neutral pH the absolute value of the electrophoretic mobility hardly increases when the electrolyte concentration is decreased from 10 mM to 1 mM and at high pH-values even slightly decreases.

The isoelectric point (i.e.p.) of all bacterial cells except for those of *Rhodococcus erythropolis* A177 is found to be at slightly lower pH-values (0.2-0.7) than the point of zero charge (p.z.c.) as determined from proton titrations with isolated cell walls⁴², see table 1. The difference between the i.e.p. and the p.z.c. may be caused by specific adsorption of anions to the hydrophobic cell walls. This phenomenon

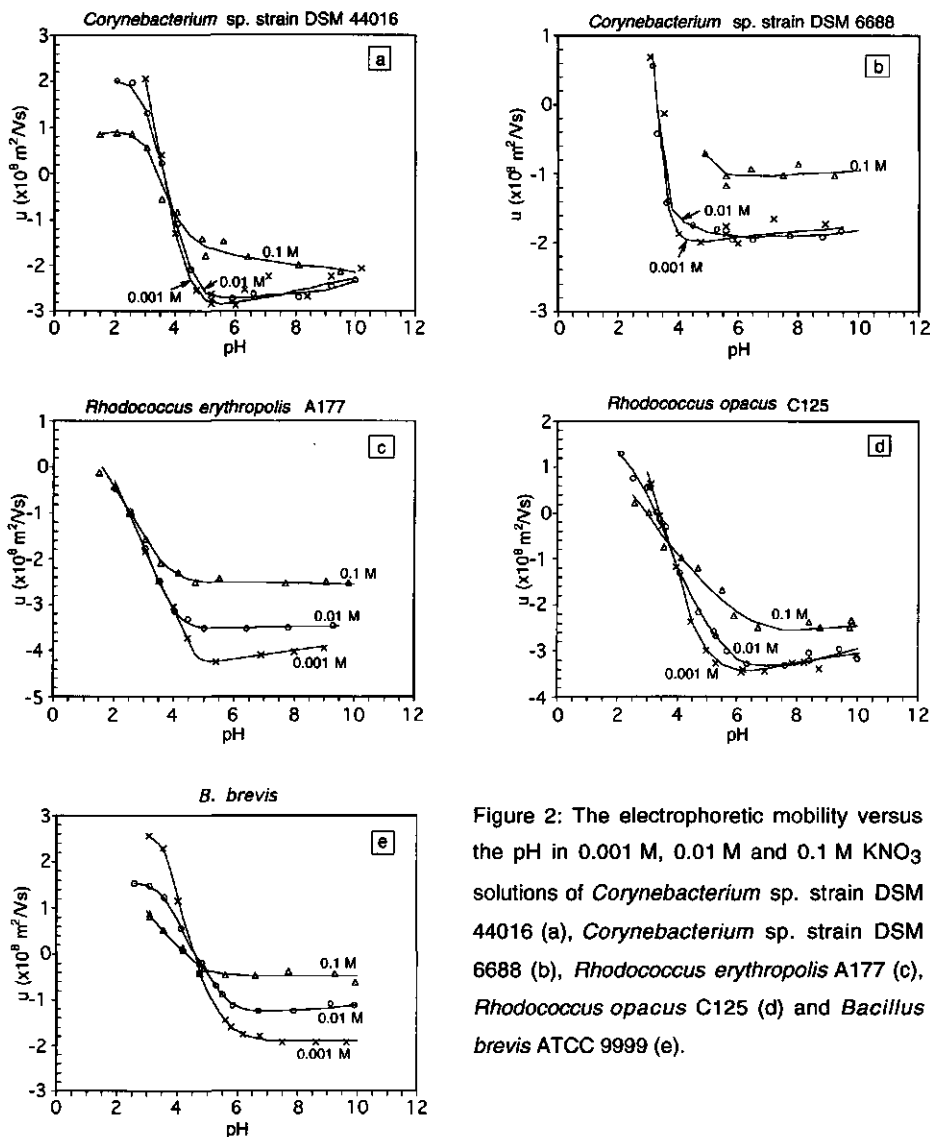


Figure 2: The electrophoretic mobility versus the pH in 0.001 M, 0.01 M and 0.1 M KNO₃ solutions of *Corynebacterium* sp. strain DSM 44016 (a), *Corynebacterium* sp. strain DSM 6688 (b), *Rhodococcus erythropolis* A177 (c), *Rhodococcus opacus* C125 (d) and *Bacillus brevis* ATCC 9999 (e).

would also explain the shift of the i.e.p. to lower pH-values in 0.1 M electrolyte solution. The difference between the p.z.c. and the i.e.p. for *Rhodococcus erythropolis* A177 is more than 2 pH-units and has been ascribed to the presence of a thin polysaccharide layer on the cell surface^{34, 42}.

strain	Length μm	width μm	a^{eff} nm	d_{cw} nm	p.z.c.	i.e.p. 1 mM	$u^{\text{I}}/u^{\text{L}}$
<i>Corynebacterium</i> sp. strain DSM 44016	1.1	0.8	570	60	3.8	3.6	0.25
<i>Corynebacterium</i> sp. strain DSM 6688	2.0	0.6	640	35	3.7	3.3	0.40
<i>Rhodococcus</i> <i>erythropolis</i> A177	2.9	1.9	1067	35	4.0	<2	0.38
<i>Rhodococcus opacus</i> C125	3.2	1.2	1074	35	4.1	3.4	0.62
<i>Bacillus brevis</i>	6.0	1.0	>500	75	5.1	4.6	>0.50

Table 1: Summary of relevant characteristics of the bacterial cells studied. a^{eff} is the effective cell radius, d_{cw} is the cell wall thickness as determined by electron microscopy, $u^{\text{I}}/u^{\text{L}}$ the relative mobility of a potassium ion in the wall compared to that in the bulk solution.

Surface conductivity in the bacterial wall is expressed in terms of the Rel-parameter given by eq. (3). The mobile charge density is computed under the assumption that $\sigma_0 \approx -(\sigma_c^+ + \sigma_c^-)$, where the cell wall charge density (σ_0) has been determined from proton titrations with isolated cell walls⁴². The mobility of the counterions in the bacterial wall, included in table 1, has been extracted from conductivity measurements⁴¹. The relations between the calculated Rel-parameter and the pH of the electrolyte solution are graphically displayed in fig. 3,

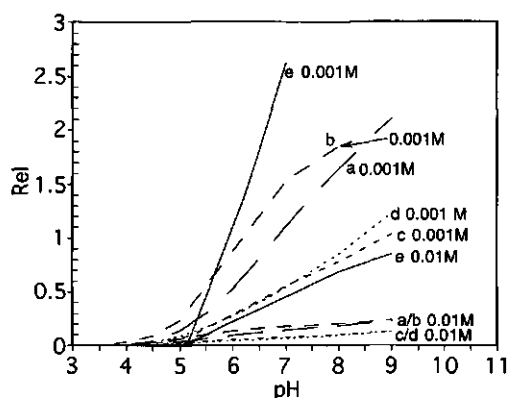


Figure 3: Values for Rel calculated from the total surface charge (σ_0) and the ion conductivities in the bacterial wall for: *Corynebacterium* sp. strain DSM 44016 (a) (— —), *Corynebacterium* sp. strain DSM 6688 (b) (— —), *Rhodococcus erythropolis* A177 (c) (---), *Rhodococcus opacus* C125 (d) (.....) and *Bacillus brevis* ATCC 9999 (e) (— · —).

for negatively charged cell walls. These results show that Rel may reach high values at low electrolyte concentrations, because then there is a high amount of mobile charge in the bacterial wall, whereas the bulk conductivity is relatively low.

With increasing electrolyte concentrations Rel gradually diminishes, as expected. In 0.1 M electrolyte solution, surface conductivity becomes negligible in comparison with the bulk conductivity resulting in negligibly low values for Rel .

In fig.'s 4^{a-e} a comparison is made between ζ -potentials, calculated according to eq. (2), which includes surface conductance and those computed from the classical Helmholtz-Smoluchowski equation. In 0.1 M salt concentration eq.(2) and the Helmholtz-Smoluchowski equation lead to the same estimate for the ζ -potential. In 10 mM and in 1 mM electrolyte solution the Helmholtz-Smoluchowski equation only applies if the cell wall charge density is low, i.e. for pH-values that are very close to the i.e.p. In all other cases, ζ -potentials, calculated according to eq. (2), may deviate considerably from those obtained from the Helmholtz-Smoluchowski equation, especially at low electrolyte concentrations. At neutral pH for example, the ζ -potential according to the Helmholtz-Smoluchowski equation is underestimated by approximately a factor of 2 and 1.3 in 1 mM and 10 mM electrolyte solution, respectively. Unfortunately, the accuracy of the estimated ζ -potentials decreases with increasing Rel , because surface conduction makes the electrophoretic mobility less sensitive to changes in the electrokinetic potential, see fig.1.

In order to calculate the potential profile across the bacterial wall, information about the cell wall thickness is required. The walls of the coryneforms are flexible structures and have been found to expand and contract in response to changes in the electrolyte concentration^{32, 42}. As a first approximation, it is assumed that the walls may shrink by a factor of 2 and 4 in 10 mM and 100 mM, respectively in comparison with 1 mM electrolyte solution. The walls of the *B. brevis* cells are much more rigid due to the presence of a dense protein rich surface layer⁴³. The thickness of these walls is therefore supposed to be insensitive to the bulk electrolyte concentration.

Potential profiles across the bacterial walls and the surrounding electrolyte solution at neutral pH are given in fig. 5. It appears that the potential rapidly decays in the outermost layers of the bacterial surface, while inside the bacterial wall it remains approximately constant. Previously, such constant potentials have been identified as Donnan potentials⁴².

Table 2 shows that the surface potential (ψ_o), i.e. the potential at the cell wall-solution-interface, at position $x=0$, is strongly influenced by the salt concentration, which indicates that the cell wall charge is effectively screened by the electrolyte. In the same table a comparison is made between the surface potential and the ζ -potential. For bacterial cells that have rather smooth surfaces, the position of the

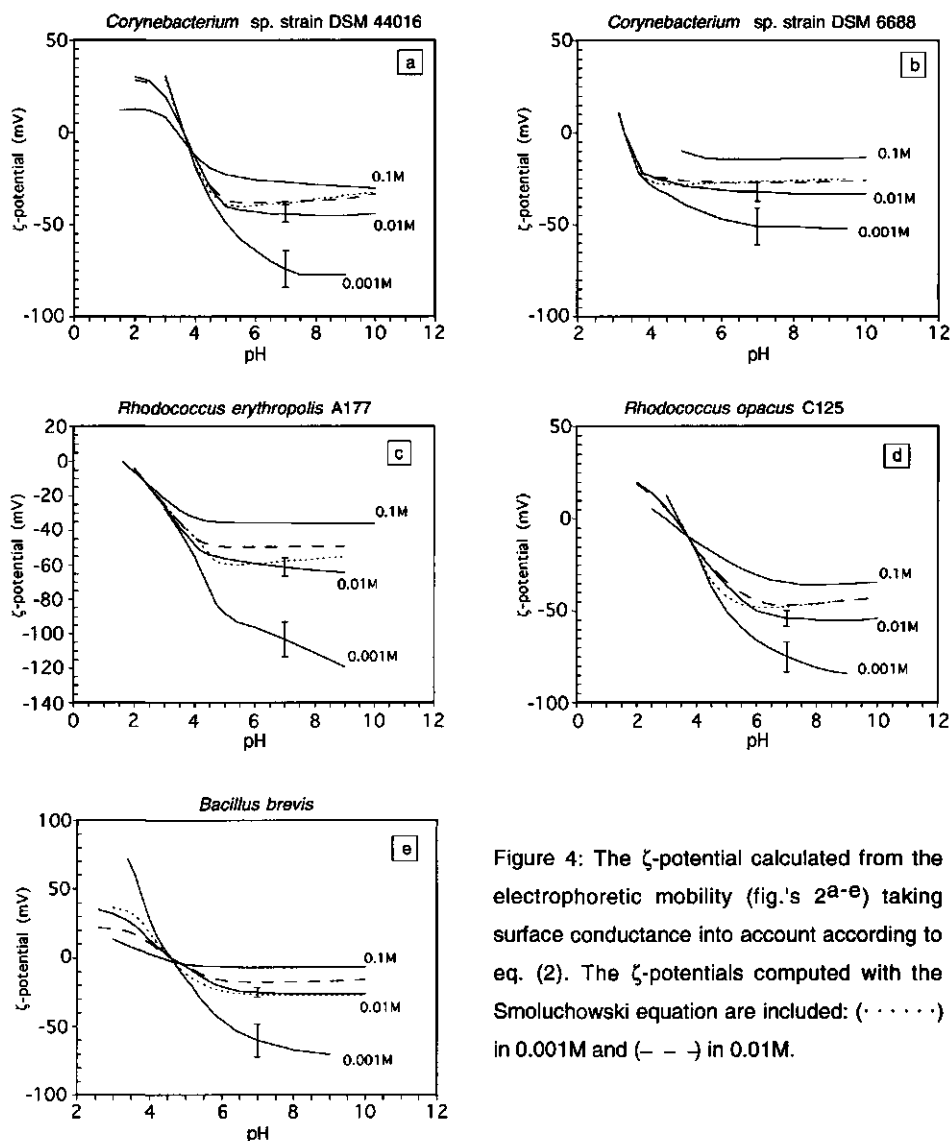


Figure 4: The ζ -potential calculated from the electrophoretic mobility (fig.'s 2a-e) taking surface conductance into account according to eq. (2). The ζ -potentials computed with the Smoluchowski equation are included: (\cdots) in 0.001M and ($- - -$) in 0.01M.

plane of shear is expected to be at a distance of only a few molecular water layers from the cell surface. For those cells the ζ -potential should therefore be close, although somewhat lower, than the surface potential. On the other hand, protruding cell wall polymers may shift the slip plane further away into the

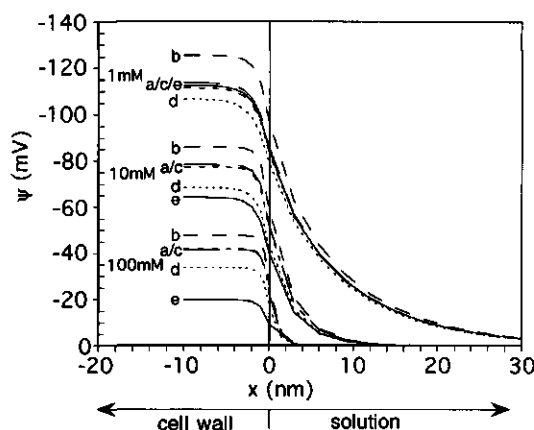


Figure 5: Potential profiles across the bacterial wall and the surrounding electrolyte solution at neutral pH, according to the Poisson-Boltzmann equation (eq. 8). For the coryneforms at 10 mM and 100 mM calculations have been made for d_{cw} values, which are resp. 2 and 4 times lower than those given in table 1. *Corynebacterium* sp. strain DSM 44016 (a) (— —), *Corynebacterium* sp. strain DSM 6688 (b) (— —), *Rhodococcus erythropolis* A177 (c) (— · —), *Rhodococcus opacus* C125 (d) (·····) and *Bacillus brevis* (e) (———).

Table 2

strain	σ_0 (C/m ²)			ψ_0 (mV)			ζ (mV)		
	1mM	10mM	100mM	1mM	10mM	100mM	1mM	10mM	100mM
<i>Corynebacterium</i> sp. strain DSM 44016	-0.50	-0.60	-0.70	-86	-52	-23	-74	-44	-27
<i>Corynebacterium</i> sp. strain DSM 6688	-0.45	-0.47	-0.53	-98	-60	-27	-51	-32	-15
<i>Rhodococcus erythropolis</i> A177	-0.28	-0.36	-0.49	-86	-52	-23	-103	-61	-36
<i>Rhodococcus opacus</i> C125	-0.22	-0.24	-0.29	-79	-44	-18	-75	-54	-35
<i>Bacillus brevis</i>	-0.56	-0.90	-1.23	-85	-40	-10	-60	-25	-7

Table 2: Comparison between the surface potential (ψ_0) and the ζ -potential at neutral pH.

electrolyte solution and consequently the ζ -potential may be quite a bit lower than the surface potential. For the coryneforms, except for *Corynebacterium* sp. strain DSM 6688, and the *B. brevis* strain the difference between the ζ -potential and the surface potential is less than approximately 10 à 20 mV. This suggests that the distance between the surface and the slip plane for these cells is not more than approximately 1 or 2 nm. The systematically lower values for the ζ -potential compared to the surface potential of *Corynebacterium* sp. strain DSM 6688 indicates the presence of a rough surface. For this strain cell wall polymers may protrude into the surrounding electrolyte solution, shifting the slip plane away from the cell surface over distances up to 4 à 5 nm.

Discussion

The analytical equation (2) for the electrophoretic mobility is based on several more or less restrictive assumptions and its applicability to bacterial cells therefore requires some attention.

In the linearisation of the electrokinetic equations only first order perturbation terms in the applied field (E) have been considered. As shown by Hunter¹⁴, this condition holds as long as $FaERel/RT \ll 1$. Although the electrophoresis measurements have been performed at rather high electric field strengths, the linearisation condition of the electrokinetic equations was satisfied as $FaERel/RT$ for all measurements was at least one order less than unity.

The cytoplasmic membrane prevents the flux of ions into the cell interior. This membrane therefore, *de facto*, plays the role of an impenetrable surface. The inner part of the bacterial cell therefore behaves as a dielectric particle. For this reason, the flux balance is not influenced by any property of the cytoplasm. The problem of calculating the electrokinetic potential from the electrophoretic mobility for bacterial cells is therefore similar to that of non-conducting inorganic particles^{29, 31}.

The dielectric constant of the bacterial wall influences the distribution of the co- and counterions in the wall and the surrounding electrolyte solution and therefore has some influence on the computed surface potential (ψ_0). However, its value does not affect the Donnan potential, because inside the bacterial wall the space charge density is approximately zero. Due to the high water content in the cell walls the dielectric constant should be close to that of the electrolyte solution. Considering that for $40 < \epsilon_r^{cw} < 80$, the uncertainty in the computed surface potential is less than 5%, it is concluded that in this respect ϵ_r^{cw} is an insensitive parameter.

For the diffuse part of the double layer the dielectric constant and the viscosity are expected to be equal to their bulk values, because the obtained ζ -potentials are sufficiently low to neglect viscoelectric effects and dielectric saturation²³.

Generally, the electrophoretic mobility of a bacterial cell is not only dependent on its size, but also on its shape. However, the aspect ratios of the bacterial cells studied are not more than approximately 2 or 3 and the effect of the shape of the particle on the electrophoretic mobility is therefore expected to be small²⁸. In those cases, where the double layer thickness is very thin in comparison with the radius of curvature of the particle surface and under the condition that surface conduction is negligible, the mobility becomes independent of both particle radius and particle shape^{25, 31}.

Furthermore, it is assumed that the charge in the bacterial wall is homogeneously smeared out, leading to a uniform ζ -potential on the cell surface. For other charge distributions, the interpretation of the electrophoretic mobility is considerably more complicated⁸ and without further information no unambiguous conclusions can be drawn.

At salt concentrations up to 0.01 M maximum expulsion of co-ions already occurs at relatively low cell wall charge densities⁴². Because of this, only the counterions have been considered in the derivation of eq.(2). However, at pH values very close to the i.e.p. the co- and counterions equally contribute to the surface conductivity and one may argue that in this case eq.(2) may not be applied. However, close to the i.e.p. the absolute value for $\text{Re}l$ is negligibly small, because of the low surface charge density. Eq.(2) is then approximately equal to the Helmholtz-Smoluchowski's equation (1) and therefore remains valid.

In order to compute the surface potential (ψ_o), the cell wall thickness had to be estimated at the various salt concentrations. For the coryneforms it was assumed that the walls may shrink by a factor of 2 and 4 in 10 mM and 100 mM electrolyte solution. If, for example, the cell walls are considered to be rigid, the surface potential would approximately be 40 mV at 10 mM and 10 mV at 100 mM electrolyte solution, respectively. However, these values are certainly too low to account for the high ζ -potentials at these salt concentrations. Our results and those of others³² suggest that the walls of the coryneforms are flexible structures that may swell or shrink upon changes in the salt concentration.

Unfortunately, the exact position of the slip plane is still uncertain. Nevertheless, for a homogeneous smooth surface it is generally assumed that the stagnant layer is only a few molecular layers thick^{15, 22}. Some authors^{5, 30} account for electro-osmotic flow in the surface layer of biological cells. However, this is very unlikely as experiments have shown that the position of the plane of shear is mainly determined by the extension of protruding tails in the surrounding solution¹⁰. For bacterial cells this implies that the thickness of the hydrodynamically stagnant layer is mainly determined by the cell wall and that the plane of shear will be situated in the very outermost surface layer, where the density of the cell wall polymers becomes very low.

ζ -potentials calculated according to the classical Helmholtz-Smoluchowski equation show a much weaker dependence on the salt concentration than as expected from calculations of the surface potential. In addition, three of the four coryneforms hardly show any change in the electrophoretic mobility, if the salt concentration is changed from 10 mM to 1 mM. According to the Helmholtz-Smoluchowski equation the ζ -potentials for these two salt concentrations would be

approximately equal. However, ζ -potentials calculated with eq.(2), in which surface conductance is incorporated, are increasing functions of the pH and salt concentrations, as would be expected from the classical Gouy-Chapman theory for the electrical double layer.

Conclusions

The necessity to incorporate surface conduction behind the shear plane in electrophoresis studies is nowadays well established. Its occurrence not only accounts for the discrepancies in the ζ -potentials estimated from different electrokinetic techniques, but it also explains the sometimes observed spurious dependence of the electrophoretic mobility on the electrolyte concentration^{13, 19, 35, 40, 46}. In the present study it has been shown that such surface conduction may also play a considerable role in the interpretation of the electrophoretic mobility of natural colloids such as bacterial cells. In the classical Helmholtz-Smoluchowski equation the effect of surface conductance on the electrophoretic mobility is not accounted for. Consequently, the ζ -potential according to this equation may be seriously underestimated, especially at low electrolyte concentrations.

In fact, bacterial cell suspensions may even be better model systems for surface conduction studies than the generally used inorganic colloids. The amount of mobile charge can rather accurately be determined for a wide range of pH values and electrolyte concentrations and is almost entirely situated in the bacterial wall, i.e. in the hydrodynamical stagnant layer.

Acknowledgement

The authors thank Dr. P. A. Barneveld for his help with the numerical solution of the Poisson-Boltzmann equation.

References

1. **Bayer, M. E., J. L. Sloyer** 1990. The electrophoretic mobility of Gram-negative and Gram-positive bacteria: an electrokinetic analysis, *J. Gen. Microbiol.* **136**, 867-874.

2. **Blake II, R. C., E. A. Shute, G. T. Howard** 1994. Solubilization of minerals by bacteria: electrophoretic mobility of *Thiobacillus ferrooxidans* in the presence of iron, pyrite, and sulphur., *Appl. Environ. Microbiol.* **60**, 3349-3357.
3. **Booth, F.** 1948. Surface conductance and cataphoresis, *Trans. Faraday Soc.* **44**, 955-959.
4. **Brinton, C. C., M. A. Lauffer** 1959. The electrophoresis of viruses, bacteria, and cells, and the microscope method of electrophoresis., In *Electrophoresis, theory, methods and applications.*, M. Bier, Eds. Academic press, New York, vol. 1, 427-492.
5. **Donath, E., A. Voigt** 1986. Electrophoretic mobility of human erythrocytes, *Biophys. J.* **49**, 493-499.
6. **Dukhin, S. S., B. V. Derjaguin** 1974. Nonequilibrium double layer and electrokinetic phenomena., In *Surface and Colloid Science*, E. Matijevic, Eds. Wiley, New York, 1974, vol. 7.
7. **Einolf, C. W., E. L. Carstensen** 1967. Bacterial conductivity in the determination of surface charge by microelectrophoresis, *Biochim. Biophys. Acta* **148**, 506-516.
8. **Fair, M. C., J. L. Anderson** 1989. Electrophoresis of nonuniformly charged ellipsoidal particles, *J. Colloid Interface Sci.* **127**, 388-400.
9. **Fixman, M.** 1983. Thin double layer approximation for electrophoresis and dielectric response, *J. Chem. Phys.* **78**, 1483-1491.
10. **Fleer, G. J., M. A. Cohen Stuart, J. M. H. M. Scheutjens, T. Cosgrove, B. Vincent** 1993. Polymers at interfaces, Chapman & Hall, London, chapter 5.
11. **Furr, J. R., G. Davies, A. R. A. Adebiti, A. D. Russell** 1981. A novel method of assaying antimicrobial agents by particle microelectrophoresis, *J. Appl. Bacteriol.* **50**, 173-176.
12. **Henry, D. C.** 1948. The electrophoresis of suspended particles. IV. The surface conductivity effect., *Trans. Faraday Soc.* **44**, 1021-1026.
13. **Hidalgo-Alvarez, R., J. A. Moleon, F. J. De las Nieves, B. H. Bijsterbosch** 1992. Effect of anomalous surface conductance on ζ -potential determination of positively charged polystyrene microspheres, *J. Colloid Interface Sci.* **149**, 23-26.
14. **Hunter, R. J.** 1989. Foundations of colloid science, Oxford university press, Oxford, vol. 2, chapter 13, 786-826.
15. **Hunter, R. J.** 1981. The zeta potential in colloid science, principles and applications, Academic press, London.
16. **James, A. M.** 1991. Charge properties of microbial cell surfaces, In *Microbial cell surface analysis*, N. Mozes, P. S. Handley, H. J. Busscher, P. G. Rouxhet, Eds. VCH Publishers, inc. 221-262.
17. **James, A. M.** 1982. The electrical properties and topochemistry of bacterial cells, *Advan. Colloid Interface. Sci.* **15**, 171-221.
18. **Kijlstra, J., H. P. Van Leeuwen, J. Lyklema** 1992. Effects of surface conductance on the electrokinetic properties of colloids., *J. Chem. Soc. Faraday trans.* **88**, 3441-3449.

19. **Kijlstra, J., H. P. Van Leeuwen, J. Lyklema** 1993. Low-frequency dielectric relaxation of hematite and silica sols, *Langmuir* **9**, 1625-1633.
20. **Krekeler, C., H. Ziehr, J. Klein** 1991. Influence of physicochemical bacterial surface properties on adsorption to inorganic porous supports, *Appl. Microbiol. Biotechnol.* **35**, 484-490.
21. **Krekeler, C., H. Ziehr, J. Klein** 1989. Physical methods for characterization of microbial cell surfaces, *Experientia* **45**, 1047-1055.
22. **Lyklema, J.** 1994. On the slip process in electrokinetics, *Colloids Surf.* **92**, 41-49.
23. **Lyklema, J., J. T. G. Overbeek** 1961. On the interpretation of electrokinetic potentials, *J. Colloid Interface Sci.* **16**, 501-512.
24. **Minor, M., A. van der Wal, J. Lyklema** Dielectric spectroscopy of model colloids and the role of conduction behind the plane of shear. Theory and experiments. Nato Advances Research Workshop on 'Fine particles science and technology from micro to nanoparticles' Ed. E. Pelizzetti, Maratea, Italy, July 15-21, 1995. in press.
25. **Morrison, F. A.** 1970. Electrophoresis of a particle of arbitrary shape, *J. Colloid and Interface Sci.* **34**, 210-214.
26. **Mozes, N., A. J. Léonard, P. G. Rouxhet** 1988. On the relations between the elemental surface composition of yeasts and bacterial and their charge and hydrophobicity, *Biochim. Biophys. Acta* **945**, 324-334.
27. **O'Brien, R. W., R. J. Hunter** 1981. The electrophoretic mobility of large colloidal particles., *Can. J. Chem.* **59**, 1878-1887.
28. **O'Brien, R. W., D. N. Ward** 1988. The electrophoresis of a spheroid with a thin double layer, *J. Colloid Interface Sci.* **121**, 402-413.
29. **O'Brien, R. W., L. R. White** 1978. Electrophoretic mobility of a spherical colloidal particle, *J. Chem. Soc. Faraday Trans. 2*, 1607-1626.
30. **Ohshima, H., T. Kondo** 1991. On the electrophoretic mobility of biological cells., *Biophys. Chem.* **39**, 191-198.
31. **Overbeek, J. T. G., P. H. Wiersema** 1967. The interpretation of electrophoretic mobilities. In *Electrophoresis, theory methods and applications*, M. Bier, Eds. Academic press, New York, vol. 2, 1-52.
32. **Plette, A. C. C., W. H. Van Riemsdijk, M. F. Benedetti, A. Van der Wal** 1995. pH dependent charging behaviour of isolated cell walls of a Gram-positive soil bacterium., *J. Colloid Interface Sci.* **173**, 354-363.
33. **Richmond, D. V., D. J. Fisher** 1973. The electrophoretic mobility of micro-organisms, *Advan. Microbial Physiol.* **9**, 1-29.
34. **Rijnaarts, H. H. M., W. Norde, E. J. Bouwer, J. Lyklema, A. J. B. Zehnder** 1993. Bacterial adhesion under static and dynamic conditions., *Appl. Environ. Microbiol.* **59**, 3255-3265.

35. **Rosen, L. A., D. A. Saville** 1991. Dielectric spectroscopy of colloidal dispersions: comparisons between experiment and theory., *Langmuir* **7**, 36-42.
36. **Shubin, V. E., R. J. Hunter, R. W. O'Brien** 1993. Electroacoustic and dielectric study of surface conductance, *J. Colloid Interface Sci.* **159**, 174-183.
37. **Solarí, J. A., G. Huerta, B. Escobar, T. Vargas, R. Badilla-Ohlbaum, J. Rubio** 1992. Interfacial phenomena affecting the adhesion of *Thiobacillus ferrooxidans* to sulphide mineral surfaces, *Colloids Surf.* **69**, 159-166.
38. **Stoer, J., R. Bullirsch** 1993. Introduction to numerical analysis, Springer-Verlag, New York.
39. **Van der Mei, H. C., A. J. Léonard, A. H. Weerkamp, P. G. Rouxhet, H. J. Busscher** 1988. Properties of oral streptococci relevant for adherence: zeta potential, surface free energy and elemental composition, *Colloids Surf.* **32**, 297-305.
40. **Van der Put, A. G., B. H. Bijsterbosch** 1980. Electrical conductivity of dilute and concentrated aqueous dispersions of monodisperse polystyrene particles. Influence of surface conductance and double-layer polarization., *J. Colloid Interface Sci.* **75**, 512-524.
41. **Van der Wal, A., M. Minor, W. Norde, A. J. B. Zehnder, J. Lyklema** 1996. Conductivity and dielectric dispersion of Gram-positive bacterial cells, chapter 4, this thesis.
42. **Van der Wal, A., W. Norde, J. Lyklema, A. J. B. Zehnder** 1996. Determination of the total charge in the cell walls of Gram-positive bacteria, chapter 3, this thesis.
43. **Van der Wal, A., W. Norde, B. Bendinger, A. J. B. Zehnder, J. Lyklema** 1996. The chemical composition of Gram-positive bacterial cell walls and the determination of the cell wall to cell mass ratio, chapter 2, this thesis.
44. **Wiersema, P. H., A. L. Loeb, J. T. G. Overbeek** 1966. Calculation of the electrophoretic mobility of a spherical colloid particle, *J. Colloid Interface Sci.* **22**, 78-99.
45. **Yelloji Rao, M. K., P. Somasundaran, K. M. Schlilling, B. Carson, K. P. Ananthapadmanabhan** 1993. Bacterial adhesion onto apatite minerals-electrokinetic aspects, *Colloids Surf. A* **79**, 293-300.
46. **Zukoski IV, C. F., D. A. Saville** 1986. The interpretaion of electrokinetic measurements using a dynamic model of the stern layer. I and II, *J. Colloid Interface Sci.* **114**, 32-44 and 45-53.

Summary and concluding remarks

Bacterial cells are ubiquitous in natural environments and also play important roles in domestic and industrial processes. They are found either suspended in the aqueous phase or attached to solid particles. The adhesion behaviour of bacteria is influenced by the physico-chemical properties of their cell surfaces, such as hydrophobicity and cell wall charge. The charge in the bacterial wall originates from carboxyl, phosphate and amino groups. The degree of dissociation of these anionic and cationic groups is determined by the pH and the activity of the surrounding electrolyte solution. Almost all bacterial cells are negatively charged at neutral pH, because the number of carboxyl and phosphate groups is generally higher than that of the amino groups. The presence of the charged cell wall groups leads to the spontaneous formation of an electrical double layer. The purpose of the present investigation is to elucidate the structure of the electrical double layer of bacterial cell surface. Such a study serves at least two goals. It allows the quantification of electrostatic interactions in the adhesion process and it contributes to gain better insight into the availability of (in)organic compounds for bacterial cells.

The characteristics of the electrical double layer of bacterial cell surfaces have been revealed by applying a combination of experimental techniques, which include: chemical cell wall analysis, potentiometric proton titration and electrokinetic studies such as micro-electrophoresis, static conductivity and dielectric dispersion measurements.

For the present study five Gram-positive bacterial strains, including four coryneforms and a *Bacillus brevis*, have been selected. Cell walls of these bacterial strains have been isolated and were subsequently subjected to chemical analyses and proton titration studies. Both methods provide information on the number of carboxyl, phosphate and amino groups.

The chemical analysis of isolated cell walls involves the quantitative determination of both peptidoglycan and protein content. These analyses indicate that the chemical composition of the walls of the coryneforms are very similar, but considerably different from that of *Bacillus brevis*. Peptidoglycan is an important cell wall constituent of the coryneform bacteria and determines about 23 to 31 % of the cell wall dry weight. The protein fractions are somewhat lower, between 7 to 14%. The cell wall structure of the *Bacillus brevis* strain is more complex and multi-layered. It contains a thin peptidoglycan layer, which only determines 5 % of the cell wall dry weight. On the other hand, the protein content of these walls is

higher than 56%. These proteins most likely can be attributed to a so-called S(urface)-layer, which is the outermost cell wall layer.

The surface charge density of the bacterial cells is assessed by proton titrations of isolated cell walls at different electrolyte concentrations. Rather high values, i.e. between 0.5 and 1.0 C/m² are found at neutral pH. The absence of hysteresis in the titration curves leads to the conclusion that the charging process can be considered as reversible. It also implies that the cell wall charge is continuously in equilibrium with the surrounding electrolyte solution, at any pH and salt concentration. This observation considerably facilitates the interpretation of the titration curves, because it allows a rigorous (thermodynamic) analysis. The anionic and cationic groups in the bacterial wall could be identified and their numbers determined by representing the differential titration curves as functions of pH and cell wall charge. The carboxyl and phosphate groups are almost entirely titrated in the pH range accessible by proton titration, allowing precise estimation of their numbers. These numbers compare very well with those based on a chemical analysis of the isolated cell walls. Estimates for the number of amino groups were less accurate, because these groups are only partly titrated in the pH range where precise titration measurements are feasible. Nevertheless, it could be concluded that the number of amino groups in the bacterial wall are lower than those of the carboxyl groups.

Information about the ionic composition of the countercharge has been obtained from Esin-Markov analysis of the titration curves and from estimates of the cell wall potential based on a Donnan-type model. The Esin-Markov analysis is purely thermodynamic and based on first principles, whereas the Donnan model requires several assumptions about the structure of the bacterial wall. Both approaches lead to the same conclusion that at salt concentrations below 0.01 M the cell wall charge is predominantly compensated by counterions, with the excluded co-ions hardly contributing to the countercharge. This observation has considerably facilitated the interpretation of the electrokinetic properties of bacterial cell suspensions.

Electrophoresis, static conductivity and dielectric response are related (electrokinetic) techniques and therefore share common physical bases. This also implies that the physical and mathematical problems that have to be solved in order to interpret the experimental data are very similar. Analytical solutions only exist for colloidal particles for which the electrical double layer is very thin compared to the particle dimensions. Most bacterial cells are relatively large colloidal particles and therefore the large κa theory may be of help in the evaluation of their electrokinetic properties. However, the original theories do not

include surface conductance in the hydrodynamically stagnant layer. Therefore, they had to be extended to account for the finite conductivity of ions in the bacterial wall.

Static conductivity and dielectric dispersion both show that the counterions in the bacterial wall give rise to a considerable surface conductance. From a comparison of the mobile charge with the total cell wall charge it is inferred that the mobilities of the counterions in the bacterial wall are of the same order but somewhat lower than those in the electrolyte solution.

Due to surface conductance the electrophoretic mobility may be strongly retarded compared to the classical Helmholtz-Smoluchowski theory, especially at low electrolyte concentrations. In 1 mM and 10 mM electrolyte solution, the Helmholtz-Smoluchowski equation underestimates the ζ -potential by approximately a factor of 2 and 1.3, respectively.

Resolving the fundamentals of the electrochemical characteristics of bacterial cell surfaces is a key step towards a quantitative understanding of the electrostatic interactions of bacterial cells with their surroundings. The success of such an investigation depends on the state of the art of the disciplines involved. Both microbiology and colloid chemistry have the microscopically small particle as object of study. Until recently there has hardly been any exchange of scientific knowledge between these two disciplines, despite their common interest. Colloid chemists preferred to study relatively simple particles to test their basic theories and bacterial cells were considered far too complex to serve as model colloids. However, the progress that has been made during the last decades in both colloid chemistry and microbiology provide the right tools for a successful cooperation. The present study is born from such a symbiosis and shows that many physico-chemical characteristics of bacterial cell surfaces are accessible with (classical) colloid chemical techniques. In fact, for testing more advanced colloid chemical theories bacteria may even be better model particles than the generally used inorganic colloids, because of their ability to produce a homogeneous population of identical cells.

For the time being only Gram-positive strains have been considered, because of their relatively less complex cell wall structures. Nevertheless, the techniques used *mutatis mutandis* also be applied to Gram-negative cells. In fact, such a study would be highly interesting, because it would contribute to a more complete description of the composition of the electrical double layer of bacterial cell surfaces.

Samenvatting

De wereld om ons heen heeft al vele van zijn aloude geheimen moeten prijsgeven. Vrijwel alle werelddelen zijn reeds gedetailleerd in kaart gebracht en het aantal gebieden waarop nog nooit een menselijke voetafdruk is gezet wordt dagelijks kleiner.

De nieuwsgierigheid van de mens lijkt echter ontoombaar. Niet alleen de direkt waarneembare wereld, maar ook datgene wat zich buiten ons gezichtsveld bevindt, moet nauwkeurig in kaart worden gebracht. Dat geldt zowel voor het eindeloos uitdijende heelal, waarin de aarde nog veel minder voorstelt dan een speldeknoopje, als ook voor de uitgestrekte wildernis van de microscopisch kleine wereld.

Sinds de ontwikkeling van de microscoop is het mogelijk om een kijkje te nemen in de wereld waar alles zo klein is dat zelfs verkleinwoorden ontoereikend zijn om de dingen goed te beschrijven. In die wereld komen hele kleine wezentjes voor, die zo'n honderd tot duizend keer kleiner zijn dan het puntje op deze j. Het krioelt er bovendien van een enorme variëteit van verschillende soorten, die alle als gemeenschappelijk kenmerk hebben dat ze slechts uit één cel bestaan. Sommige van die cellen hebben ingewikkelde structuren en zijn bovendien wat groter dan de rest. Dat zijn de algen, de schimmels, de gisten en de protozoa. De wat kleinere cellen zien er veel eenvoudiger uit en lijken veel minder complex. Dat zijn de bacteriën.

De microscopisch kleine organismen blijken werkelijk overal voor te komen in omgevingen variërend van een gezellige huiskamer tot en met het ontoegankelijke Himalaya-gebergte. En natuurlijk niet te vergeten ons eigen lichaam, waarin ze in miljardentallen op de meest verborgen plekjes te vinden zijn. Sommige van die minuscule organismen zijn echte parasieten, die er voortdurend op uit zijn om het leven van de mens te veronaangenamen. Echter de meeste microorganismen zijn de mens goedgezind en spelen zelfs een belangrijke rol bij de instandhouding van het leven op aarde. Ze zijn van onschatbare waarde bij de reiniging van vervuilde grond, huishoudelijk afvalwater en besmet oppervlaktewater, omdat ze vrijwel alle organische stoffen, inclusief de meest toxische kunnen afbreken.

Het leven van een microorganisme is niet eenvoudig. Hij is voor zijn overleven volledig overgeleverd aan zijn direkte omgeving en heeft nauwelijks mogelijkheden om daarop enige invloed uit te oefenen. Zijn dagelijkse maaltijd wordt helemaal bepaald door wat de pot schaft en dat is meestal heel weinig. De bewegingsvrijheid van de microorganismen is vaak erg beperkt. Dat komt omdat

ze aan krachten onderhevig zijn waar je als gewoon mens geen weet van hebt. Om dat in te zien is het noodzakelijk om iets dieper in te gaan op de wetmatigheden die algemeen gelden voor kleine deeltjes, ook wel kolloïden genoemd.

Kolloïdale deeltjes zijn vanuit moleculair oogpunt gezien betrekkelijk groot, maar tegelijk zijn ze voldoende klein om in een vloeistof (b.v. water) te kunnen oplossen. Vrijwel alle kolloïdale deeltjes in oplossing zijn ofwel positief danwel negatief electrisch geladen. Het ladingsteken is heel gemakkelijk vast te stellen door b.v. een kolloïdale oplossing in een elektrisch veld te brengen en vervolgens te kijken (b.v. met een microscoop) in welke richting ze bewegen. Kolloïdale deeltjes in oplossing leven in een soort van haat-liefde samenlevingsverband. Aan de ene kant hebben ze een natuurlijke aantrekkingskracht tot elkaar, terwijl ze tegelijk sterk de neiging hebben om wederzijds contact te ontlopen. Die aantrekking tussen de deeltjes is een direkt gevolg van een elementaire natuurkracht tussen molekulen die pas duidelijk merkbaar wordt als ze heel dicht in elkaars nabijheid komen. De afstotingskracht tussen de deeltjes houdt verband met de hoeveelheid electrische lading die aanwezig is op het deeltjesoppervlak.

Er is een fundamentele natuurwet die zegt dat alle positieve lading op de een of andere manier gecompenseerd moet worden door een gelijke hoeveelheid negatieve lading. Het bestaan van de lading op het deeltjesoppervlak leidt daarom tot het ontstaan van een gelijke hoeveelheid lading met tegengesteld teken in de direkte omgeving van het deeltje, zodat de som van alle ladingen precies gelijk aan nul is. In waterige milieus is de tegenlading erg diffuus en zit daardoor relatief ver van het deeltje vandaan. Bevindt het kolloïdale deeltje zich echter in een omgeving met veel zout dan zit de tegenlading in de direkte nabijheid van het deeltje. De zoutionen zijn dus in staat om de oppervlaktelading af te schermen, zodat het net lijkt alsof het deeltje minder geladen is. In een omgeving met veel zout kunnen de kolloïdale deeltjes elkaar heel dicht naderen en zelfs gaan samenklonteren. Daarentegen bij voldoende oppervlaktelading in een omgeving met weinig zout is de afstotingskracht groter dan de aantrekkingskracht en blijven de deeltjes in oplossing. De stabiliteit van een kolloïdale oplossing wordt dus bepaald door het samenspel van de hoeveelheid electrische lading op het deeltjesoppervlak en de neutraliserende werking daarvan door het aanwezige zout.

Van de microorganismen zijn het met name de bacteriecellen die kolloïdale afmetingen hebben. Het is een enorme uitdaging om te zien in hoeverre bestaande theoriën die tot nu toe ontwikkeld en getest zijn voor relatief

eenvoudige dode kolloïdale deeltjes toegepast kunnen worden op biologische kolloïden zoals b.v. de bacteriecellen.

Het binnenste deel van een bacteriecel bestaat uit cytoplasma en is omringd door een dun vliesje, de cytoplasma-membraan. Deze membraan is erg kwetsbaar en wordt daarom beschermd tegen de buitenwereld door een dik vezelig omhulsel, de celwand. Zo'n celwand bestaat uit een mengelmoeis van eiwitten, suikers en vetten, die samen een sponsachtige structuur vormen met een stevigheid die overeenkomt met die van een autoband. In de eiwitten en in mindere mate ook in de suikers zitten bepaalde groepen, die een positief geladen waterstofatoom kunnen afscheiden en dan zelf met een negatieve lading blijven zitten. Dat is de reden dat vrijwel alle bacteriën negatief geladen zijn. Er is slechts een gering aantal groepen in de bakteriewand die in potentie de mogelijkheid heeft om te dissociëren en zelfs die doen dat maar gedeeltelijk. Op het aantal groepen in de wand dat dissocieert heeft de bacteriecel zelf geen enkele invloed. Het is het milieu waarin de bacterie zich bevindt en dan met name de zuurgraad en de zoutconcentratie, dat bepaald hoe sterk de bacteriecel geladen is.

Om het gedrag van de bacteriecel te kunnen begrijpen is het nodig om zijn elektrische eigenschappen te kennen. Om daar achter te komen is het noodzakelijk om de bacteriecel vanuit de vrije natuur over te brengen naar een groeimedium, zodat het zich kan vermenigvuldigen. Op die manier is het mogelijk om een populatie te kweken van miljardentallen volledig identieke individuen, die vervolgens gebruikt kunnen worden voor diverse experimenten. Zo kun je b.v. de celwand van de bacterie losspellen en chemisch analyseren om te kijken wat voor soort molekulen daarin voorkomen. Vervolgens kun je voor een hele reeks van verschillende zoutconcentraties en zuurgraden bepalen hoeveel groepen in de bakteriewand een positief waterstofatoom zijn kwijtgeraakt, zodat je dus exact kunt uitrekenen hoeveel lading er in de bakteriewand voorkomt. Eveneens is het mogelijk om precies vast te stellen hoe de tegenlading rondom de bacteriecel verdeeld is.

Om te weten te komen hoe effectief die celwandlading is kun je de bacteriecellen in een elektrisch veld brengen. Vanwege de lading in de bakteriewand zal het elektrische veld dan aan de cellen gaan trekken, zodat ze gaan bewegen. Echter ook de zoutionen rondom de cel voelen de aanwezigheid van het elektrische veld en zullen eveneens in beweging komen. Je kunt beide effecten bestuderen en vervolgens met speciaal daarvoor ontwikkelde theorie bepalen hoeveel celwandlading op zekere afstand van de bacteriecel nog gevoeld wordt. Ook kun je dan te weten komen hoe de zoutionen rondom de cel en in de celwand bewegen en met welke snelheid ze dat doen.

Als de elektrische eigenschappen van bacteriecellen zijn opgehelderd is het mogelijk om hun lot in de vrije natuur beter te begrijpen. In de bodem bijvoorbeeld zitten bepaalde bacteriën stevig gebonden aan gronddeeltjes, terwijl andere soorten veel meer bewegingsvrijheid hebben. Datzelfde geldt ook voor bacteriën die in meren of rivieren voorkomen. Beweeglijke bacteriën hebben in principe de mogelijkheid om op zoek te gaan naar een ander plekje in tijden van voedselschaarste, terwijl gehechte bacteriën dan gedwongen zijn om op een houtje te bijten. In andere gevallen is het veel gunstiger om stevig verankerd te zitten aan bijvoorbeeld een grote zandkorrel. Dat geldt bijvoorbeeld voor een zoetwaterbakterie die zich in de riviermond bevindt. Vrijlevende bacteriën kunnen gemakkelijk door de stroming worden meegesleurd naar open zee, waar ze al snel het loodje zullen leggen, vanwege de veel te hoge zoutconcentratie. De gehechte bacteriën daarentegen zijn in dat geval veel beter af en kunnen bovendien profiteren van een continu aanbod van niet te versmaden organische stoffen.

Om een inschatting te maken van de bruikbaarheid van bacteriën voor technologische processen is het eveneens noodzakelijk om de oppervlakte-eigenschappen te kennen. Het zuiveren van huishoudelijk- en industrieel afvalwater is in veel gevallen het werk van bacteriën. Uiteraard mogen ze niet zelf in het gereinigde afvalwater aanwezig zijn. Daarom worden alleen die bacteriën gebruikt die sterk de neiging hebben om zich aan elkaar of aan andere deeltjes te hechten. Om uit de veelheid van verschillende soorten de juiste bacteriecellen te selecteren is het daarom van belang om hun oppervlakte-eigenschappen nauwkeurig te kennen.

Curriculum Vitae

Albert van der Wal werd op 22 januari 1965 geboren te Kantens in het Noord-Oosten van Groningen. Op 3-jarige leeftijd verhuisde hij naar het drie kilometer verderop gelegen Middelstum en op 11-jarige leeftijd naar het eveneens nabijgelegen Ten Boer. In 1983 behaalde hij het Atheneum diploma aan het Gomarus College te Groningen. In hetzelfde jaar begon hij aan de studie Moleculaire Wetenschappen aan de toenmalige Landbouwhogeschool te Wageningen. Na het propaedeutisch examen in augustus 1984 werd de studie voortgezet met de doktoraal fase in de fysisch-chemische oriëntatie. In november 1989 werd de studie afgerond met de hoofdvakken fysische chemie, microbiologie, filosofie en een bijvak wiskunde. Vervolgens werd een zes-maands onderzoek gedaan in het "Bioengineering Department" van de Universiteit van Utah, USA, naar het adsorptiegedrag van bloedeiwitten. Dit onderzoek werd uitgevoerd onder begeleiding van Dr. Vladimir Hlady en Dr. Joseph Andrade. Vanaf juli 1990 tot en met november 1994 werkte hij, binnen het kader van het Speerpuntprogramma Bodemonderzoek, als assistent in opleiding bij de vakgroep Fysische en Kolloïdchemie en de vakgroep Microbiologie van de Landbouwuniversiteit te Wageningen. In deze periode is het in dit proefschrift beschreven onderzoek uitgevoerd. Vanaf 1 april 1995 is hij werkzaam als assistent onderzoeker bij de vakgroep "Chimie Minérale Analytique et Appliquée" van de Universiteit van Genève, Zwitserland.